HEAT FLOW IN PARTICLE MAT AND PROPERTIES OF PARTICLEBOARD UNDER STEAM-INJECTION PRESSING(Dissertation_全文)

AUTHOR(S):

Hata, Toshimitsu

HEAT FLOW IN PARTICLE MAT AND PROPERTIES OF PARTICLEBOARD UNDER STEAM-INJECTION PRESSING

TOSHIMITSU HATA

1993

HEAT FLOW IN PARTICLE MAT AND PROPERTIES OF PARTICLEBOARD UNDER STEAM-INJECTION PRESSING

TOSHIMITSU HATA

1993

CONTENTS

INTRODUCTION [1]

In the production of particleboard, the pressing process is the most important for both productivity and board quality. For that reason, efforts are being made to develop the new methods of pressing technology and new types of resin[2,3].

The efforts for the former were crowned with successfully developing a multi-opening press, single-opening press and continuous press[4-8], which are based on a hotpressing. On the contrary, a steam-injection pressing in which high pressure steam is injected into a mat during pressing have awakened a world interest recently. The mechanism of heat transfer in mats during steam-injection pressing is different from that in the conventional hotpressing. In the former, a high-pressure steam flow governs the heat transfer through particle mat, while in the latter the hot-platens supply heat energy to the mat by heat conduction. In this regard, the steam-injection pressing is expected to have the advantage of shortening the total pressing time than the conventional hotpressing.

Studies on isocyanate bonded particleboard have been conducted in an effort to develop new types of resin[9-11]. In Japan many studies on low-density particleboard with a density of about 0.4 g/cm^3 have been done in order to substitute particleboard for plywood. Low-density particleboards bonded with an isocyanate compound adhesive suitable for both exterior and interior uses have been reported[3,12-14]. The features of the isocyanate compound resins are as follows: 1)hot pressing time can be shortened as the adhesive reactivity is higher; and 2)the allowable range of moisture is broader.

The remarkable features of the low-density board include high dimensional stability and internal bond strength in spite

of its lower density, although the flexural properties are rather poor. The simple way to improve the flexure property is to increase the board thickness. However, the pressing time increases in direct proportion to the board thicknesses in the conventional hotpressing, thus the production efficiency is decreased.

The purpose of the present study is to establish the technology for the steam-injection pressing process and to apply this technology in the production of thick low-density particleboard. The present paper consists of four chapters;

Chapter 1: The history of technology and study on the steam-injection pressing;

Chapter 2: The temperature behavior in particle mats during hotpressing and steam-injection pressing;

Chapter 3: The effect of particle geometry on the temperature behavior in particle mat and on the gas permeabilities in the particleboard;

Chapter 4: The effects of injection time and timing, and particle geometry on the board properties, and the trial of shortening the press cycle with steam-injection.

CHAPTER 1

LITERATURE REVIEW

The pressing process in the production of particleboard and other efforts that have been done in order to shorten the total pressing time are discussed in this chapter. The emphasis and significance of this study are focused more by reviewing the historical development of the steam-injection pressing technology and citing some research highlights on the subject.

1.1 Methods of shortening the pressing time

Two ideas can illustrate the pressing process of particleboard production. These are:

1. Pressing the mat in order to make the particles come into close contact with each other;
2. Heating the mat to cure the adhesives.

Adding to those two ideas mentioned above, it is also necessary to adjust the pressing time so that the optimum moisture content of the mat would take effect.

In the production of particleboard, the pressing process is considered to be a bottleneck. Thus, shortening the pressing cycle would eventually improve productivity. The heat conductivity of particleboard is poor because it has small pores and few free electrons which is different in the case of metal where the influence of evaporated water under heat is neglected. The simplest way to shorten the total pressing time is to increase the platen temperature, that is, to increase the temperature gradient in the mat. In this case, however, wood particles deteriorate at a temperature over 170 °C for a certain time, and the energy consumption maintaining the platen temperature at a higher level increase[15]. Spring back of the

boards, when pressing pressure is released, should also be taken into account in deciding the pressing time, because spring back tends to increase with a decrease of the pressing time[15].

When moistened materials are heated, the repetition of boiling, evaporation, and condensation of water start from the surfaces and the heat from the platens is conducted throughout the core at once. This kind of heat conduction which is applied for heat exchange equipments, steam boilers, and atomic power applications in a daily life is much greater than single phase conduction taking place in materials without water because of its greater heat conductivity.[16].

"Steam shock" is a process that enhances heat transfer by moisture distribution. A "Novopan process", or "steam shock" was first explained by Fahrni[17], and Klauditz showed the possibility of a remarkable shorter pressing time[18]. In this process, particles with distinctly different moisture content are used or these are sprayed with the required amount of water on the mat surfaces just prior to hotpressing, so that the moisture content in the face layers is higher than that of the inner layers. The method shortens the pressing time due to the fast heat transfer by the steam evaporated from the mat surfaces to the core, thus the temperature at the core reaches 100 °C in a fraction of a minute.

However, longer pressing time is required when too much water is sprayed on the surface layers because it prevents the adhesives from curing[19]. It is least expected for the mat core temperature to be more than 100 °C because most of the heat energy from the hot platens is used for evaporating water. Therefore, this process cannot be an effective way to shorten the pressing time when the adhesives need a temperature over 100 °C for curing. Mat thickness is another limitation for this

process. When the mat is too thick, it is unlikely for the steam to penetrate into the core within a desired pressing time. This is because of the fact that the rate of steam diffusion is lower when no pressure is applied from the outside.

A steam-injection pressing shows a possibility of widening the range of the mat thickness because externally applied pressures make the steam move much faster in the mat than the self-pressures of the steam.

1.2 Technology of the steam-injection pressing

1.2.1 Patents and studies

Patents on reducing the total pressing time by injecting steam into the mat have been issued since 1950s, however, in 1973 Shen applied this technology to the experiment of producing waferboard for the first time. Since then, years of research and development in the steam-injection pressing have been conducted for practical use.

Klauditz got a German patent in 1959 on a process where boards were produced by injecting superheated steam into the mat after reaching the final thickness[20]. The patent described the details of drying time necessary to reduce the mat moisture increased by steam-injection to an appropriate moisture content. The process is limited to phenol formaldehyde bonded boards with 0.35 g/cm^3 low density. Corbin obtained a US patent assigned to Weyerhaeuser Co. Ltd. in 1966 on a method where superheated steam was injected into the mat sprayed with a urea formaldehyde resin[21]. The superheated steam made the pressing time shortened, and the pressure reduced, and a 19-mm thick, 0.7 g/cm^3 density board was produced by a 5-sec superheated-steam injection at a total pressing time of 120 seconds. The patent describes that the use of the superheated steam made the

condensation in the mat reduced. Stegmann and May reported on experiment in 1968 involving the movement of steam edgewise through panels[22]. Voelskow et al. obtained a German patent issued in 1972 on a continuous steam-injection press[23]. Steam was injected from the steam-injection equipment installed at the entrance of the press in order to reduce the closing pressure on the mat.

A US patent issued to Shen in 1975, an assignor to Canadian patents and Development Ltd[24]. The patent describes the method where saturated steam was injected into the mat after the particle mat was pressed to the final thickness in an edge-sealed press. The steam injected into the mat from one side is exhausted from the other in the specially designed press. For example, a 0.76 g/cm^3 density, 25 mm thick board was manufactured with the pressing time of a minute using a steam pressure of 21 kgf/cm^2. A German patent issued in 1974 to Alenius details a device by which gas or liquid can be injected into panels during pressing[25]. A French patent issued to Okhotskii et al. in the same year describes the method of producing boards with superheated steam injected into the mat without adhesives[28]. This patent describes the long periods of steam-injection followed by periods of hotpressing. Thoman manufactured boards with the same press system as Shen's and tested the board properties[27]. The steam-injection pressures were 7 - 8 kgf/cm^2 and the total pressing times were in the range of 1 - 3 minutes. Optimum board properties were obtained in 2 min pressing time. Steam condensation in the press prevented the adhesives from curing, which caused less bending property and internal bond strength than those of the conventional hotpressing. A patent modifying Shen's was issued in 1980 to Nyberg, assignor to Hawker Siddeley Canada Ltd. It

describes the equipment similar to Shen's forming a steam chamber in pressing[28]. The saturated steam injected into the mat from the platens was exhausted through the same platen after the steam-injection.

Nishikawa et al. discussed the optimum conditions in the production of phenol formaldehyde bonded particleboards with the steam-injection press[29]. Board properties increased in the case where both heat and steam-injection system have less steam pressure. Acceptable properties of 40 mm thick board were obtained at 7 kgf/cm^2 steam pressure for the heat system and 4.5 kgf/cm^2 for the steam-injection system. The optimum condition is a pressing time of 10 - 17.5 min and a steam-injection time of 2.5 - 10 min. In this case, a certain period before steam-injection is applied. The total pressing time was much greater, when compared with the other reports such as Shen's or Geimer's. Nishikawa et al. produced OSB from thin larch flakes under the optimum conditions taken in the previous paper[30]. The obtained MOE value of OSB, 70 x 10^3 kgf/cm^2, passed the standard specified by FPL for structural boards.

Instead of using the sealed steam-injection pressing system as Shen's or Thoman's, Geimer developed an unsealed steam pressing technique. A US patent issued in 1983 to Geimer describes a process where saturated steam is injected through both top and bottom surfaces during pressing[31]. In this system, the mat itself works as an outlet valve. He produced 0.64 g/cm^3 density, 13 mm thick phenol formaldehyde bonded particleboard in 1.5 min pressing time. Geimer also examined the properties of 1.27 - 5.08 cm thick, 0.48 - 0.801 g/cm^3 density, isocyanate bonded particleboard[32]. Isocyanate adhesive is suitable for board production with the steam-injection pressing because of the broad range of suitable moisture content. A Patent of "hot

gas" system was issued to Tayler and Reid in 1985, assignors to Weyerhaeuser Co. in USA[33]. His method is similar to Geimer's, however, the sequence of steam-injection and exhaustion is different. Geimer produced a large size of flake boards with a prototype steam-injection press in 1986[34]. The board properties decreased because the adhesive was diluted by the steam condensation. The inner vapor-pressure increased with an increase of the mat density. In this system, the push-through stage is necessary to remove air pockets wherein steam is introduced into the mat from the lower platen and is exhausted to atmosphere through the top platen. A patent assigned to Hsu of Forintek Canada Corp. developed a self-sealing technology in 1989[35]. Narrow and thin frames were attached around the outer edges of the upper platen. The periphery of the mat was highly densified during pressing so that the steam pressure in the mat became greater when the steam injected into the mat[36].

Bambang Subiyanto et al. examined the relationships between a heat environmental temperature, that is, an adhesive temperature in test tubes and the adhesive gelation as the basic study of the steam-injection pressing[37,38]. The results showed that all resins such as urea melamine formaldehyde, phenol melamine formaldehyde, and phenol formaldehyde resin follow the Arrhenius equation in curing behaviors. No apparent relation was observed between the average resin-temperature and the gelation time[39]. The mechanism of adhesive curing under higher pressures or temperature was also examined, and it was shown that the curing of the adhesives under higher steam pressure is different from that under the atmospheric conditions[40]. It was concluded in the paper that the polymerization and decomposition of the adhesives always go on one after another under both higher steam pressures and atmospheric conditions.

Sasaki et al. tried to produce a 0.4 g/cm³ density, 100 mm thick particleboard with a semi-continuous steam-injection press[41]. The temperature behaviors in the mat during pressing and the board properties were also measured. The optimum curing condition for the semi-continuous press was obtained by adjusting the steam-injection time and by separately opening or closing the steam-pores at each section of the perforated platens. Overlapped pressing was required between each press. It is possible to make 60 - 100 mm, thick low density particleboard in a 90-second total pressing time including 8 - 15 second steam-injection time. The internal bond strength and thickness variation in the lengthwise direction at the joint part of the consecutive pressing were improved by closing the steam-injection pores at both ends of the press platen[42]. Sasaki et al. reported the temperature distribution, the temperature behaviors during pressing, and the board properties on the continuous steam-injection press[43]. Uniform steam diffusion is difficult to get especially in the higher density mat.

1.2.2 Merits and demerits of steam-injection methods

The differences of the steam-injection methods are summarized in three points when the studies and patents mentioned in the previous section were surveyed.

1. Sealed or unsealed press.
2. Saturated or superheated steam.
3. Single-daylight or continuous press.

From these points of view, merits and demerits of each steam-injection pressing process are as follows:

Unsealed superheated steam-injection pressing

Corbin and Hall adopted the method where the superheated steam generated was being passed through the superheater and is

injected into the mat[21]. A schematic diagram of the system is shown in Fig.1.1. The merits are that the superheated steam prevents the steam from condensing to water in the mat. Effective curing of the adhesives is expected even in relatively lower pressure because the potential of the superheated steam is greater. The demerits are that, there is a large loss of the superheated steam as it flows from mat sides to atmosphere, and that the temperature is inconsistently distributed in the mat.

Externally sealed saturated steam-injection pressing

Shen was the one who developed this method of pressing[24]. The schematic diagram of the apparatus is shown in Fig. 1.2. The following serves as the advantages: Little steam leak from the edge-sealed press is observed during steam-injection. High temperature in the mat is accomplished easily and uniformly so that gives the board high dimensional stability. On the other hand, the demerits of this process are as follows: The heavy sealing wall is difficult to deal with. Reliable sealing system is required. The sealing wall makes the movement of the press machines complicated. The maintenance cost of the sealing wall becomes expensive.

Unsealed saturated steam-injection pressing

The schematic diagram of the apparatus adopted by Geimer is illustrated in Fig. 1.3[31]. The merits are that no peripheral wall is required and that the system is much simpler. The demerits are: the usable area of the board is narrower; steam easily condensates to water especially at the periphery of the mat; difficult to raise the mat core to higher temperature; a large loss of the steam; and easy to form the air pocket in larger size panels. When considering the sequence of injection and exhaustion, the air pockets can be avoided, however, other demerits still exist.

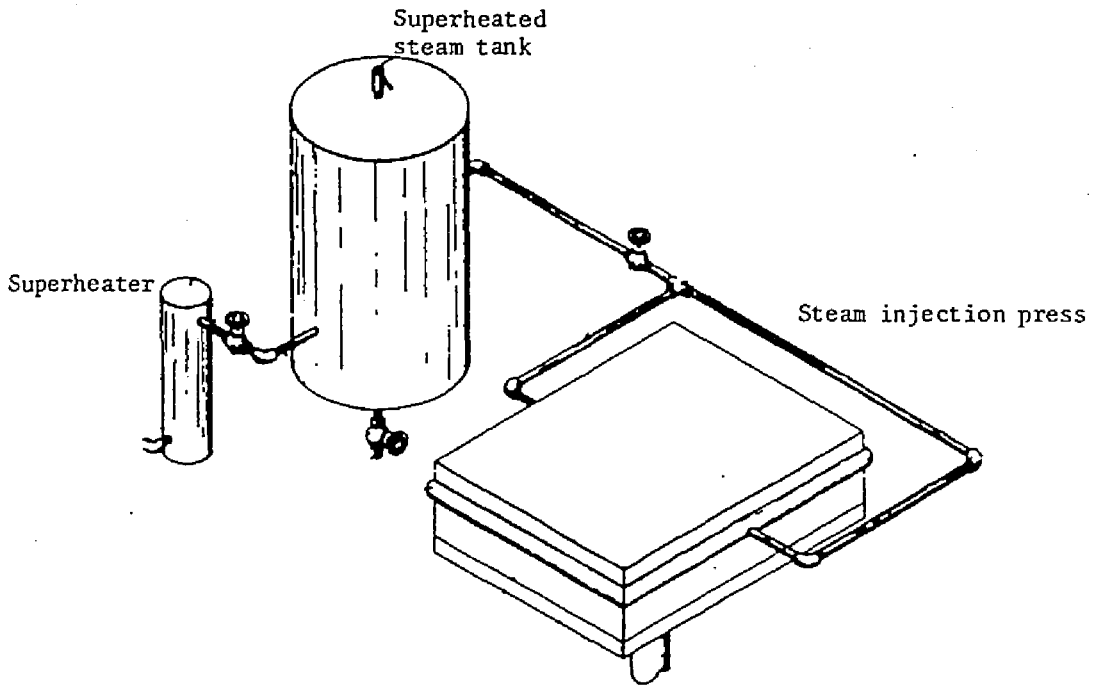

Fig. 1.1 Schematic of an Unsealed Superheated Steam Pressing System.

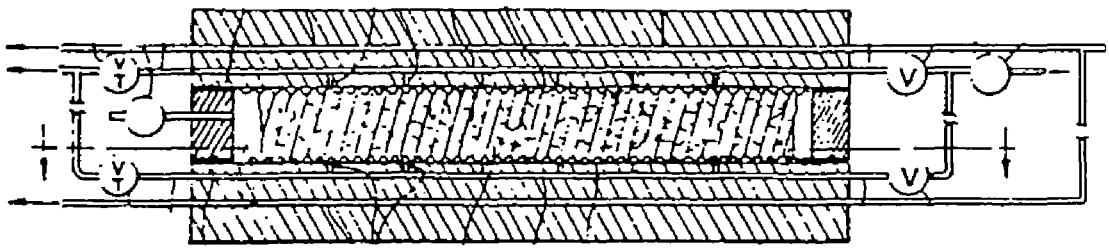

Fig. 1.2 Cross-Section of an Externally Sealed Steam Press.

Self-sealing steam-injection pressing

Hsu developed this method in order to overcome the disadvantages mentioned before[35]. The schematic diagram of this apparatus is shown in Fig. 1.4. The merits are: there is little loss of the steam; the mat edges are densified so that the steam can be closed up in the press; the sealing frame is maintenance free because the mat periphery itself works as seal; and high temperature in mats is obtained easily. The demerits are: the yield of board production is not so good because of the thicker boards: and the area of the board edges densified are more.

Continuous steam-injection pressing

Sasaki developed this type of method[41]. The schematic diagram of the apparatus is shown in Fig. 1.5. Compared with the single daylight press, greater productivity and higher thickness accuracy are expected in the continuous steam-injection press. More effective steam-injection is possible when the steam is injected from the side of the perforated platens, because the air permeability is greater in horizontal direction of the platen. Moreover, this steam-injection system makes it possible to produce laminated veneer lumber.

1.2.3 Other applications of the steam-injection pressing

Gas is injected into porous materials and adhesives are cured by the heat carried by the steam in the steam-injection pressing. So, other gases working as catalysts can be applied to this system. Examples of this are the gassing process and the Sunds Defibrator process.

Tomimura et al. injected triethilamine gas into the mat during pressing and manufactured fiberboards by using the catalytic action[44]. The board properties were almost the same as those made by the conventional hotpressing, except the re-

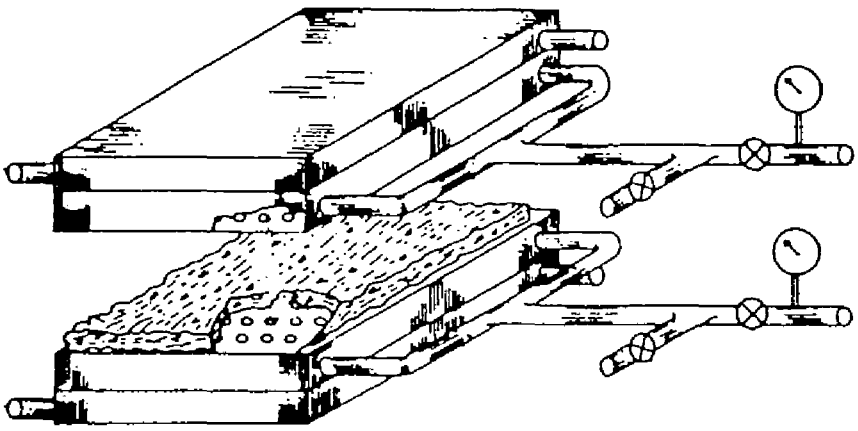

Fig. 1.3 Schematic of an Unsealed Steam Press.

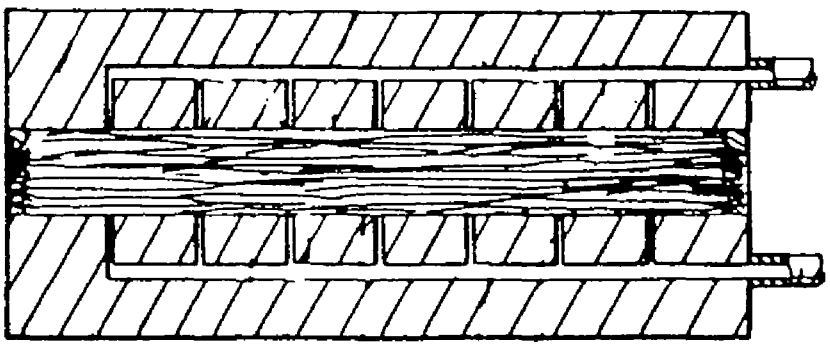

Fig. 1.4 Cross-Section of a Self-Sealing Steam Press.

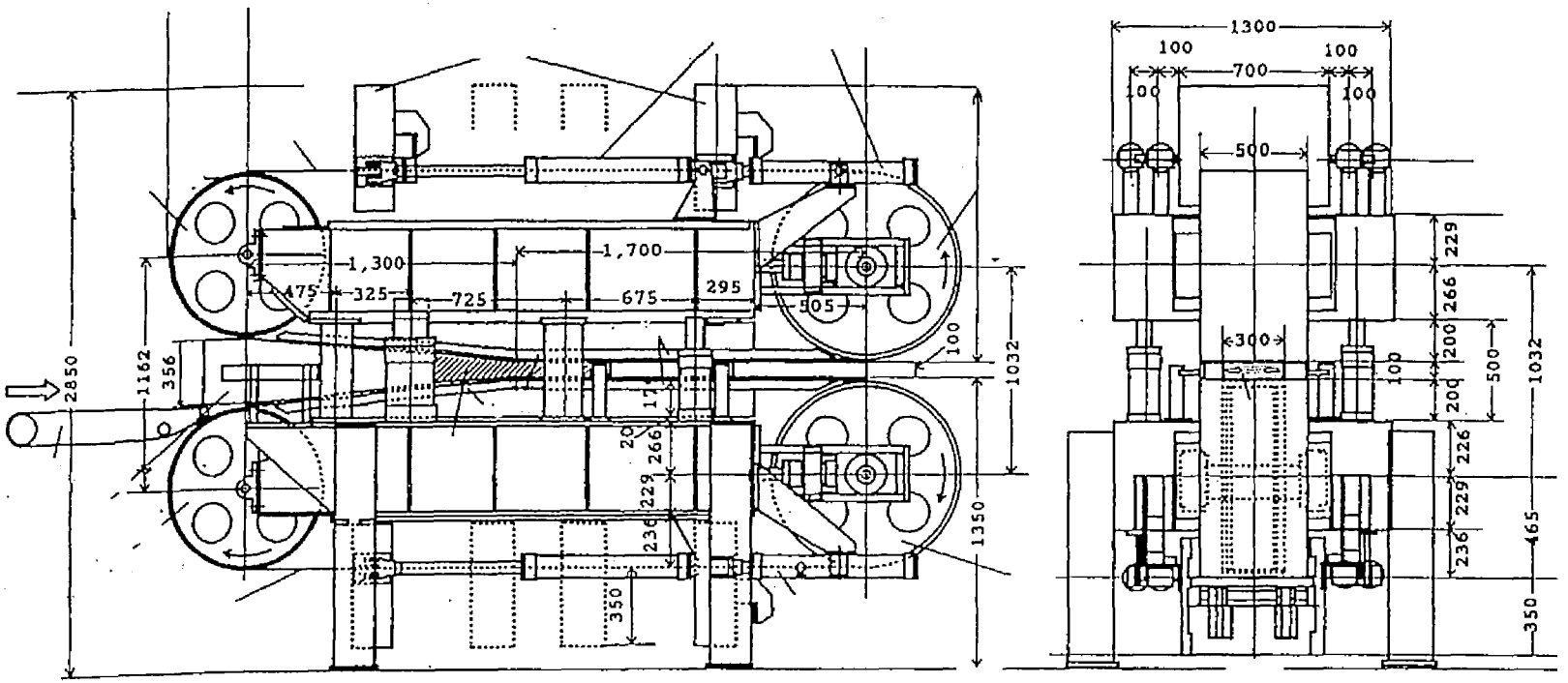

Fig. 1.5 Schematic of Continuous Press with Steam-Injection Heating from Both Sides.

markably excellent internal bond strength. Hata and Ebihara reported the experiment where dimethilethanol amine gas was injected into the mat during pressing and the properties of MDI bonded particleboard were discussed[45]. Satisfactory board properties were achieved even at lower temperature of 60 °C. The paper describes that the moisture content of the particleboard was an important factor. Sunds Defibrator Co. Ltd. shortened the press cycle to 4 - 5 minutes by injecting a CO_2 gas into the mat in the production of cement bonded particleboards[46]. The wood cement board was produced in Hungary in 1988. The uniformity of the gas diffusion in the mat seem to be an important factor, especially in larger size panels.

1.3 Recent developments and practical application

There have been ideas of the steam-injection press for a long time. However, recently has the press been developed into a commercially successful production unit. Up to now, four steam-injection plants are on the stream. Each press is a single opening press producing panels with distinctive features. The present conditions of each plant are shown in Table 1.

Northern pulp Ltd. in New Zealand was the first to install the steam-injection press in 1987[47] to produce "Triboard", which is the combination of building board with MDF surfaces and OSB core[48,49]. The products have many uses, mainly for furniture. The steam injection press owned and operated by Weyerhaeuser is working at the Marshfield, Wisconsin, particleboard plant producing door cores[50]. The Madiberia MDF plant in Nelas, Beira Alta, Portugal, started up their new line with this type of press with a capacity of 112,500 m^3/yr of board a few years ago[51,52]. The last one is working at the Trus Joist Macmillan Ltd. plant and has started the production in

Table 1. The present conditions of steam-injection plants.

Company Name	Place	Products	Application	Press size	Daylight	Press cycle
Juken Nissho	Kaitaia, New Zealand	Triboard Strandboard	Door, Furniture Flooring, Partition	8' x 13'	Single	79sec/30mm
Weyerhaeuser	Marshfield, Wis. USA	Particleboard	Door core	7' x 9'	Single	52sec/40mm
Madiberia	Portugal	MDF	Furniture	8' x 48'	Single	120sec/19mm 180sec/40mm (16mm)
Trus-Joist Mac Millan	Deerwood Min., USA	PSL OSB	Outdoor application	8' x 36'	Single	

Company Name	Capacity	Board thickness	Board density	Adhesives	Materials
Juken Nisho	350m^3/day	20-100mm	450-720kg/m^3	UF UMF	Radiata pine
Weyerhaeuser	350m^3/day	25-50mm	450-530kg/m^3	UF	Aspen pulp chip
Madiberia	430m^3/day (16mm)	8-60mm		UF	Pinaster pine
Trus-Joist Mac Millan		45-140mm		MDI	Aspen log

November 1991[53,54]. Oriented strand lumber is produced from 300 mm Aspen flakes. The product, called Timber Strand, has higher modulus of rupture and excellent dimensional stability.

In Japan, there are no steam-injection press plants, however, Sasaki et al. have bent their energy to the studies for the research and development on the steam-injection pressing[55-57]. They designed and developed the prototype of a semi-continuous steam-injection press in 1990. By this method, the process continues by compressing the particle mat while the press is moving with the same speed as that of the belt conveyors. Steam is then injected from both upper and lower perforated platens followed by hot-pressing which is maintained until the end of the pressing cycle. Finally, the upper platen is raised while the press returns to the initial position at a fast speed. Sasaki et al. also designed and developed the continuous steam-injection press[43]. In this system, steam is injected into the mat through the pores on the injection platens installed on both press sides at the entrance of the press.

1.4 Future prospects

The steam-injection pressing makes it possible to produce a variety of thicker wood based materials which is impossible for the conventional hotpressing. Many new types of wood based products will be developed by using steam-injection press in the near future. The higher internal bond strength and excellent water resistance of the products make it possible to substitute wood and plywood which are getting more and more expensive because of the lack of raw materials. The use of water proof adhesives such as MUF and isocyanate promotes more substitutions. Examples of such products are as follows: thick MDF, low density MDF, thick insulation board made from low

density materials, structural oriented strand lumber, and so on[53].

A full scale continuous steam-injection press will be developed in the near future, as the next step. It is said that Siempelkamp Ltd. is going to complete a new prototype of the steam-injection press. It is high time for the industries of wood processing machinery in Japan to start getting down in the development of the steam-injection press, because the plywood industry is declining due to the availability of raw materials.

1.5 Significance of this study

Although the steam-injection pressing has commercially been successful and there have been various studies on this process, few theoretical approaches on how the steam diffuses in the mat during pressing have been done yet. The observation of the temperature in the mat has been taken as an indication for investigating the steam diffusion in the mat. It is true that some reports regarding temperature behaviors were mentioned, however these are only examples under a specified conditions. Few papers systematically discussed the temperature behaviors under various conditions. Limited papers are avilable with regards to gas permeability in the mat[58].

The present condition in the plants is that, optimum conditions are found from their experiences. As the theoretical studies about the steam-injection pressing are few, any change in the production factors such as a furnish size, board density, resin type, mat moisture content, platen temperature, steam temperature, injection schedule, or steam movement in the mat make the decision of the optimum condition through trials and errors. In such a situation, little attention can be given to the development of new products for each plant.

It is concluded that the effect of the production factors on heat flow in the mat should be systematically discussed. The possibility of shortening the pressing cycle has to be studied and the mechanism of the steam diffusion in the mat should be made clear. It is confirmed that the establishment of the heat flow theory under the steam-injection pressing lead to the further successful research and development of new types of wood composite products and wood processing machineries.

CHAPTER 2

HEAT FLOW IN PARTICLE MAT DURING PRESSING

The temperature behavior, which is the most fundamental information to decide optimum conditions during pressing is examined. The theory for heat conduction in wood was discussed by Maku[59,60]. This theory which was analytically applied to wood drying, can also be applied to calculate the temperature distribution in a particle mat during conventional hotpressing. Heat transfer in a mat during hotpressing accompanying steam injection, however, has not been discussed yet. The thermal flow in a dry particle mat is theoretically discussed for both pressings, and the theoretical equations proposed are examined by use of experimental data in this chapter. The core temperature curves during pressing can be simulated by means of a computer under various conditions according to the obtained equations.

2.1 Temperature behavior in particle mat during hotpressing and steam-injection pressing[61]

2.1.1 Experimental

Flake-type particles of seraya (Shorea spp.) 13 mm long, 1.6 mm wide and 0.6 mm thick on the average were prepared. Upper and lower hot platens were regulated at the same temperature of 160 ℃, and for convenience no binders were applied to the particles.

The temperature distribution along the mat thickness was measured by means of Copper-Constantan thermocouples with wire diameters of 0.2 mm, inserted into the center of the mat plane

at different layers. These were connected to a data processor via a data-logger, and the temperature at each point was recorded at certain time intervals. In a preliminary experiment, the temperature distribution at each layer of the mat was uniform during hot-pressing. Figure 2.1 shows the measuring point along the mat thickness. The error was estimated at ±0.5 ℃.

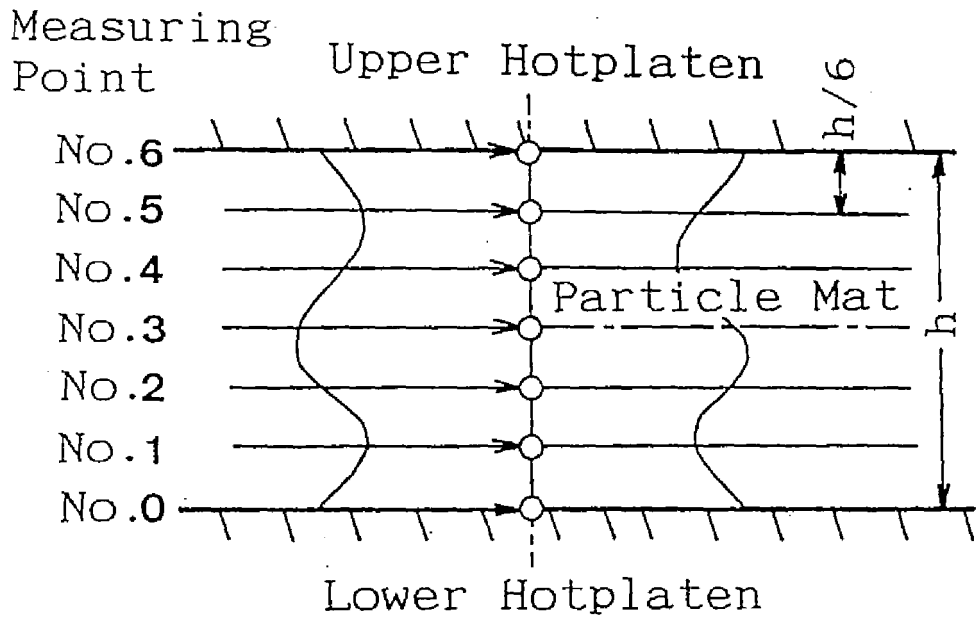

Fig.2.1 Measuring points of temperature of mats during hot-pressing and steam-injection pressing.

The measurement started at the moment when pressure was applied to a particle mat. In hotpressing, the target mat densities were 0.4 and 0.6 g/cm³ at thicknesses of 20, 30 and 40 mm, which was controlled by distance bars inserted on both sides of the mat in the press. The effect of moisture content on the

temperature distribution was examined by use of particles with different moisture contents and by use of wetted papers covering the top and bottom of the mat so that the moisture content in the face layers is higher than that of the inner layers. This method shortens the pressing time due to the fast heat transfer by the steam evaporated from the mat surfaces to the core, thus the same effect as that of steam-injection pressing can be ecpected. The factors and levels taken in the hotpressing experiment are summarized in Table 2.1.

Table 2.1 *The factors and levels taken in the experiment on hot-pressing*

Parameters	Measurement of temperature distribution within a layer	Measurement of the temperature at the center of the layers	
		Uniformly distributed moisture content	Higher moisture content in mat surface
Mat thickness (mm)	20, 40	20, 30, 40	20, 30, 40
Mat density (g/cm^3)	0.4, 0.6	0.4, 0.6	0.4, 0.6
Particle m.c. (%)	10.1	0, 11, 30	0
Equivalent m.c.* of wet paper (%)			20, 26, 31, 35

*Moisture content in the wet papers covered the both surfaces of mat in expressed as the equivalent moisture content which would be calculated on whole particle mat if the moisture would distributre uniformly in the mat.

For steam-injection pressing, a set of 600 x 600 x 30 mm perforated plates for steam-injection were prepared to fit the surfaces of the hotplatens of the conventional laboratory hotpress. The upper and lower plates were perforated with 2 mm-diameter holes drilled through half the depth of the plates with a 25 mm x 25 mm spacing pattern, which covered an area of 450 mm x 375 mm for the upper plate and of 475 mm x 400 mm for the lower plate. The holes on the upper platen and those on the lower platen were drilled in staggered position relative to each

other. A vapor seal on the edge of the mat as reported by Shen[55] was not used.

Thirty seconds into pressing time, or after the press pressure had begun to build up, high pressure steam was injected. The steam-injection periods were 3, 10, 30 and 120 seconds. Adjusted initial steam pressures were 6.2 and 10.0 kgf/cm² corresponding to 160 and 180 ℃, respectively. However, the effective steam pressure during the injection was reduced to some extent. In mats with a density of 0.4 g/cm³, the effective steam pressure were 4 and 6 kgf/cm², when the initial pressures were set at 6.2 and 10.0 kgf/cm², respectively, while the effective steam pressure was 5.5 kgf/cm² for a mat with a density of 0.6 g/cm³ at the initial steam pressure of 6.2 kgf/cm². The target air-dry densities of the mats were 0.4 and 0.6 g/cm³ and target thicknesses were 20 and 40 mm.

The factors and levels taken in the experiment on steam-injection pressing are summarized in Table 2.2.

Table 2.2 *The factors and levels taken in the standard of the experiment on steam-injection pressing*

Parameters	Measurement in the horizontal plane	Measurement in the thickness direction
Mat thickness (mm)	20	20, 40
Mat density (g/cm³)	0.4	0.4, 0.6
Particle m.c. (%)	10.1	0.4, 11
Injection time (sec)	30	3, 10, 30, 120
Vapor pressure (kgf/cm²)	6.3	6.3, 10.2

2.1.2 Results and discussion

The temperature distribution in the middle layer of the mat during hotpressing was as uniform as that in hotplatens (coefficient of variation 1.6 %). A more uniform distribution which was independent of the location of steam perforations was observed in steam-injection pressing. Therefore, in the present paper only the temperature behavior through the mat thickness at the center of mat plane is discussed.

Figure 2.2 shows a typical example of temperatures in different layers of the particle mat as a function of time during hotpressing and steam-injection pressing. Because of the seasonal changes of temperature, the initial mat temperature in the case of hotpressing is slightly different from that of steam-injection pressing. The temperatures of all the mat layers increased to more than 100 ℃ almost immediately after the start of steam-injection. As soon as steam is injected, vapor diffuses through the mat with the driving force of steam pressure gradient. On the other hand, the temperature increase in the mat during hotpressing depends very much on the position within the mat. The core temperature increases slowly and requires about 11 - 11.5 minutes for a mat of 40 mm thickness to reach 100 ℃. The press time of a low density particleboard of 40 mm thickness bonded with an isocyanate compound adhesive is taken to be 12 minutes at a platen temperature of 160 ℃[13]. It took about 1 minute to cure the resin in the middle layer of the mat after the temperature of the layer had reached 100 ℃. Therefore, in steam-injection pressing can it be predicted to shorten the pressing time to 1/10 (for a board of 40 mm in thickness) of that of conventional hotpressing.

Conventional hotpressing

The core temperature of particle mats with different densities and moisture contents are shown in Figs. 2.3 - 2.5 as a function of elapsed time.

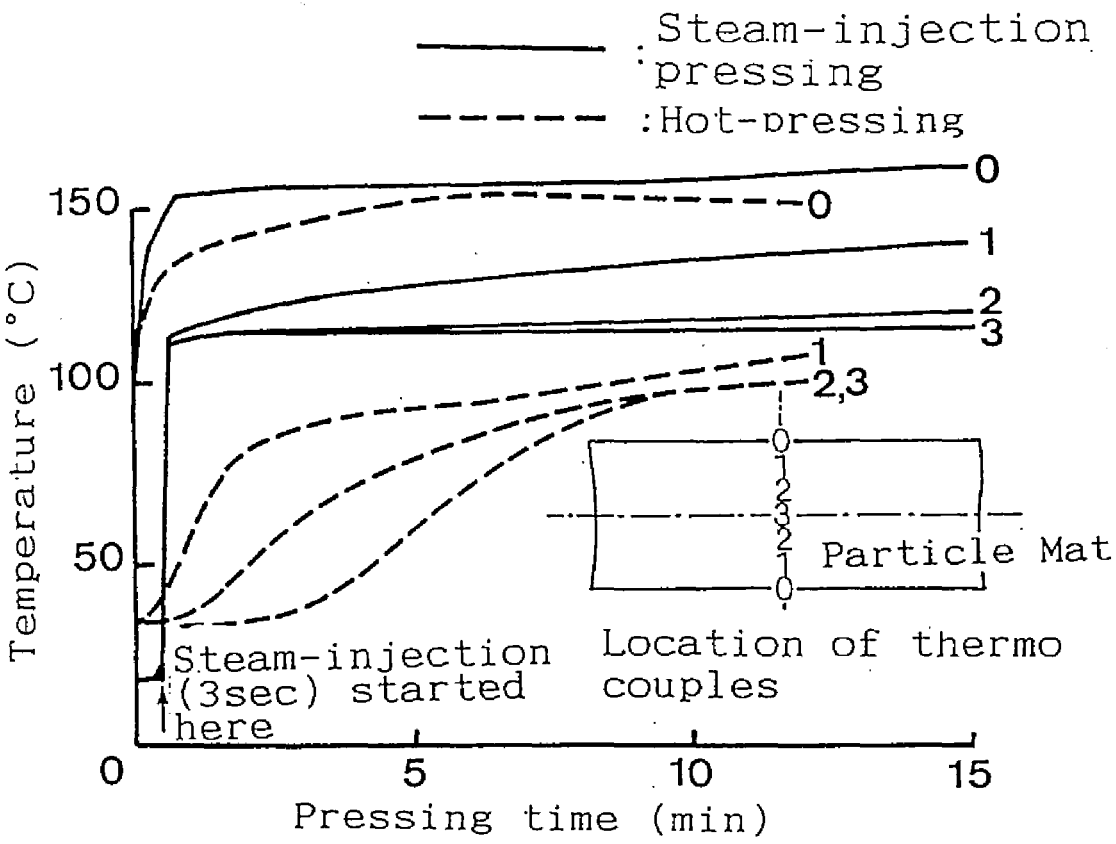

Fig.2.2 Temperature behavior of mat during hot-pressing and steam-injection pressing.

Note: Mat density = 0.4 g/cm^3, mat thickness = 40 mm, moisture content of mat before pressing 0% (steam-injection pressing), 11% (hot-pressing).

Figure 2.3 shows the core temperature of mats with a different density and thickness at a moisture content of 11 % as a function of time. With the increase of the mat thickness from 20 to 40 mm, the slope of the temperature curve decreased. It was calculated that it takes about 3 and 11 minutes for the core temperatures of mats with a thickness of 20 and 40 mm, respectively, to reach 100 ℃. According to the heat conduction theory, when the thickness of the mat is doubled, the time required to increase core temperature to a certain level should increase four times. The experimental result shows that the temperature behavior of particle mat with low moisture content in hotpressing obeys principally the heat conduction law.

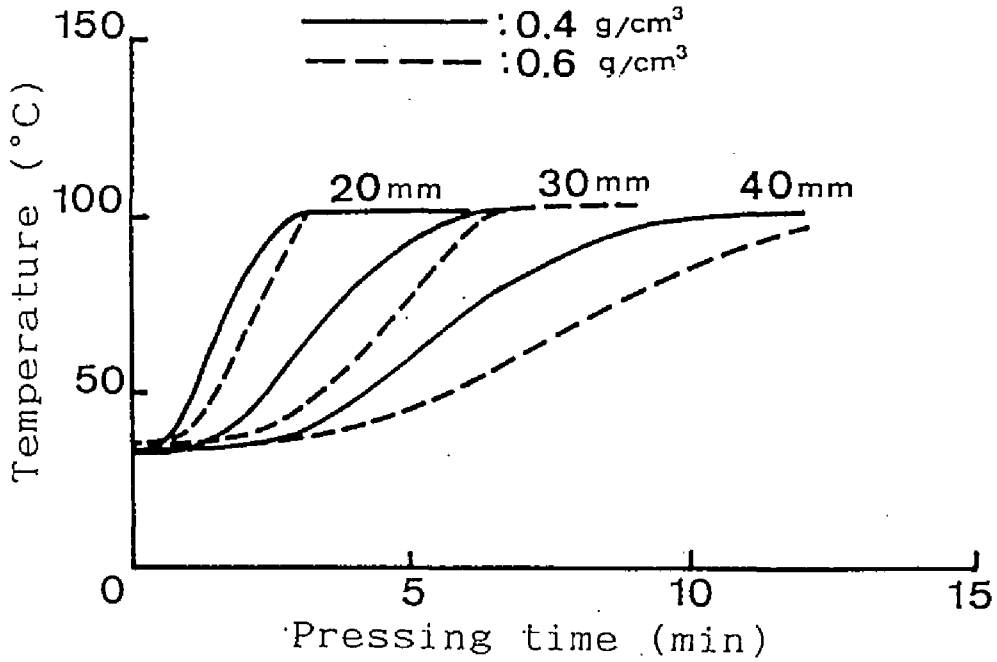

Fig.2.3 The effect of mat density and thickness on the core temperature of mats as a function of time during hot-pressing.
Note: Mat moisture content before pressing = 11%.

The effect of mat density on the temperature increase with passage of time is very slight, as shown in Figure 2.3. However as the density increased, the rate of temperature increase seems to decrease due to the increase of heat capacity per unit volume of mat.

Figure 2.4 shows the effect of the initial moisture content of the particles on the core temperature of the mats as a function of time. The density and the thickness of the mat were 0.4 g/cm^3 and 30 mm, respectively. From the figure, the following can be observed; the higher the moisture content is, the shorter is the time necessary for the core of mat to reach 100 ℃, while the time to stay at a constant temperature about 100 ℃ is longer. It has been confirmed that the core temperature begins to rise again from 100 ℃ as the particles lose moisture below 10 % moisture content[82,83]. When dry particles are used, no equilibrium state of temperature at 100 ℃ is observed.

Figure 2.5 shows the core temperature of dry mats covered on both surfaces with wet papers. The basis weight of the paper was 80 g/m^2. In the figure, moisture contained in the wet papers is expressed as an equivalent moisture content which would be calculated on the whole particle mat if the moisture were distributed uniformly in the mat. When both the face and the back of the mat have a higher moisture content, the increase of mat thickness from 20 to 40 mm does not affect the time required for the core temperature to reach 100 ℃ and the rate of increase is much higher than without wet papers. Comparing Figure 2.5 with Figure 2.4, the rate of increase of the temperature of mat overlaid with wet papers shows more than four times as much as that of a mat which has a uniform moisture distribution. It is noteworthy that the temperature in the

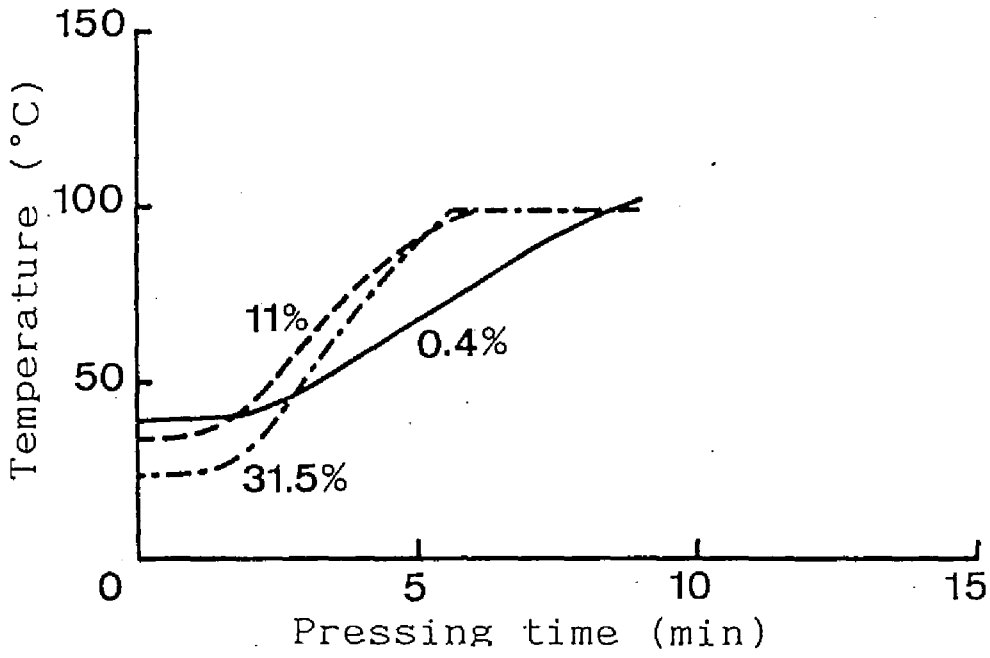

Fig.2.4 The effect of moisture content of mat before pressing on the core temperature of mats along the thickness as a function of time during hot-pressing.
Note: Mat thickness = 30 mm.

middle layer rose to more than 100 ℃ when the equivalent moisture content of wet paper was more than 30 %, while it remained at 100 ℃ for mats having less than 30 % equivalent moisture content. This suggests that the water vapor moving toward the middle layer of the mat exceeds the vapor moving out of this layer when enough water exists at the surface, and the sorption heat of water on particles may promote the temperature increase in the core, so that internal vapor pressure increases.

Steam-injection pressing

During steam-injection, the variation of temperature within the plane of the middle layer of mat was less than in the conventional hotpressing.

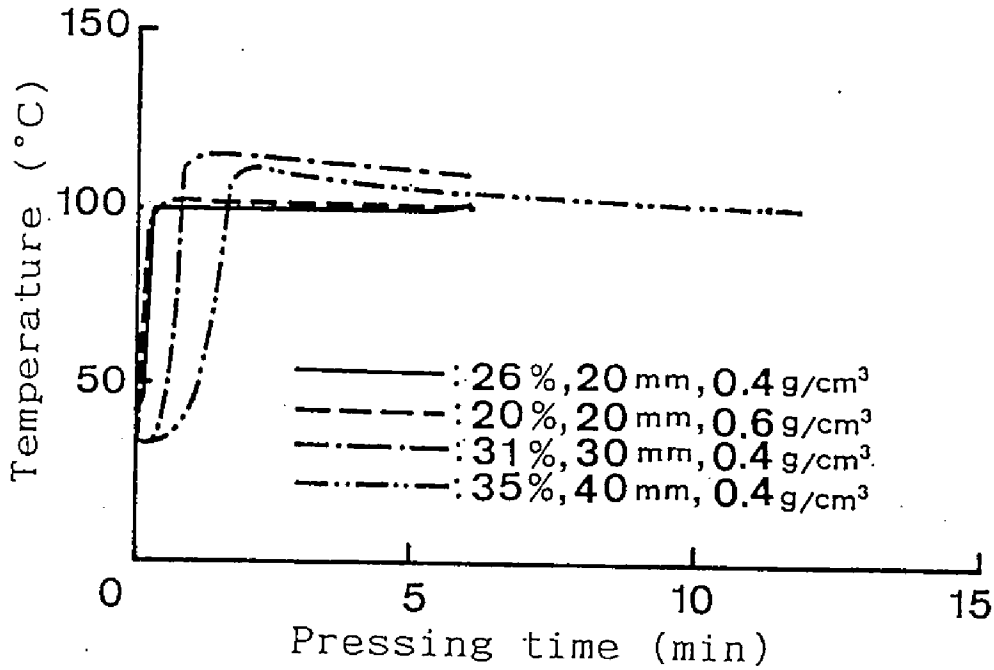

Fig.2.5 The core temperature of mats with wet paper overlays.
Note: Particle moisture content = 0 %, e.m.c.= equivalent moisture content which expresses the moisture contained in the wet papers as if distributed uniformly in the whole mat.

Figure 2.6 shows the effect of steam-injection time on the core temperature of the mat. The target density and the mat thickness were 0.4 g/cm³ and 20 mm, respectively. Dry particles (0% moisture content) were used for this series of experiments. When steam was injected for a longer time, the core mat

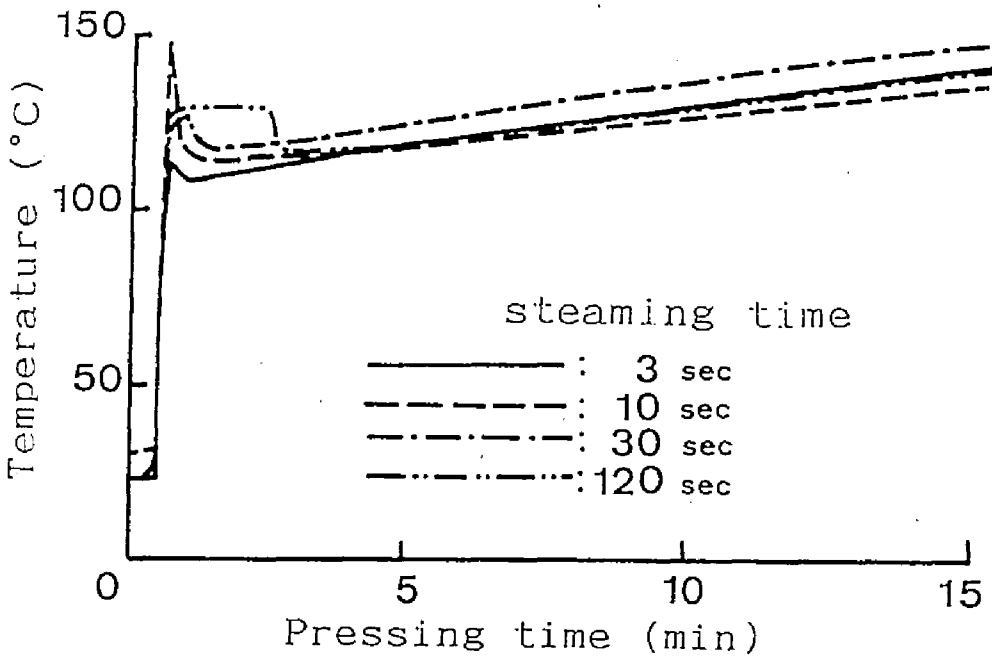

Fig.2.6 The effect of steam-injection time on the core temperature of mats.

Note: Mat density = 0.4 g/cm^3, mat thickness = 20 mm, moisture content = 0%, effective steam pressure = 4 kgf/cm^2.

temperature was kept constant during injection. This suggests that with the increase of the steam-injection time the inflow and outflow of steam in the middle layer of mat was kept balance, and the inner vapor pressure maintained constant. After injection was stopped, the inner vapor pressure or the temperature of the middle layer falls down due to the outflow of steam from edges of mat. However, the temperature goes down once, then increases gradually again, and the increasing curves with different injecting time show almost similar figure, which is quite different from that in the case of mats with wet paper overlay. This suggests that steam-injection up to 120 seconds

does not increase moisture content of the middle layer of mat to more than 10 %[62·63]. This result agrees with those obtained by Geimer[2] and Shen[64].

Figure 2.7 shows the effects of mat thickness and moisture content on the core temperature of mats with density of 0.4 g/cm³ during steam-injection pressing. The core temperature of a mat with a thickness of 40 mm immediately rises to more than 100 ℃ in the same way as that of a mat with a 20 mm thickness during steam-injection in the range of steam pressures used in this experiment. However, the maximum temperature reached at the middle layer during steam-injection showed a tendency to decrease with an increase of the mat thickness. The temperature curves after stopping the steam-injection were greatly affected by the mat thickness, which depends greatly on heat conduction from the hot platens.

When steam is injected, the temperature curves of air-dry (11 %) particle mat are similar to those of dry mats, and seem to be independent of the moisture content. This suggests that most of the steam injected does not interact with the moisture present in the particles and diffuses through the particles from the hot-platens to the middle mat layer. However, the temperature of the middle layer of air-dry mats decreases to 100 ℃ after stopping the steam-injection and then increases gradually at a rate lower than that of the dry-mat, because the heat energy supplied from the hot-platens is partly consumed for evaporation of water present in the particles.

Figure 2.8 shows the core temperature of mats with a density of 0.6 g/cm³ under different conditions of moisture content and steam-injection time. When steam is injected, the core of a mat with a density of 0.6 g/cm³ reaches a higher temperature than that of a mat with the density of 0.4 g/cm³.

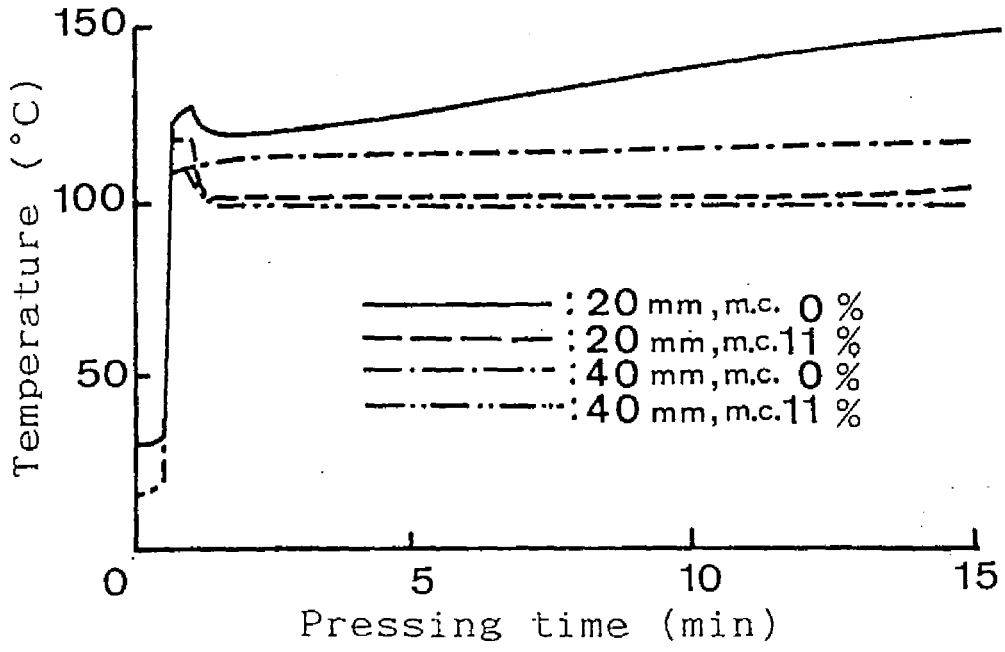

Fig.2.7 The effect of mat thickness and moisture content on the core temperature of mats during steam-injection pressing.

Note: Injection time = 30 sec, mat density = 0.4 g/cm^3.

With increasing density, the gaps among the particles, which are considered to be the main paths of the steam, become narrower. This means that the resistance to the diffusion of vapor in the mat becomes greater with increasing mat density. On the other hand, resistance to the outflow from the edges of mat also increases. Therefore, when the supply of steam is sufficient, the inflow and outflow of steam in mat balances at a higher vapor pressure, and the core mat temperature reaches a higher level.

When steam with higher pressure is injected, the core

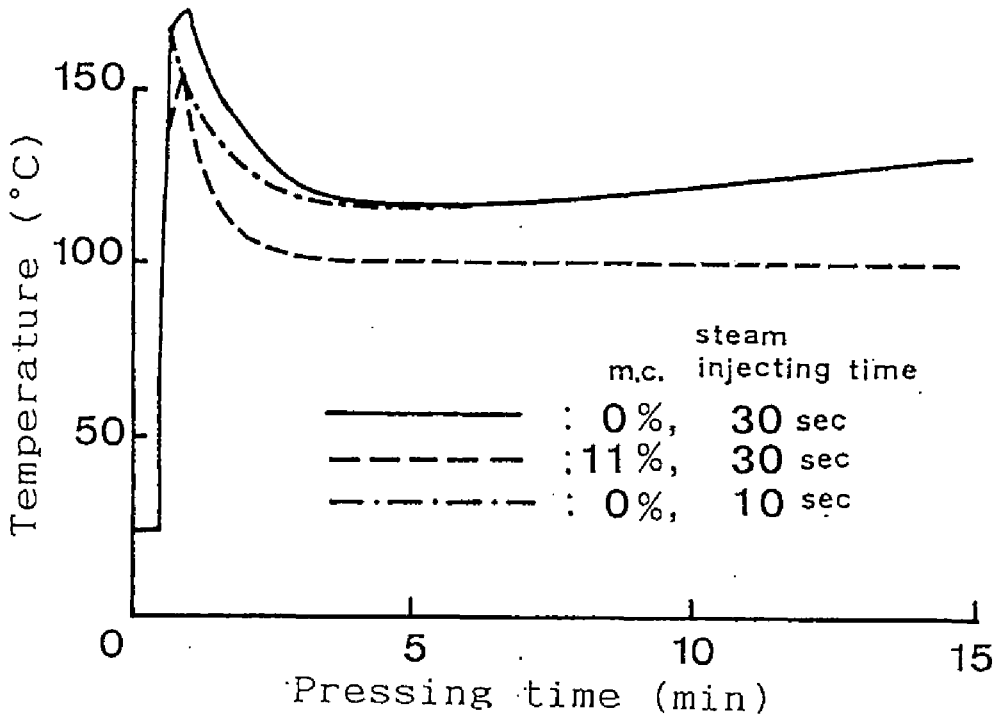

Fig.2.8 The core temperature of mats during steam-injection pressing.
Note: Mat thickness = 20 mm, mat density = 0.6 g/cm^3.

pressure as shown in Figure 2.9.

2.2 Computer simulation of temperature behavior in particle mat during steam-injection pressing[65,66]

2.2.1 Theory for the prediction of temperature behavior in mat

During steam-injection and period following the injection, the mat temperature increase is mainly caused by the high temperature steam moving among particles through the mat. The steam movement is presumed to be a diffusion phenomenon based on vapor pressure gradient as a driving force. The equation for the diffusion analysis is similar to that of heat conduction.

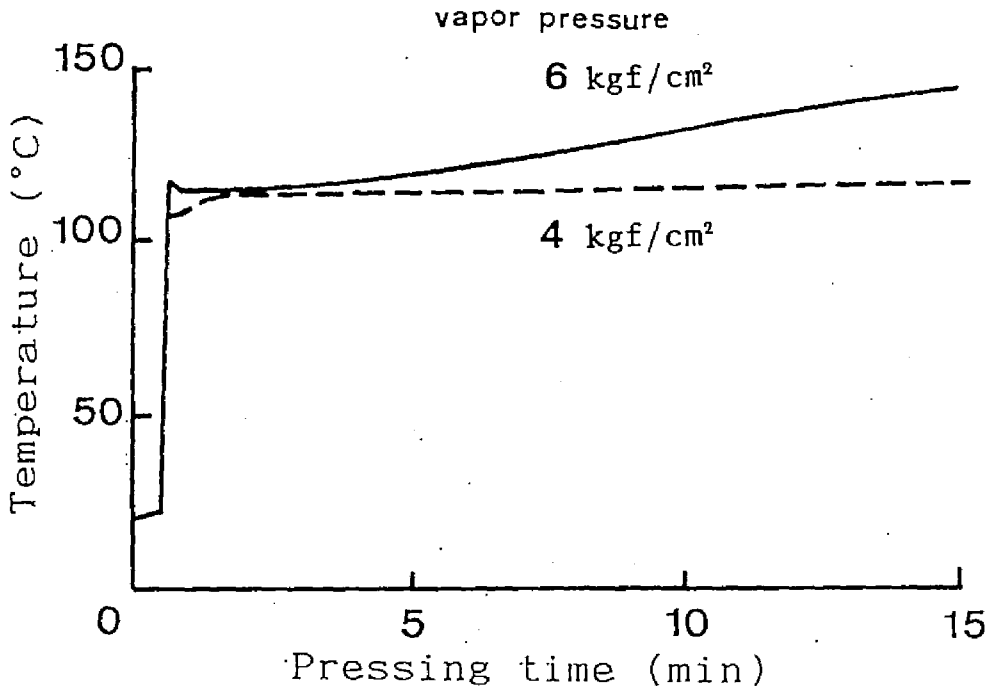

Fig.2.9 The core temperature of mats during steam-injection pressing.
Note: Mat thickness = 20 mm, mat density = 0.4 g/cm³.

Therefore the finite element equation applied for the heat conduction analysis would also be applicable.

In general, mass flow in a porous matrix is controlled by many driving forces. When these forces are treated as a potential gradient of a whole, the mass flow is expressed as follows:

$$\text{flux} = Q/A = k(\partial\phi/\partial x), \qquad (1)$$

where Q/A is a mass flow [$g\cdot sec^{-1}\cdot cm^{-2}$], k is a proportional coefficient [$g\cdot cm^{-1}\cdot atm^{-1}\cdot sec^{-1}$], $\partial\phi/\partial x$ is a potential gradient which is expressed as follows:

$$\partial\phi/\partial x = \partial(P_1 + P_2 + P_3 + \cdots)/\partial x. \quad (2)$$

The driving forces, shown at the right of Eq. (2), are given the gradients of external pressure potential, pneumatic potential, osmotic potential, gravitational potential, and so on[67].

As in the case of steam-injection pressing where steam is injected into a particle mat, the external pressure gradient, (dP_1/dx), and the concentration gradient, (dP_2/dx), can be given as the main potential gradient $(\partial\phi/\partial x)$. Therefore, Eq. (1) becomes

$$\text{flux} = -k_1 dP_1/dx - k_2 dP_2/dx. \quad (3)$$

The first and second terms of the right of Eq. (3) correspond to Darcy's law for gases and Fick's law of diffusion, respectively, and k_1 and k_2 of the potential coefficients are called as gas permeability and diffusion coefficient, respectively.

When the interaction of adsorption and desorption on wood by steam is ignored, and the gas transportation such as air through the pores among particles in a mat is assumed, the first term of Eq. (3) mainly controls the flux because k_1 is greater than k_2 during steam-injection. On the other hand, after stopping the steam-injection, the external steam pressure gradient dP_1/dx becomes zero, and the second term of Eq. (3) controls the flux. As the concentration, the pressure, and the temperature of saturated steam are considered to be functions of each other, the driving force, dP_2/dx, can be expressed as a pressure gradient.

Therefore, steam transported through mats during steam-injection pressing is approximated with the following equation:

$$\text{flux} = -k\, dP/dx \quad (4)$$

Comparing this equation with Eq. (3), the right term of Eq. (4) corresponds to $k_1(dP_1/dx)$ during steam-injection and to $k_2(dP_2/dx)$ after the injection of steam.

By using the continuous equation, the unsteady state diffusion equation is derived from Eq. (4) as

$$\frac{\partial}{\partial t}\rho_s=\frac{\partial}{\partial x_i}\left(k\frac{\partial P}{\partial x_i}\right) \tag{5}$$

where, ρ_s is a steam density [g·cm^{-3}].

When the interaction between steam and particles is neglected, the gradient of the saturated steam pressure P to steam density ρ_s is constant. Using the gradient of the steam mass density $\partial\rho_s/\partial x_i$ [g· cm^{-4}], Eq. (5) can be expressed as

$$\frac{\partial\rho_s}{\partial t}=\frac{\partial}{\partial x_i}\left(k_\rho\frac{\partial\rho_s}{\partial x_i}\right) \tag{6}$$

where, $k_\rho=k\,(\partial P/\partial\rho_s)$ (7)

k_ρ is the gas permeability of a particle mat based on steam density gradient [cm^2·sec^{-1}].

When the diffusion coefficient is independent of the steam density, Eq.(6) is expressed as

$$\frac{\partial\rho_s}{\partial t}=k_{\rho x}\frac{\partial^2\rho_s}{\partial x^2}+k_{\rho y}\frac{\partial^2\rho_s}{\partial y^2}+k_{\rho z}\frac{\partial^2\rho_s}{\partial z^2} \tag{8}$$

where, $k_{\rho x}$, $k_{\rho y}$, and $k_{\rho z}$ is a diffusion coefficient [cm^2·sec^{-1}] of steam moving in the direction of the x, y and z axes, respectively.

If the diffusion coefficient is uniform in all directions and in every part of the mat, from Eq.(8) we obtain the equation,

$$\frac{\partial\rho_s}{\partial t}=k_\rho\left(\frac{\partial^2\rho_s}{\partial x^2}+\frac{\partial^2\rho_s}{\partial y^2}+\frac{\partial^2\rho_s}{\partial z^2}\right) \tag{9}$$

where, $k_\rho(=k_{\rho x}=k_{\rho y}=k_{\rho z})$ is the diffusion coefficient of steam in a particle mat [cm^2·sec^{-1}].

The steam density on the boundary between a mat surface and a hot-platen is defined as,

$$\rho_s=\bar{\rho}_s \tag{10}$$

where, $\bar{\rho}_s$ is the saturated steam density at a regulated vapor pressure [$g \cdot cm^{-3}$].

The mass flux J_p of steam evaporation from mat sides [$g \cdot cm^{-2} \cdot sec^{-1}$] is given as

$$J_p = k_p(p_w - p_c) \tag{11}$$

where, k_p is the surface evaporation coefficient [$g \cdot cm^{-2} \cdot sec^{-1} \cdot mmHg^{-1}$], p_w the steam pressure at the surface of the mat sides [mmHg], and p_0 the steam pressure in environmental air [mmHg].

Eq.(11) can be expressed in terms of steam density as

$$J_\rho = k_\rho(\rho_w - \rho_0) \tag{12}$$

where, J_ρ is the steam flux [$g \cdot cm^{-2} \cdot sec^{-1}$] corresponding to J_p, k_ρ the surface evaporation coefficient of steam based on the steam density gradient [$cm \cdot sec^{-1}$], and ρ_w, ρ_0 the steam densities in $g \cdot cm^{-3}$ corresponding to the steam pressures p_w and p_0, respectively.

The initial condition is expressed as

$$\rho(r, 0) = \Omega(r) \tag{13}$$

where, $\rho(r, 0)$ is the steam density at the position r and at the time 0, $\Omega(r)$ is a known function.

The standard equation of the finite element method derived from Eq.(9) is expressed in the same way as that of conventional hotplaten pressing;

$$[K]\{\psi\} + [C]\{\partial\psi/\partial t\} = \{F\} \tag{14}$$

where, $\langle\psi\rangle$ the grid point vapor density vector for the whole elements,

$$[K] = \sum_e \left\{ \int_{V^e} k_\rho \left(\frac{\partial[N]^T}{\partial x}\frac{\partial[N]}{\partial x} + \frac{\partial[N]^T}{\partial y}\frac{\partial[N]}{\partial y} + \frac{\partial[N]^T}{\partial z}\frac{\partial[N]}{\partial z} \right) dV + \int_{S^e} k_\rho [N]^T [N] \, dS \right\}, \tag{15}$$

$$[C]=\sum_e\left\{\int_{V^e}[N]^T[N]\,dV\right\},\ \text{and} \tag{16}$$

$$[F]=\sum_e\left\{\int_{S^e}k_\rho\rho_0[N]^T\,dS\right\}. \tag{17}$$

Approximating the time term of Eq.(14) by the difference method, we obtain,

$$\left(\frac{1}{2}[K]+\frac{1}{\Delta t}[C]\right)\{\psi(t+\Delta t)\}=\left(\frac{-1}{2}[K]+\frac{1}{\Delta t}[C]\right)\{\psi(t)\}+\langle F\rangle \tag{18}$$

When $\langle\psi\rangle$ is known, the equation of the finite element method for the unsteady state diffusion problem can be solved step by step using Eq.(18).

It was found from experimental measurements that the temperature distribution in mat during hotpressing was symmetric with respect to the horizontal and vertical axes through the mat center. As shown in Figure 2.10 the mat section was divided into four parts by two axes, one of which was taken as the range for calculation. The range was divided by 20(lengthwise) x 50 rectangular elements.

2.2.2 Input data for the calculation of temperature behavior

The particle geometry and the compaction ratio (board density/particle density) are the important factors that influence the steam diffusion in the mat[88,89]. The effect of particle geometry on the gas permeability of mats is to be discussed in the next section.

When the particle size is 13 mm long, 1.6 mm wide, and 0.6 mm thick as given in the experiment of section 2.1.1 and steam is injected at the compaction ratio of 1.0, k in the vertical direction to the platen is 5.68 $g\cdot cm^{-1}\cdot atm^{-1}\cdot sec^{-1}$ [88]. As $\partial P/\partial\rho_s$ of saturated steam is 1,893 $g^{-1}\cdot cm^{-1}\cdot atm^{-1}$ from Eq.(7),

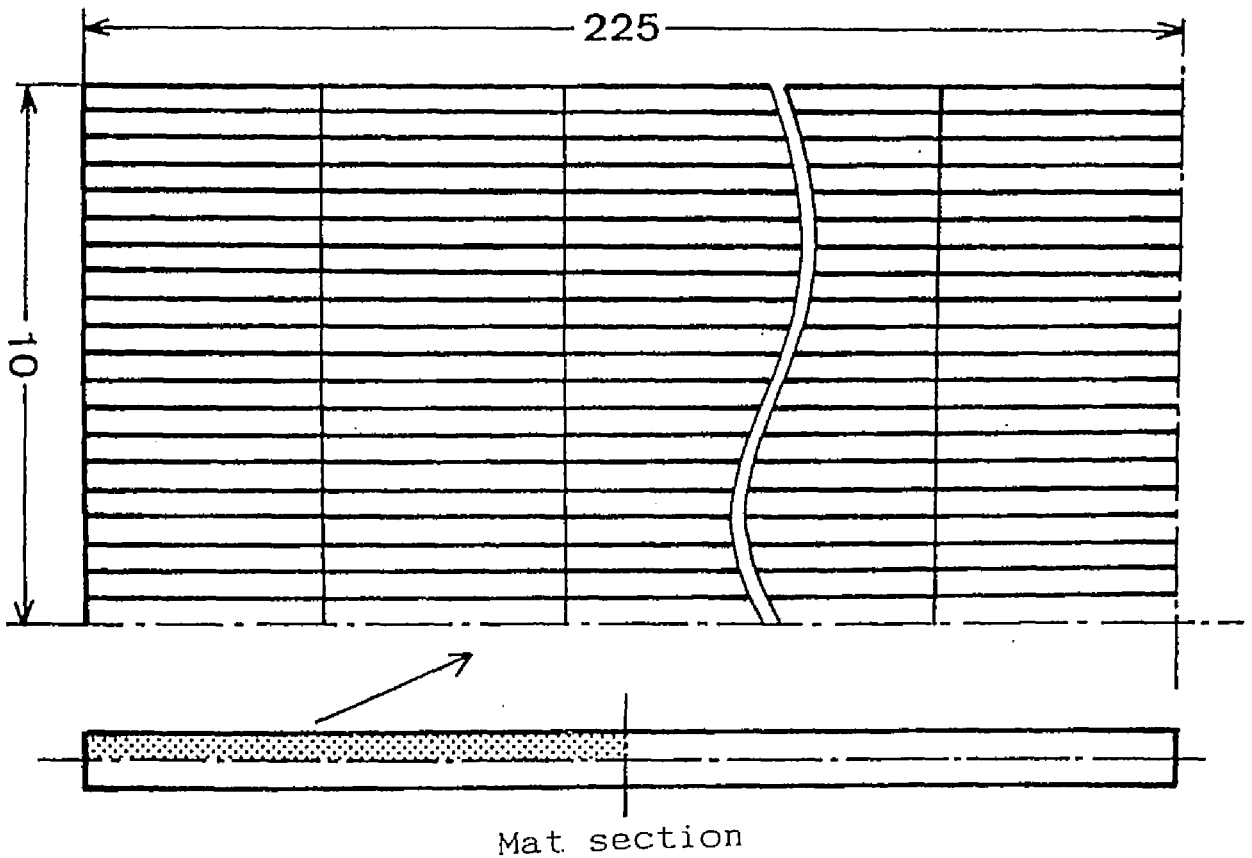

Fig.2.10 Typical elements division (in the case of a 20 mm thick mat)

k_p is calculated to be 10,753 cm^2/sec from Eq.(7).

The initial steam density is taken as 0 $g \cdot cm^{-3}$. The steam density at mat surfaces as the boundary condition is of 0.001081, 0.002101, and 0.003132 $g \cdot cm^{-3}$ corresponding to steam pressure of 2, 4, and 6 kgf/cm^2, respectively. The steam evaporation condition at mat sides is given in Eq.(12) where the surface evaporation coefficient based on the steam density gradient, k_p has a value of 1.434 $cm \cdot sec^{-1}$ [70].

The time increment for the calculation was 0.25 seconds. The factors and the levels of the numerical analysis on steam-injection pressing are summarized in Table 2.3. Two cases were analyzed to investigate the effect of the vertical density gradient of the mat on the temperature behavior of mat. One was given from the observed values for boards with average densities of 0.6 and 0.8 g/cm^3 and the other was for uniform density boards with densities of 0.3 and 0.4 g/cm^3.

Table 2.3 *The factors and levels of the numerical analysis in steam-injection*

Mat moisture content (%)	Mat density (g/cm^3)	Mat thickness (mm)	Equilibrium vapor pressure in injection (kg/cm^1)	Steam-injection time (sec)
0	0.3, 0.4* 0.6, 0.8**	10, 20, 40 60, 100	2, 4, 6	1, 3, 10, 30, 60

*Flat vertical density profile.

**Vertical density profile based on the data.

2.2.3 Numerical procedure

The program for analysis of the two dimensional problem on heat transfer[50] was improved so as to allow analysis of the

temperature distribution commonly in both hotpressing and steam-injection pressing. Figure 2.11 shows the flow chart of the FORTRAN program. The procedure is explained as follows:

1) First gridpoint co-ordinates and element numbers are input.

2) Before steam injection, the initial condition, the boundary conditions of the regulated mat surface temperature, and that of the heat outflow at the mat sides are input for the heat conduction analysis. The temperature $\Phi(t)$ is calculated from the finite element equation, which is continued to be solved until the time step immediately before the diffusion analysis. In the analysis with hotpressing, the heat conduction analysis is continued to the end of the pressing time, while in that with steam injection pressing all grid point values are initiated at this time step.

3) During steam-injection, the boundary condition of the regulated steam density at the mat surface and that of the steam evaporation from mat sides are input. The steam density $\psi(t)$ is calculated from the finite element equation obtained by these data. The equation which was substituted by the obtained $\psi(t)$ at the next time step is continued to be solved. The initial value is taken before $\psi(t)$ reaches the saturated steam density corresponding to the initial temperature. In output $\psi(t)$ is converted into $\Phi(t)$.

4) Immediately after stopping steam-injection, the boundary condition of regulated steam density at the mat surfaces is cancelled.

5) After a further 10 seconds at the time stopping steam injection, $\psi(t)$ which was obtained at the step 10 seconds after steam-injection is converted into Φ(t) and is put in as the initial values of the heat conduction equation. After the

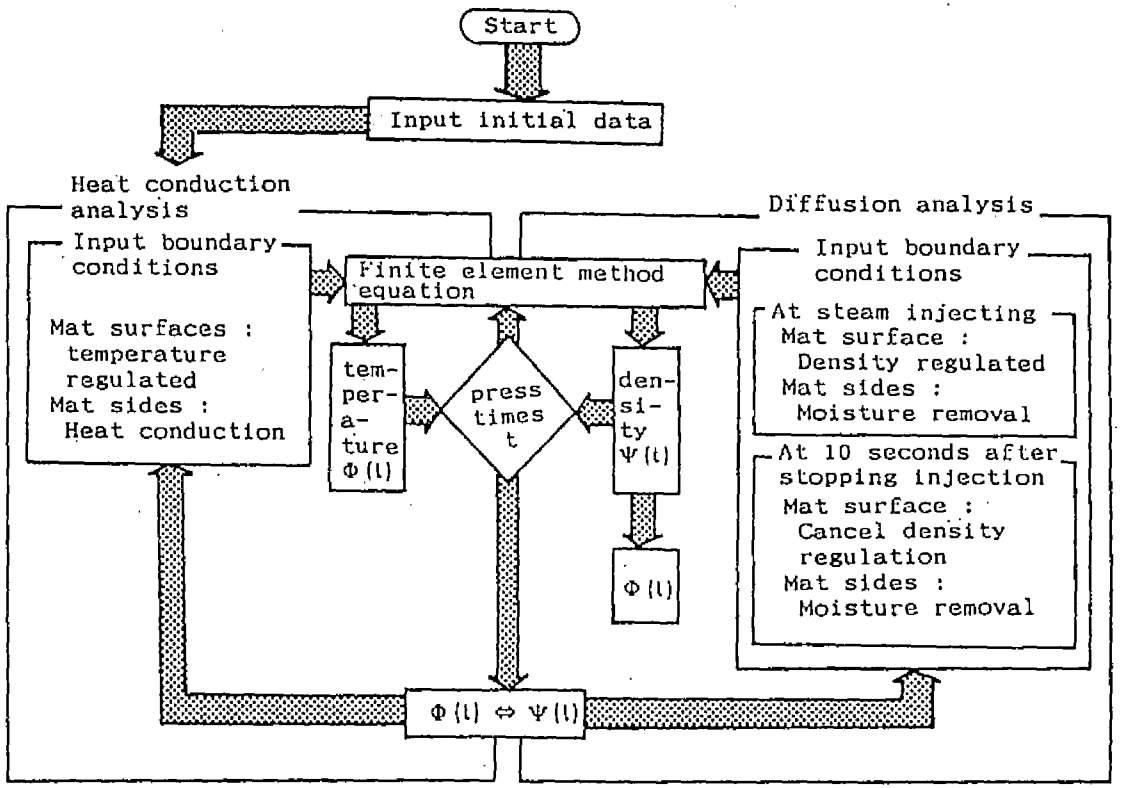

Fig.2.11 The program flow chart

boundary condition of the regulated temperature and that of the heat outflow from the mat sides are input the heat conduction analysis is continued to the end of the pressing time.

2.2.4 Results and discussion

Figure 2.12 shows a comparison of the experimental results with a calculated temperature distribution along the mat thickness in steam injection pressing. The calculated temperature distribution in the inner layers agrees relatively well with the observed values during steam injection. The experimental values at mat surfaces, however, are slightly below 160 ℃. In the experiment, temperature increase was delayed by the Teflon sheet (0.1 mm thick) inserted between mat surface and hotplaten, and the thermocouples sank a little into the mat during pressing. After steam-injection the experimental values for a 20 mm thick mat decreased by about 10 °C and then increased gradually again. It seems that the flux and influx of steam got out of balance after steam injection had been stopped, and that the condensed moisture in mat withdrew latent heat from the mat. The theoretical values of temperature increased after a slight decrease, because interaction between injected steam and particles is neglected in the program. Just after steam injection, the experimental temperature values increased slightly more than those of the theoretical values. This is probably due to the absorption heat generated in the wood particles.

Figure 2.13 shows the effect of steam pressure on the core temperature-time curves in steam-injection pressing. Core temperature immediately after steam injection rose with an increase of steam pressure for both 20-mm-and 40-mm-thick mats.

Figure 2.14 shows the calculated results of the effect of

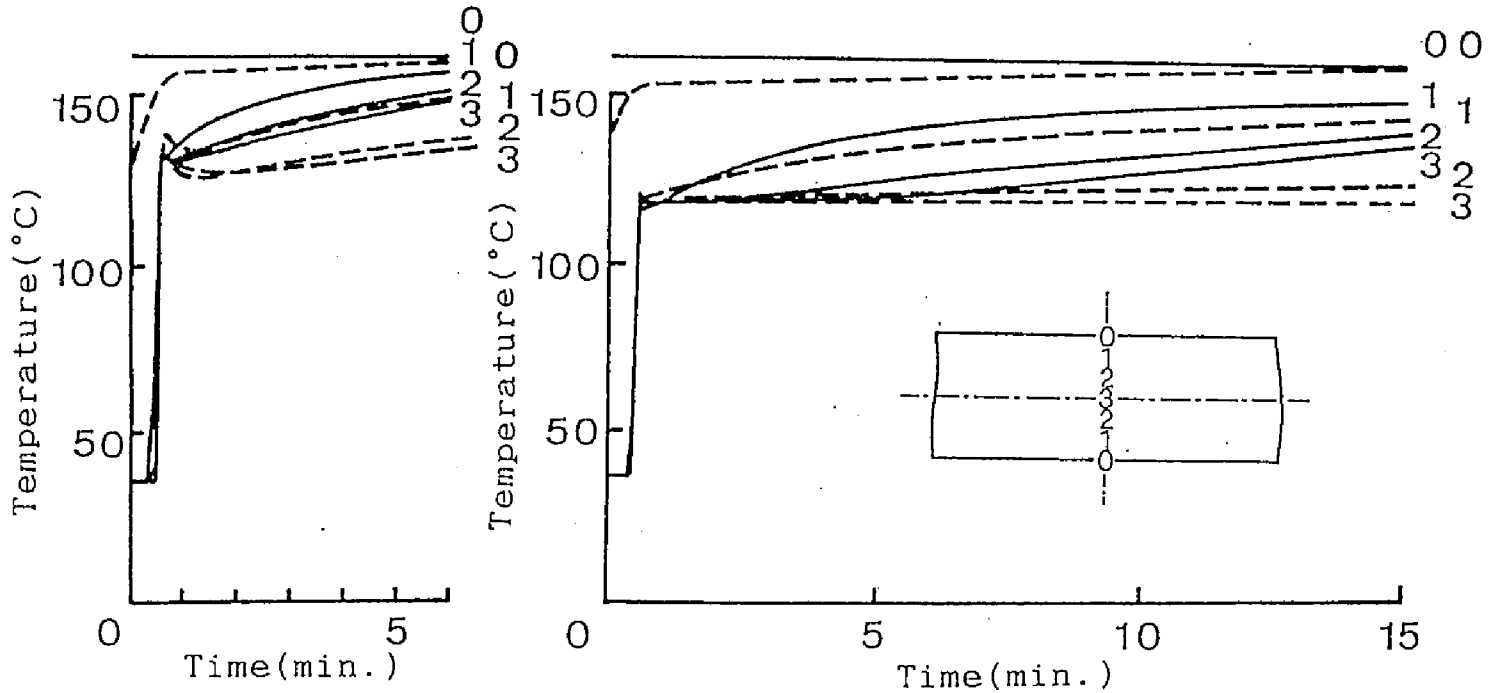

A) Mat density 0.4 g/cm³, Mat thickness 20 mm
B) Mat density 0.4 g/cm³, Mat thickness 40 mm

Fig.2.12 Comparison of experimental and calculated results of the temperature distribution along the mat thickness in steam-injection pressing
(Steam pressure 4 kgf/cm², Injection time 3 sec, Mat moisture content 0 %, ———— : calculated values, — — — —: experimental values(The positions of the thermocouples are 0, 1, 2, 3 from the top graph in each case))

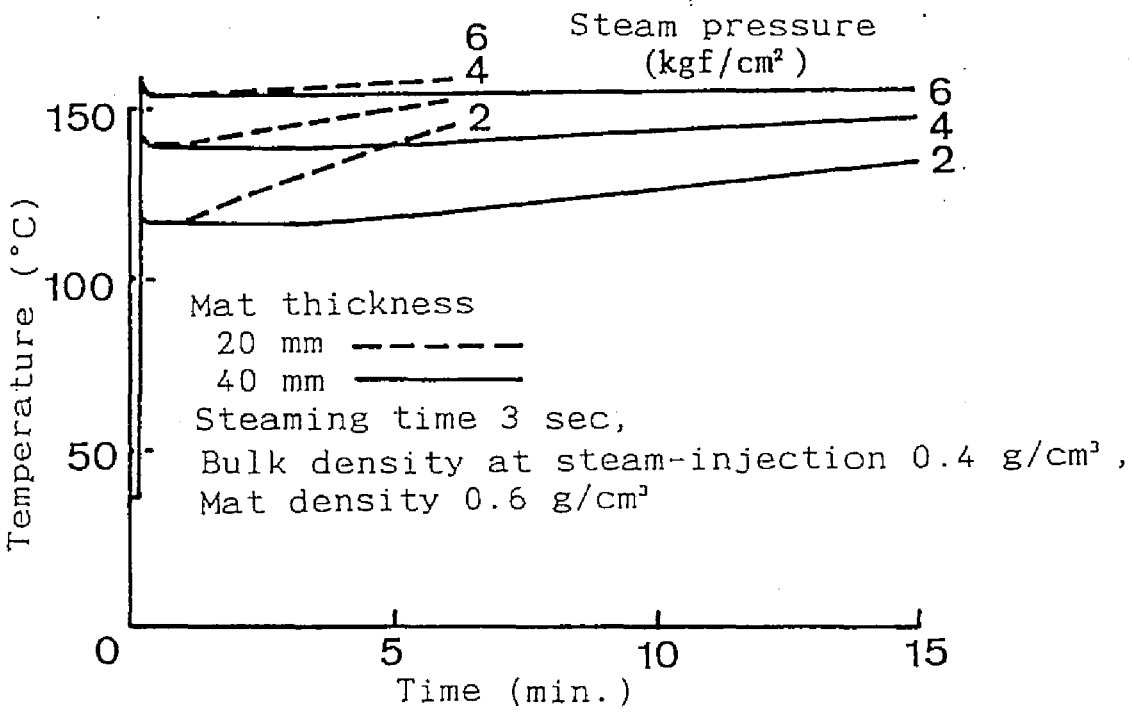

Fig.2.13 Calculated results of the effect of steam pressure on the core temperature curves in steam-injection pressing.

mat density on the core temperature curves in steam-injection pressing. The increase of mat density does not significantly affect the mat core temperature by steam-injection. The rate of temperature increase after steam injection, however, decreases slightly with an increase in mat density because of the increase in thermal capacity of the whole mat.

Figure 2.15 shows the calculated results of the relationship between mat thickness and steam injection time necessary for a mat core to reach 100 ℃. With increase in mat thickness the injection time required to reach 100 ℃ increases.

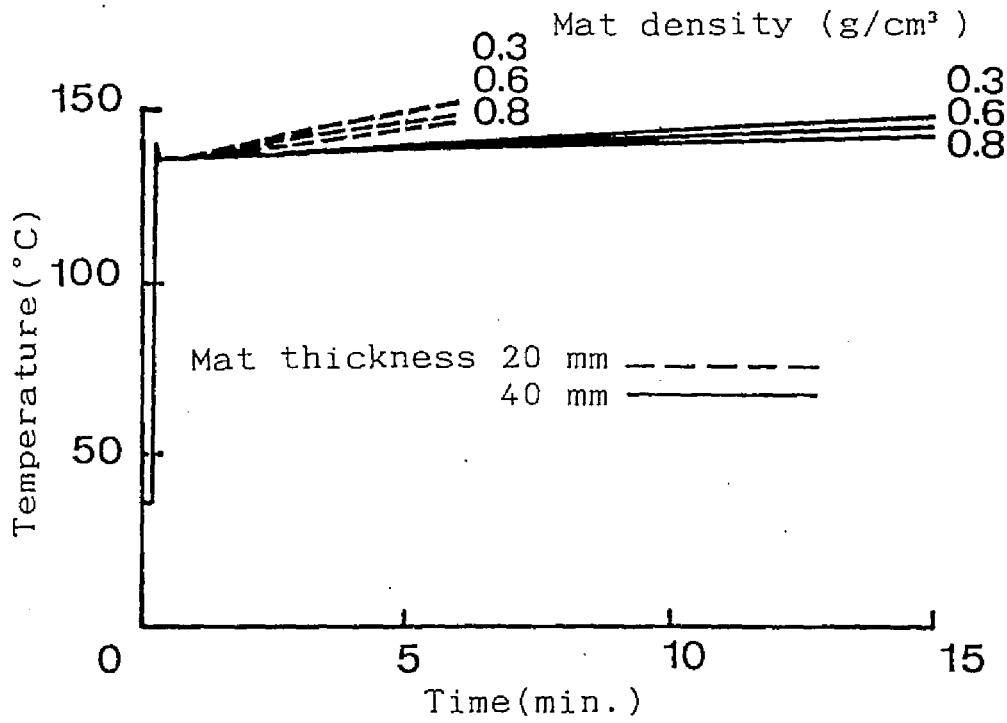

Fig.2.14 Calculated results of the effect of mat density on the core temperature in steam-injection pressing.

Note: Steam pressure = 4 kgf/cm², injection time = 3 sec, bulk density at steam injection = 0.4 g/cm³ (0.3 g/cm³ bulk density for 0.3 g/cm³ mat).

It is apparent that about 8 seconds steam injection is required for the core of 1000-cm-thick mat to reach 100 ℃, the temperature necessary for an isocyanate resin to cure within 1-2 minutes[37,61]. Therefore, the simulation predicts that such a thick board can be produced with a 2-3 minute press time by steam-injection pressing.

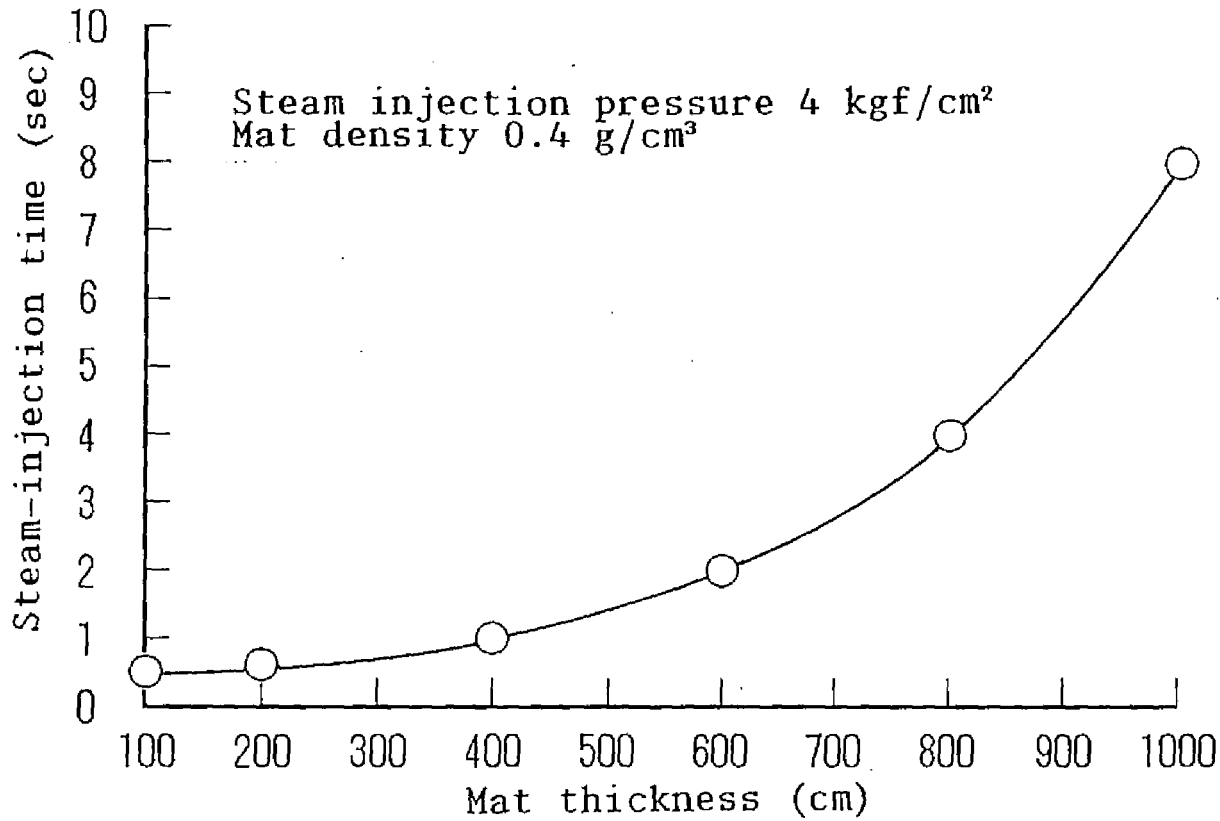

Fig.2.15 Calculated results of the relationship between mat thickness and steam-injection time necessary for mat core to reach 100 °C.

2.3 Summary

The temperature behavior of the particle mat during hot-pressing and steam-injection pressing was investigated under various conditions. With an increase of moisture content, the time necessary for the middle layer to reach 100 ℃ tended to shorten, whereas the time to maintain a constant temperature (about 100 °C) was prolonged in the case of hotpressing. The temperature in the middle layer of a mat with a higher moisture content in the face layers increased more than that of a mat with a uniform distribution of moisture content. In the case of steam-injection pressing, the temperature in the middle layer of the mats immediately increased to a specific degree decided by injection pressure and the characteristics of mats at the moment of steam-injection, and maintained a constant level during steam-injection. After stopping steam-injection, the temperature decreased a little, and then started to rise again. The rates of temperature increase in the middle layers of mats were independent of thickness, moisture content and density in the range of the experimental conditions.

The temperature distribution in particle mats during steam-injection pressing was numerically analyzed with the finite element method under various conditions. Calculated results agreed comparatively well with the observed results, which proved that the analytical theory was useful to predict the temperature behavior of particle mats during steam-injection pressing. In steam-injection pressing, with increases of mat thickness, the injection time necessary for raising core temperature up to 100 ℃ gradually increased. For example, it will take about 8 seconds for the core temperature of a 1000-cm-thick-mat, to reach 100 °C.

CHAPTER 3

STEAM DIFFUSION IN PARTICLE MAT DURING STEAM-INJECTION PRESSING

In the process of steam-injection pressing, it is very important to know the influence of the particle geometry on the steam diffusion because steam is the main medium to control the heat energy through the particle mat. The curing conditions of adhesives depend very much on how the steam diffuses in the mat. The compaction ratio (CR: board density / particle density) of particles and pressing conditions are considered as important factors that influence the diffusion of steam in the mat[58].

In the previous chapter, the mechanism of heat flow in the mat with stem-injection pressing was discussed and the optimum production conditions were determined. This chapter discusses the effects of particle geometry, CR, and pressing conditions of the steam-injection on the temperature behavior in the mat and the air permeability of the boards.

3.1 Effects of particle geometry on temperature behaviors in particle mats[68]

3.1.1 Experimental

Regulation of particles

A series of model particles of regulated sizes in three dimensions were prepared as follows: First, the boards with a thickness corresponding to the required particle width were cut from sawn lumber of Japanese red pine (*Pinus densiflora* Sieb. et Zucc.) with an air-dry density of 0.4 g/cm^3. Second, the boards with a width equal to a needed particle length were cut into blocks across the grain. Third, the blocks after having been soaked in water for a day were cut to a certain thickness

with a cross section disk planer.

Seven kinds of particle sizes, that is, the particle lengths (l) of 10, 20, 50, and 80 mm, widths (w) of 2 and 10 mm, and thicknesses (t) of 0.3, 0.6, and 0.9 mm, were prepared. The standard particle length, width, and thickness is 20 mm, 2 mm, and 0.3 mm, respectively. Dimensions of each particle were measured to calculate the mean and the standard deviation which are shown in Table 3.1. As the particles were prepared with strict control of particle sizes, the variations of coefficients were very small.

Table 3.1 Model particle configuration.

a. Prepared particles.

Particle No.	l (mm)	w (mm)	t (mm)	Particle No.	l (mm)	w (mm)	t (mm)
1	10	2	0.3	5	20	10	0.3
2	20	2	0.3	6	20	2	0.6
3	50	2	0.3	7	20	2	0.9
4	80	2	0.3				

b.Measurement of particle size.

l (mm) Target	l (mm) Measured	S.D.	C.V.	w (mm) Target	w (mm) Measured	S.D.	C.V. (%)	t (mm) Target	t (mm) Measured	S.D.	C.V. (%)
10	10.02	0.04	0.00	2	2.04	0.05	0.02	0.3	0.303	0.03	0.10
20	20.01	0.02	0.00	10	9.99	0.10	0.01	0.6	0.602	0.02	0.04
50	49.99	0.06	0.00					0.9	0.906	0.04	0.04
80	79.92	0.27	0.00								

Legend: l, w, and t : Particle length, width, and thickness, respectively.
S.D. and C.V.: Standard deviation and coefficient of varience, respectively.

Note: The number of particles measured in each configuration = 50-100 particles.

Temperature behaviors in mats

No binders were applied to the particles with the moisture content of 0 % for convenience. The temperature distribution in

the middle layer was measured by means of copper-constantan thermocouples with wire diameters of 0.2 mm connected to a porous glass-fiber reinforced teflon sheet that was inserted into the center layer. These were connected to a data processor via a data logger, and the temperature at each point was recorded at time intervals. Fig.3.1 shows the locations of each measuring point in the mat plane. The temperature at nineteen spots were measured. The error was estimated to be ± 0.5 °C.

For the steam-injection pressing, a set of 550 × 550 × 30 mm perforated plates were prepared to fit the surfaces of the hot-platens of the conventional hot-press. The upper and lower plates were perforated with a hundred and forty-four 2 mm-diameter holes drilled through half the depth of the plates with a 25 mm × 25 mm spacing pattern, which covered an area of 150 mm × 150 mm of each plate.

The temperature measurements started at the moment when pressure was applied to a particle mat. Steam was injected into the mat at a mat density of 0.2 and 0.4 g/cm³ for the target density of 0.4 g/cm³, and 0.2 and 0.6 g/cm³ for the target density of 0.6 g/cm³, for three seconds. The temperatures were recorded every two seconds. The initial steam pressure were 2, 4, and 6 kgf/cm²; upper and lower hot-platens were regulated at the same temperature of 160 °C, the mat size was 20 mm (t) × 200 mm × 200 mm, and the total pressing time was 3.5 min.

3.1.2 Results and Discussion

A uniform temperature distribution in the middle layer of the mat was observed in the steam-injection. As the mat plane was symmetric in two directions, the average of twelve spots in one-forth part of the whole plane is discussed in this paper. The temperature of two spots between the center and the surface

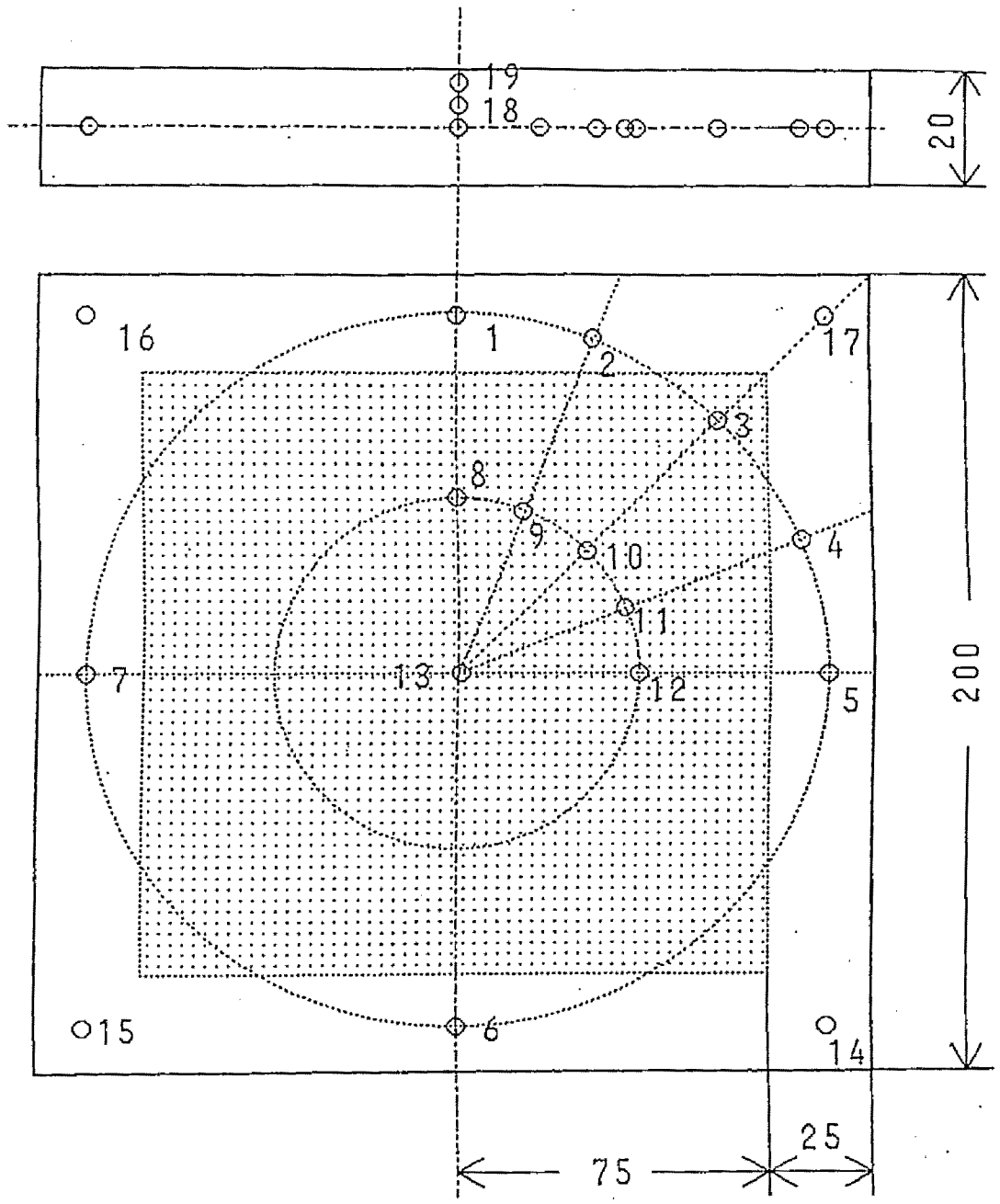

Fig.3.1 Location of thermocouples in mat.
Note: The mesh shows an area of steam perforations.

always started increasing earlier than the others. This behavior gave us a clue for deciding the start of steam-injection.

Fig. 3.2 shows the effects of particle lengths on the temperature behaviors in the middle layers. The rate of temperature increase after steam-injection becomes less at the length of 50 mm than for other lengths in the case of 2 mm wide particles. A remarkable difference was observed by changing the particle length in the case of 10 mm wide particles. The temperature increased more slowly with increases of particle lengths. It took more than three minutes to reach the temperature of 100 °C, that is, the temperature for isocyanate resin to cure in a minute. The resistance for steam to diffuse in the mat became greater with longer particles. The temperature behavior in the case of 80 mm long particles was the same as that in the mat of which the moisture content before pressing was 11 % [81]. This means that the steam did not reach the middle layer, and that the temperature increased by heat conduction.

Fig. 3.3 shows the effect of the particle thickness on the temperature behavior in the mat. The rate of the temperature increase is greater as the particle thickness increases after increasing more than 100 °C by steam-injection. The number of voids seen on the sides of the manufactured boards increased by increasing particle thicknesses, when the other two dimensions were constant. It seems that these voids have an influence on the rates of temperature increases.

Fig. 3.4 shows the effects of mat densities at injection on the temperature behaviors in the middle layers. In the case of 0.4 g/cm^3 density board, the temperature started increasing at the moment that steam was injected, whereas in 0.6 g/cm^3 density board, the start of temperature increase was delayed. In the latter, there was a time lag in the case of the 0.2 g/cm^3 mat

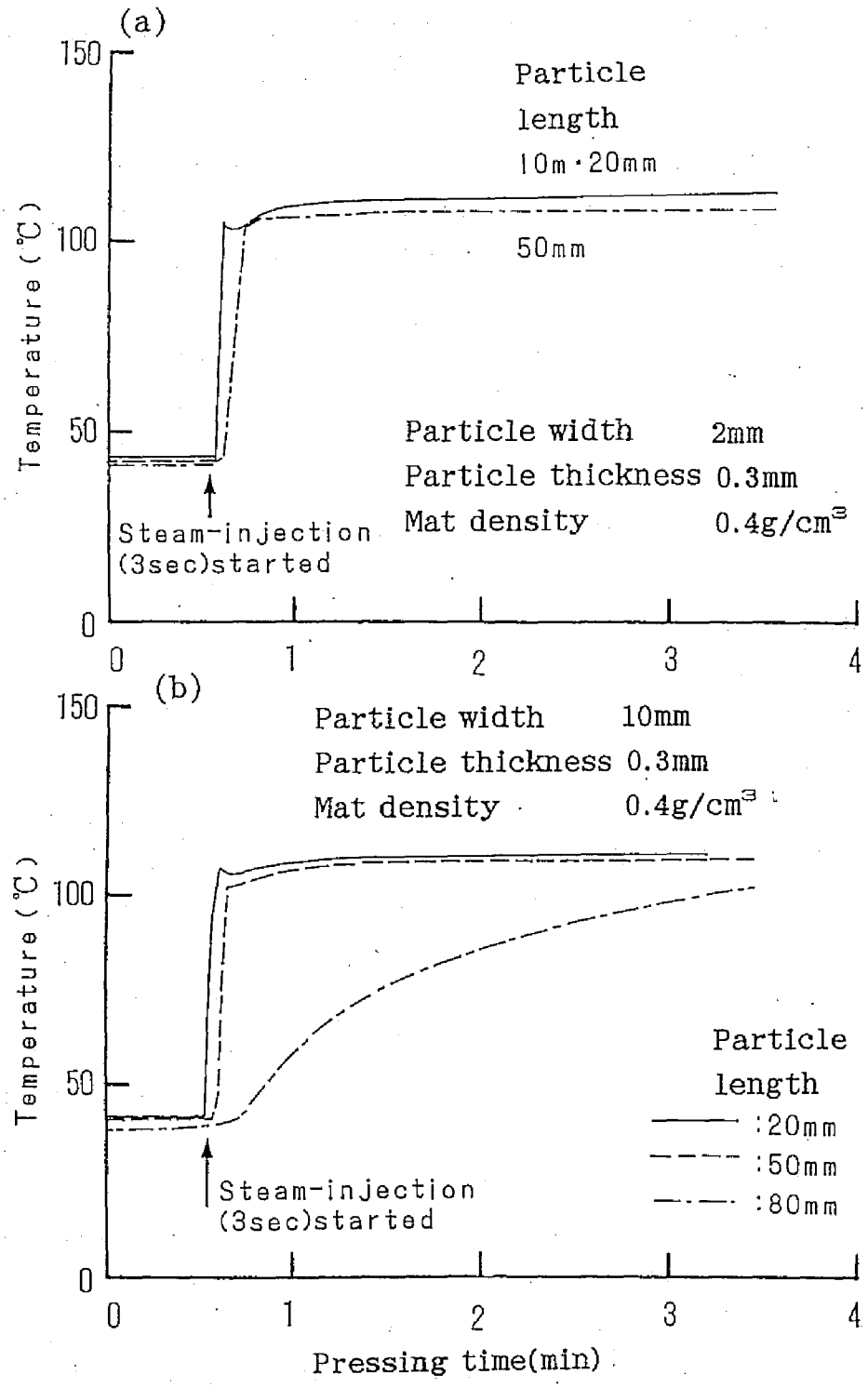

Fig.3.2 Effect of particle length on temperature behavior of mat core.

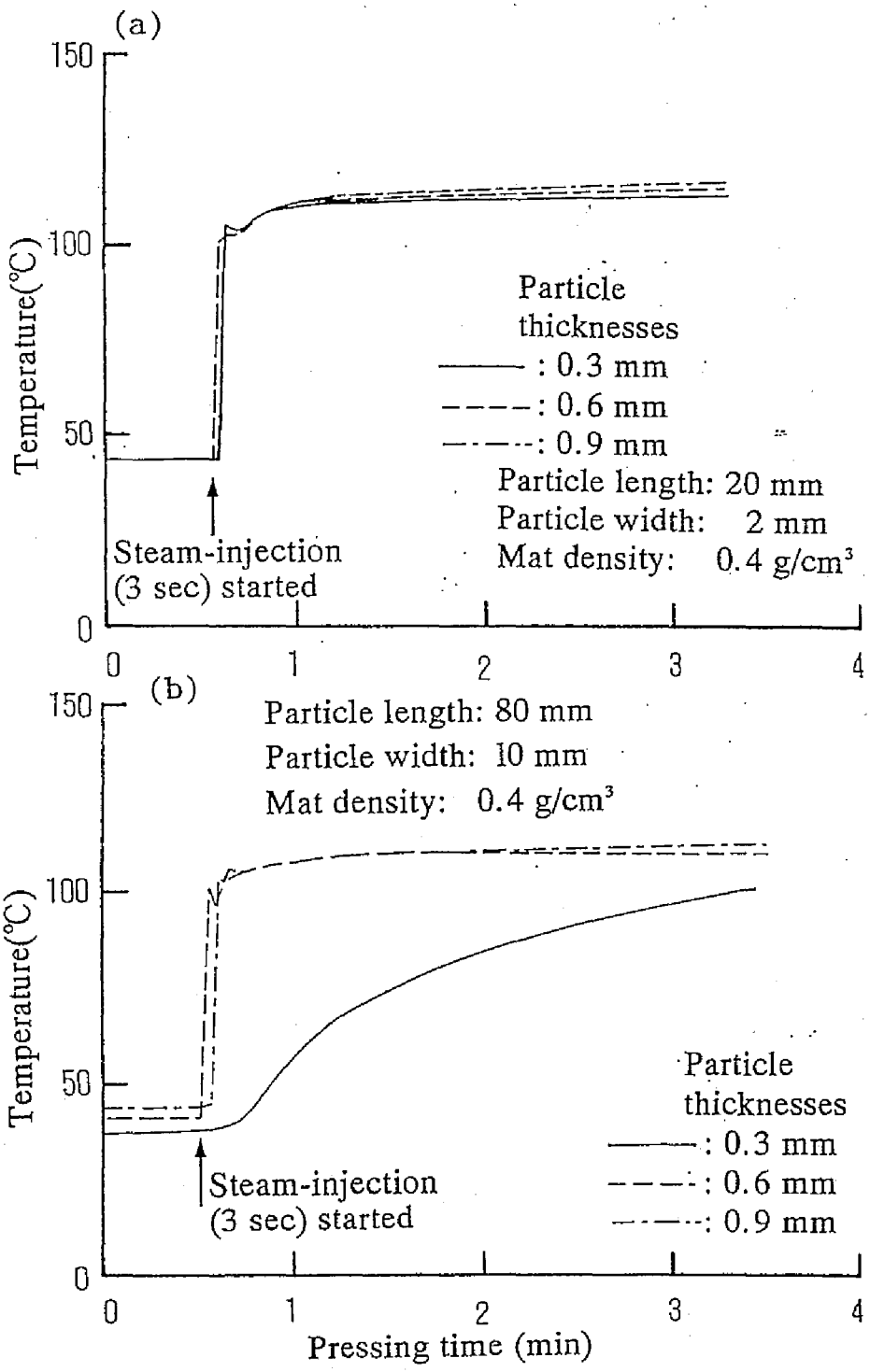

Fig.3.3 Effect of particle thicknesses on temperature behaviors of mat cores.

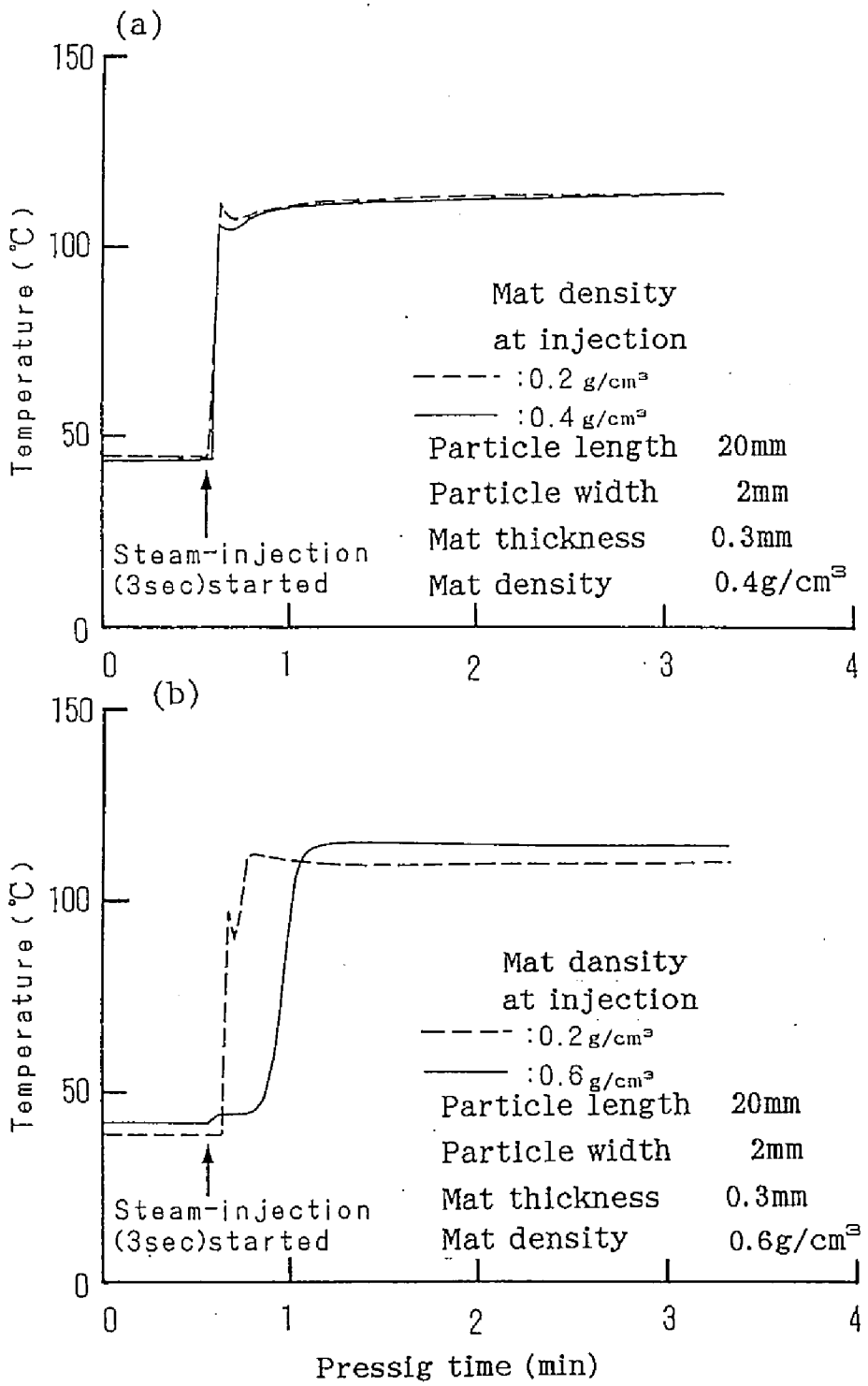

Fig.3.4 Effect of mat density at injection on temperature behavior of mat core.

density at injection. This may have been due to the fact that it is more difficult for steam to flow in a mat with a greater thickness in spite of the same mat density. It took about 15 seconds before the temperature in the middle layer started increasing when steam was injected at the mat density of 0.6 g/cm^3. The maximum temperature achieved by steam-injection was greater in the case of 0.6 g/cm^3 density board because of greater steam pressure in the mat.

The effect of the initial steam pressure also was examined. However, no apparent differences of temperature behaviors were seen in the range of 2 to 6 kgf/cm^2 initial steam pressure.

3.2 Effects of particle geometry on the gas permeabilities of boards[88)]

3.2.1 Experimental

Measurements of air permeabilities of boards

Under the same conditions as those of the temperature behavior experiment, two boards with dimensions of 10 x 340 x340 mm were produced for each level of particle geometry and pressing condition. That is, the mat density at injection was 0.2 and 0.4 g/cm^3 for the target density of 0.4 g/cm^3, and 0.2 and 0.6 g/cm^3 for that of 0.6 g/cm^3, the steam-injection time was three seconds, and the initial steam pressure were 2, 4, and 6 kgf/cm^2.

Adhesive used was an isocyanate compound resin, UL-4811 formulated by Gun-ei Kagaku Kogyo Co. Ltd. Acetone was added at 20 % based on resin solids to reduce the viscosity of the adhesive. The resin was sprayed on the particles (having a moisture content of 12 %) using a drum-type rotary blender by means of an airless gun. The resin content was 10 % of the resin

solids/dried particle weight. Hand-formed particle mats were pressed in a hotpress with the temperature of 160 °C. Both top and bottom surfaces of the particle mats were covered with porous glass-fiber reinforced Teflon sheets so as to prevent the mat from sticking to the platens. The total pressing time was 1.5 min.

The sample boards were conditioned for two weeks at 20 °C and 65 % RH, followed by the cutting of test specimens for use in measuring the air permeability.

Fig. 3.5 shows the system[71] for measuring air permeability. The specimens were rectangular blocks, 100 x 10 x 10 mm, for measuring the air permeability in the direction horizontal to the heat platens and three to five piled cubes with each having a size of 10 x 10 x 10 mm for measuring in a vertical direction. Before starting the measurements, the sides of each specimen were covered with plastic film. Then, each specimen was inserted into a plastic tube to prevent the leakage of air. Air was flowed through the specimens from the end by a microfeeder at the flow rate of 4.80×10^{-3} to 1.78×10^{-2} cm^3/s, and the pressure was measured at a steady state. The permeability was estimated by the following equation of Darcy's law :

$$k_p = (Q \cdot P \cdot L)/(\Delta P \cdot A \cdot \bar{P}) \qquad (19)$$

where, k_p: air permeability, cm^3 (air)/cm·atm·sec,

Q: volumetric flow rate, cm^3/sec,

P: air pressure, atm,

L: length of the specimen in the flow direction, cm,

ΔP: air pressure difference between the specimen edges, atm,

A: cross-sectional area of the specimen, cm^2,

$\bar{P}$: average air pressure of the specimen, atm.

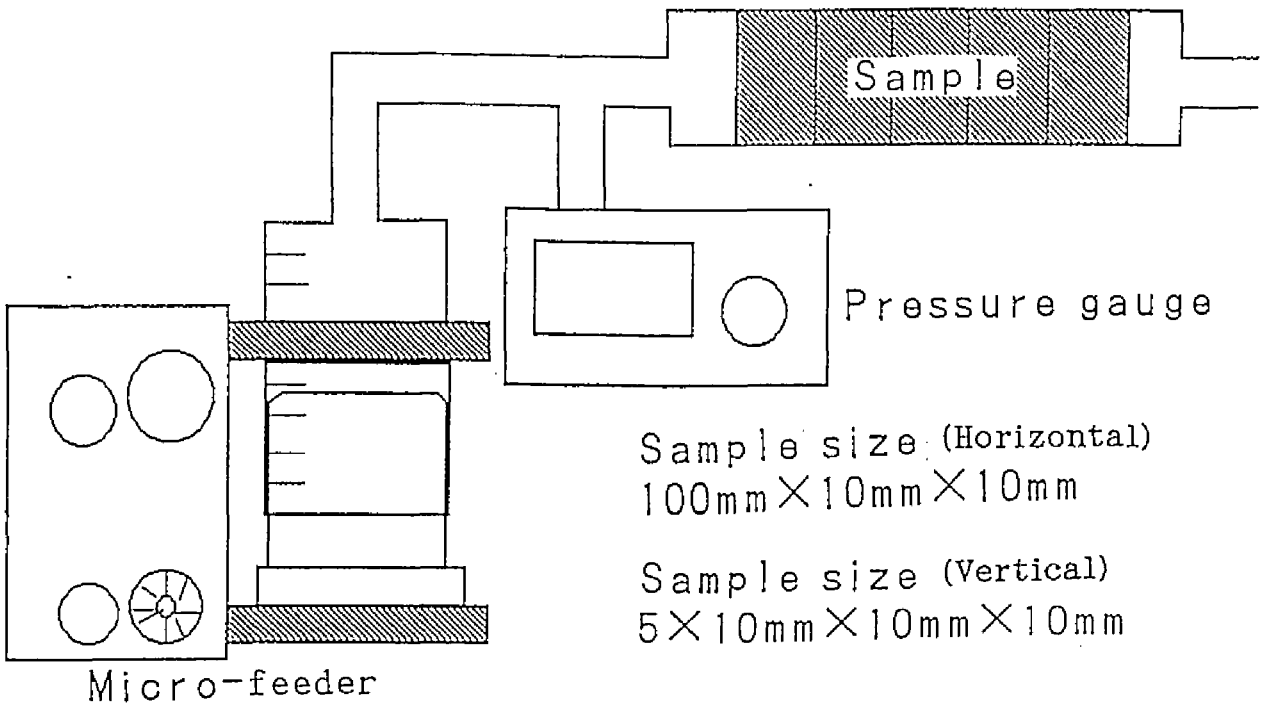

Fig.3.5 System for measuring air permeability.

3.2.2 Results and discussion

Air permeabilities of boards

Fig. 3.6 shows the effects of particle lengths on the air permeability. The air permeability decreased with increases of the particle lengths when the particle thicknesses and widths were constant. It decreased as well with increases of the widths at the same length. The air permeability in the horizontal direction was always greater than in the vertical direction. Fig. 3.7 shows the effects of the particle thicknesses on the air permeabilities. The air permeabilities of both horizontal and vertical directions tended to increase with increases of the particle thicknesses.

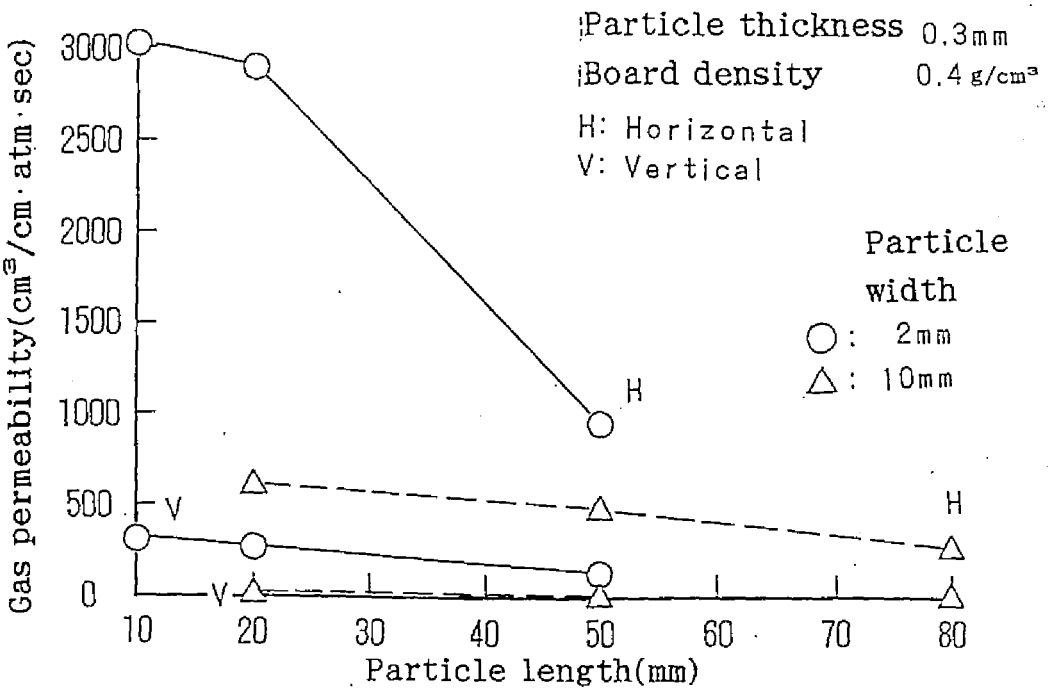

Fig.3.6 Effect of particle length on gas permeability of boards.

These results of the air permeabilities of boards well ex-

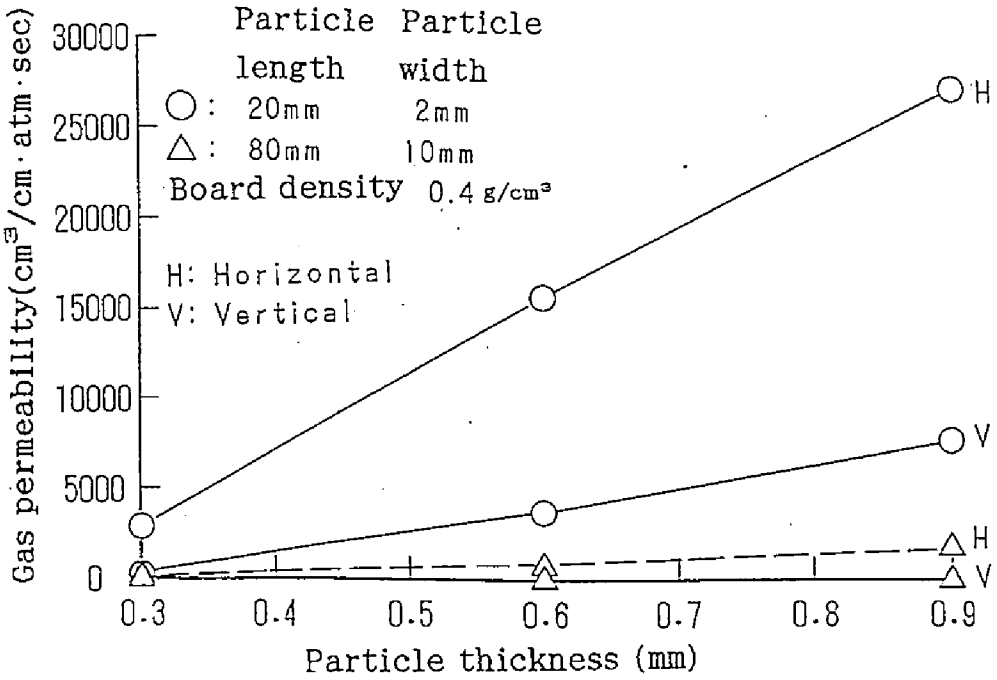

Fig.3.7 Effect of particle thickness on gas permeability of boards.

plains those of the experiment on temperature behaviors through the particle mats during steam pressing.

Fig. 3.8 shows the effect of the mat densities at injection on the air permeabilities of manufactured boards. The air permeabilities of boards were independent of the mat densities at injection. This may have been due to the fact that permanent paths are not formed by steam injection and that the injected steam diffuses through the paths between the particles which already existed because if any paths had been formed by the steam-injection, there should have been influences on the air permeability of the boards produced by changing the injection timing.

Fig. 3.9 shows the effects of board densities on air permeabilities. The greater the board density, the less the air

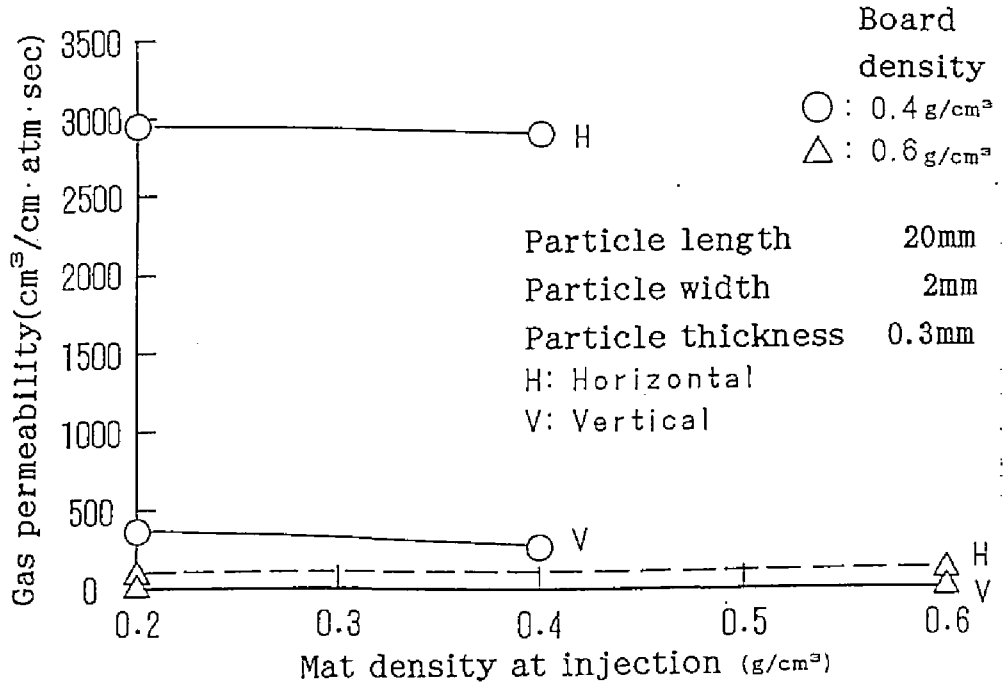

Fig.3.8 Effect of mat density at injection on gas permeability of boards.

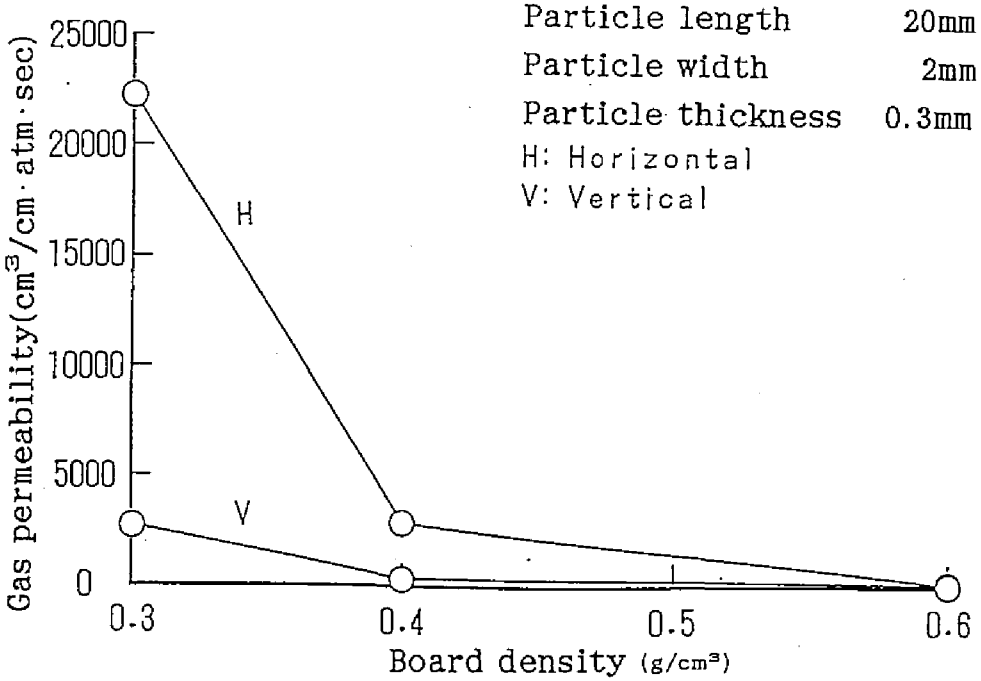

Fig.3.9 Effect of board density on gas permeability of boards.

permeability. The air permeability was remarkably greater at the CR of 0.75. This may have been due to the fact that the resistances against the steam flows in the mats become less because the voids among particles increased with decreases of CRs. As the range of the vertical line is greater in the figure, the air permeability for the horizontal direction appears to be equal to that for the vertical direction at a 0.6 g/cm^3 board density; however, in fact, the former was about 25 times as great as the latter. Boards with a greater CR always have lower air permeabilities. The ratios of air permeabilities in horizontal and in vertical directions are 3 - 400, depending on the particle sizes and CRs.

Fig. 3.10 shows the effects of the initial steam pressures on the air permeabilities of boards. With increases of the steam pressures, the air permeabilities of boards in a horizontal direction decrease, whereas that in a vertical one increase. Thus the difference of the permeabilities in the two directions decrease. This may be due to the fact that wood particles deform non-elastically by the injected steam, and the contact area of each particle becomes greater. This result suggests the possibility of developing products with more uniform and with greater dimensional stabilities by injecting steam with greater pressures.

Multiple regression analysis [72]

The influences of the particle geometry and the timing of the injection on air permeability were analyzed by multiple regression analysis. The program used was "micro-CDA" developed by Professor T. Haga. In this program, degrees of freedom double adjusted coefficients of determination, are used for the standard of the selection of variables, and a stepwise regression

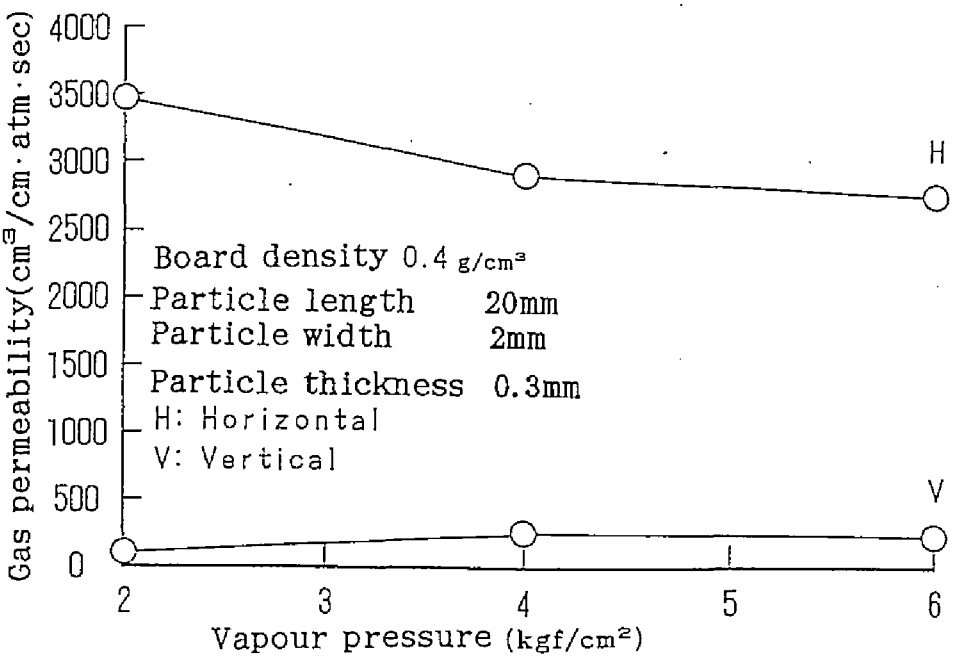

Fig.3.10 Effect of steam-injection pressure on gas permeability of boards.

procedure also is used. The obtained equation by this analysis is as follows:

$$k_{ph} = 1,110\,l - 4,540\,w + 531,450\,t + 700\,w \cdot l - 63,300\,l \cdot t + 1.1 \exp(15.42 - 7.32\,CR) - 14,252 \quad (20)$$

$$k_{pv} = 590\,l - 260\,w + 163,460\,t - 20,300\,l \cdot t + 1.14 \exp(13.87 - 8.12\,CR) - 4,915 \quad (21)$$

where k_{ph}: gas permeability in the horizontal direction [cm³ (air)· cm^{-1}·atm^{-1}·sec^{-1}], k_{pv}: gas permeability in the vertical direction [cm³ (air)·cm^{-1}·atm^{-1}·sec^{-1}], l: particle length [cm], w: particle width [cm], t: particle thickness [cm], and CR: compaction ratio.

When a linear regression equation with only variables of length, width, and thickness of particles, the degrees of freedom double adjusted coefficients of determination are less for both directions. By adding the predictor variables of $w \cdot l$,

$l \cdot t$, and CR to Eq. (20), and $l \cdot t$ and CR to Eq. (21), each of the degrees of freedom double adjusted coefficients of determination show the large values of 99.6 % and 99.7 %, respectively. Thus, the diffusion phenomena of air in mats can be interpreted as follows: air, not only move linearly, but also diffuse in two dimensions through between the particle surfaces. It may be concluded that the steam diffusion in the whole mat is the phenomena that is resulted from the repeat of the diffusion among particle surfaces in two dimensions.

Eqs. (20) and (21) are valid only under the conditions of this experiment. However, it is important to predict the air permeabilities of boards in extreme conditions in developing new materials. When both the equations are valid out of the range of this experiment and each material is very small, such as powder, then

$$k_{ph} < 0 \quad (l,\ w,\ t \to 0),$$
$$k_{pv} < 0 \quad (l,\ w,\ t \to 0).$$

On the other hand, when t is a constant, and l and w are greater such as in sawn boards, it is obvious from the signs of Eqs. (20) and (21) that the next relationships should be held:

$$k_{ph} < 0,$$
$$k_{pv} < 0.$$

Therefore, it is predicted that the air permeabilities approach 0 in either case of much smaller or greater particle sizes.

3.3 Summary

Each of seven types of Japanese red pine particles with different dimensions, strictly controlled for length, width, and thickness, was prepared in order to investigate the temperature behavior in the mat, and the air permeability of the boards with

specific gravities of 0.30-0.60. The variables influencing the temperature behavior in the mat by steam-injection press is directly related to the air permeability of mats. The air permeability of the boards in the horizontal direction to the heat platen is always higher than in the vertical direction. A functional equation with a higher coefficient of determination that explains the air permeability is obtained by a multiple regression analysis. It is inferred that the temperature increase in the mat result from the repetition of the steam diffusion among particles in two dimensions.

CHAPTER 4

PHYSICAL AND MECHANICAL PROPERTIES OF PARTICLEBOARD PRODUCED BY STEAM-INJECTION PRESSING

In the production of boards with the steam-injection pressing, the production factors auch as injection time, injection timing, pressing time, and the way how steam diffuse in the mat are important because they decide the properties of final products.

In the previous chapter, the mechanism of heat flow in the mat was discussed and the effects of particle geometry, CR, and pressing conditions of the steam-injection on the temperature behaviors in the mat and the air permeabilities of the boards.

In this chapter, firstly the effect of injection timing and injection time on physical properties of boards are examined. Secondly, 20-mm-thick isocyanate bonded particleboards were manufactured with various total press time under the obtained conditions and then the effect of total press time on physical properties of boards were examined. Finally, the physical and mechanical properties of boards produced with various particle size and pressing conditions.

4.1 Effect of steam-injection time and timing on board properties[73)]

4.1.1 Experimental

Raw materials used were Seraya (Shorea spp.) end-logs with an air dry density of 0.4 g/cm^3. Chips of the materials prepared by drum chipper were converted into flake-type particles with a knife-ring flaker (Pallmann PZ-8). The average dimensions of particles were 9.1 mm long, 0.28 mm thick and 5.7 mm long, 0.38

mm thick for the experiment on steam-injection time and for that on injection timing, respectively. One half part of the particles were dried with a vacuum dryer to about 0 % moisture content for steam-injection pressing, in order to investigate only the influence of injected steam and the remainder was conditioned to 11 % moisture content for conventional pressing.

Resin binder used was an isocyanate compound (IC) adhesive, UL-4800, formulated by Gun-ei Kagaku Kogyo Co. Ltd. The resin content level was ten percent of resin solid, based on oven-dry weight of particles. To obtain a suitable viscosity of adhesive for spraying, acetone was added to the IC resin at 20 percent based on the weight of resin solids. The resin was sprayed on the particles in a drum-type rotary blender by means of an airless gun. Hand-formed particle mats were pressed at 160 °C. Both upper and lower surfaces of the mat were covered with teflon coated glass-fiber nets to prevent the mat from sticking to the platens. Target board densities in an air-dry condition were 0.4 and 0.6 g/cm^3, and the dimensions of the boards were 500 x 450 x 20 mm.

In the experiment on the effect of steam-injection time, the target steam pressure was 6 kgf/cm^2 (160 °C) with an effective steam pressure of 4 kgf/cm^2 (140 °C). Steam-injection time was varied at 3, 10, and 30 sec. Steam was injected 30 sec after the start of press pressure build-up. The total pressing-times were 3.5 and 5.5 min for steam injected- and conventional pressed-board (no steam-injection), respectively.

In the experiment of steam-injection timing, steam was injected in the bulk densities of 0.3 and 0.4 g/cm^3 for board density of 0.4 g/cm^3, and 0.3, 0.4, 0.5, and 0.6 g/cm^3 for board density of 0.6 g/cm^3. Steam-injection time was 3 sec with an effective steam pressure of 4 kgf/cm^2. Total press times were 3

minutes for all boards.

Specimens cut from the above boards were tested after conditioning for 2 weeks at 20 °C and 65 % relative humidity (RH). Modulus of elasticity (MOE) and modulus of rupture (MOR) both in air-dry and wet conditions, internal bond strength (IB), screw withdrawal resistance (SW) in air-dry condition and thickness swelling (TS) after a 24-hour water immersion were measured according to Japanese Industrial Standard (JIS) A 5908. For the wet treatment in the bending test the specimens were boiled for two hours and then immersed in water for one hour at a room temperature. Density distributions across thickness were determined by measuring weight and dimensions of specimens at each of sanding from the surface to core.

4.1.2 Results and Discussion

Effect of steam-injection time

Density profiles across thickness of boards produced by conventional and steam-injection pressing are shown in Figure 4.1. From the Fig. 4.1, it can be understood that different density distributions across board thickness were produced by conventional and by steam-injection pressing; In conventional pressing, the density distribution across board thickness showed a "U"-shaped distribution with higher density layers near the both surfaces and a low-density layer in the core. In steam-injection pressing, however, this distribution was rather uniform. In the case of steam-injection pressing, steam was used as a medium of heat transfer and it diffuses through the particle mat much faster than heat conduction. Consequently, temperature in all parts of particle mats suddenly increased in the very short time[61,65], and uniform plasticization through

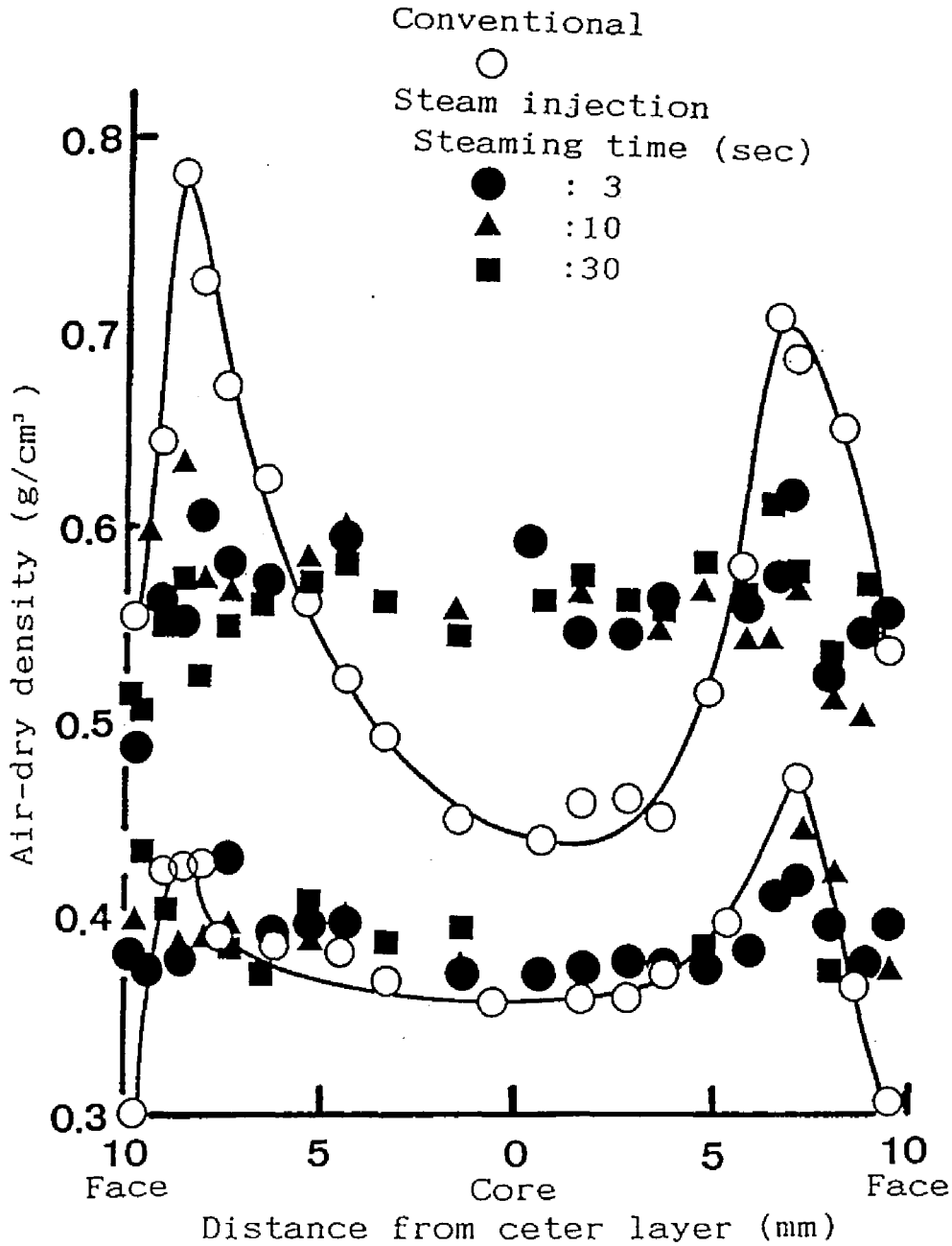

Fig.4.1 Density profiles through the thickness of boards

the particle mat occurred under high steam pressure. Wood particles remarkably plasticize under an unsteady state of both moisture and heat.

The effect of steam-injection time on density distribution across board thickness was not significant for 20 mm thick steam-injection pressed-board. This proves that 3-second-steam-injection gives the uniform plasticization of the whole particle mat.

In the case of conventional pressing, the difference of density between surface and core layers of particleboards with a density of 0.6 g/cm^3 is greater than that of 0.4 g/cm^3. This uniform density distribution of steam-injection pressed boards across thickness will give certain improvement of IB and dimensional stability, but a little decline in bending properties, as described in the following paragraph.

Figure 4.2 shows the effect of steam-injection time on MOE and MOR of boards under both dry and wet conditions. The MOE and the MOR of steam-injection pressed boards with a density of 0.6 g/cm^3 showed a little lower values than those of conventionally pressed boards. This can be explained by the difference in density distribution across board thickness. Bending properties of particleboard depend mostly on stiffness and strength of surface layers. Boards produced by conventional pressing have dense surface layers, which was more favorable for bending properties than boards with homogeneous density profile produced by steam-injection pressing. The effects of steam-injection time on MOE and MOR were, however, not significant for both board densities of 0.4 and 0.6 g/cm^3. The bending strength of boards with a density of 0.4 g/cm^3 showed almost the same value as those of boards produced by conventional pressing in the same target density.

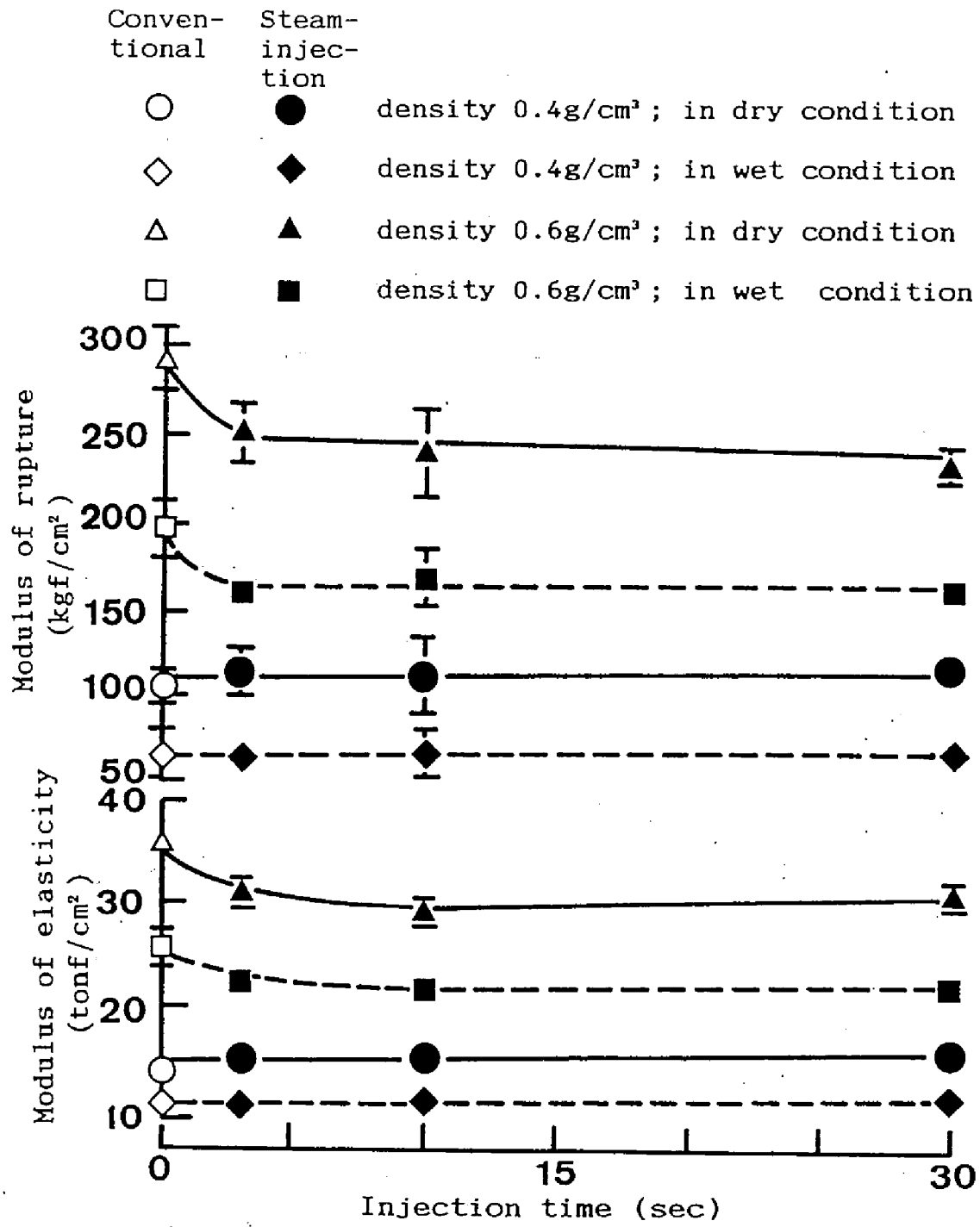

Fig.4.2 Relationships between steam-injection time and modulus of elasticity and modulus of rupture in dry and wet condition.

Legend:

The ranges of the mean values show 95% confidence intervals.

Furthermore, the figure suggests that a board with a thickness of 20 mm can be produced with very short steam-injection as 3 sec; namely, 3 sec steam-injection can raise the core temperature of particle mat to enough level for curing adhesive[11], as predicted in Fig. 2.18.

The relationship between steam-injection time and internal bond strength (IB) is shown in Fig. 4.3. The IB value of particleboards with a density 0.6 g/cm^3 produced by steam-injection pressing were about 20 kgf/cm^2, that is, 2 times greater than that of particleboards produced by conventional pressing. Furthermore, IB values for boards with a density of 0.4 g/cm^3 produced by steam-injection pressing showed also a little higher than that of boards produced by conventional pressing. A linear correlation between IB and the density in the core layer (which is usually lower than in the surfaces in hot-platen pressed boards) has been found[13]. The results obtained in this experiment corresponded with the above mentioned report, since the density in the core of particleboard produced by steam-injection pressing is always higher than that of boards produced by conventional pressing.

In the range of this experiment, the screw withdrawal resistance (SW) of particleboards produced by steam-injection pressing did not depend on steam-injection time. The SW values of 31 and 72 kgf for board densities of 0.4 and 0.6 g/cm^3, respectively, were almost the same as those of boards produced by conventional pressing.

The relationship between steam-injection time and thickness swelling (TS) is shown in Figure 4.4. Similar TS values were observed in steam-injection pressed boards and hot-pressed boards for a density of 0.4 g/cm^3. On the other hand, the improvement of the dimensional stability was observed on steam-

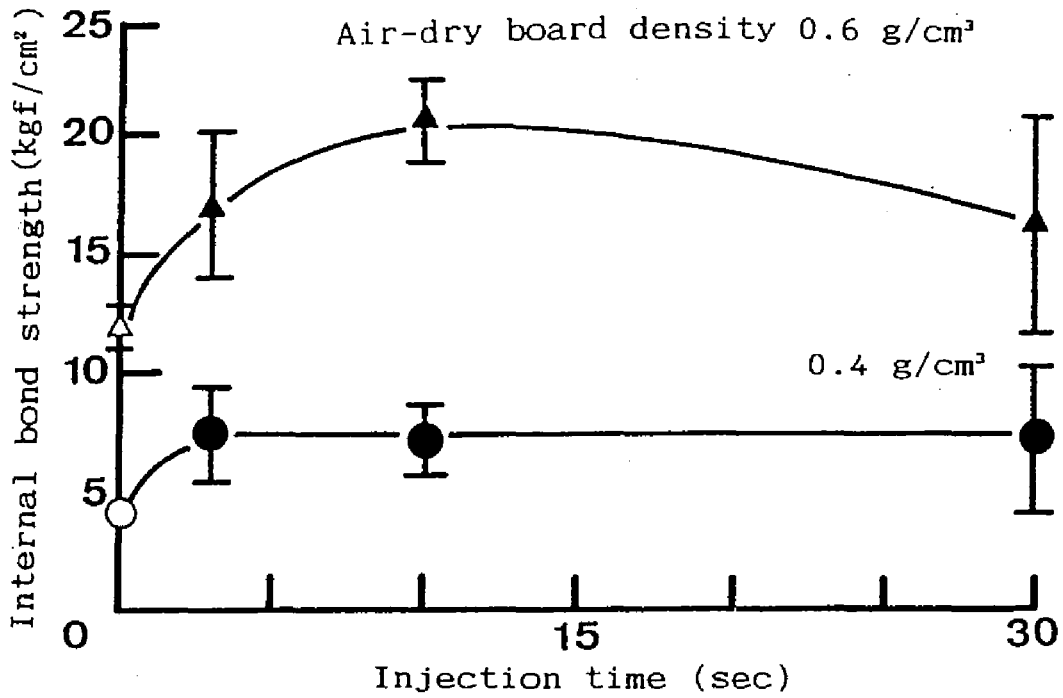

Fig.4.3 Relationships between steam-injection time and internal bond strength.

Legend: ○, △ : Conventional; ●, ▲ : Steam injection. The ranges of the mean value show 95% confidence intervals.

injection pressed boards with a density of 0.6 g/cm³ when steam-injection time was more than 10 sec. Thickness recovery of the dense surface layer formed during hot-pressing process seems to have greater influence on the TS[3,13,14]. In other words, the steam-injection pressed boards has the uniform density distribution across board thickness and results in better dimensional stability. High-pressure steam-treatment, also helps the relaxization of the internal stress which was built up in compressed particles during pressing[36]. As a result, steam-injection pressed particleboards have better dimensional stability than conventional boards, especially in high density range. Similar trend was observed in the accelerated aging test

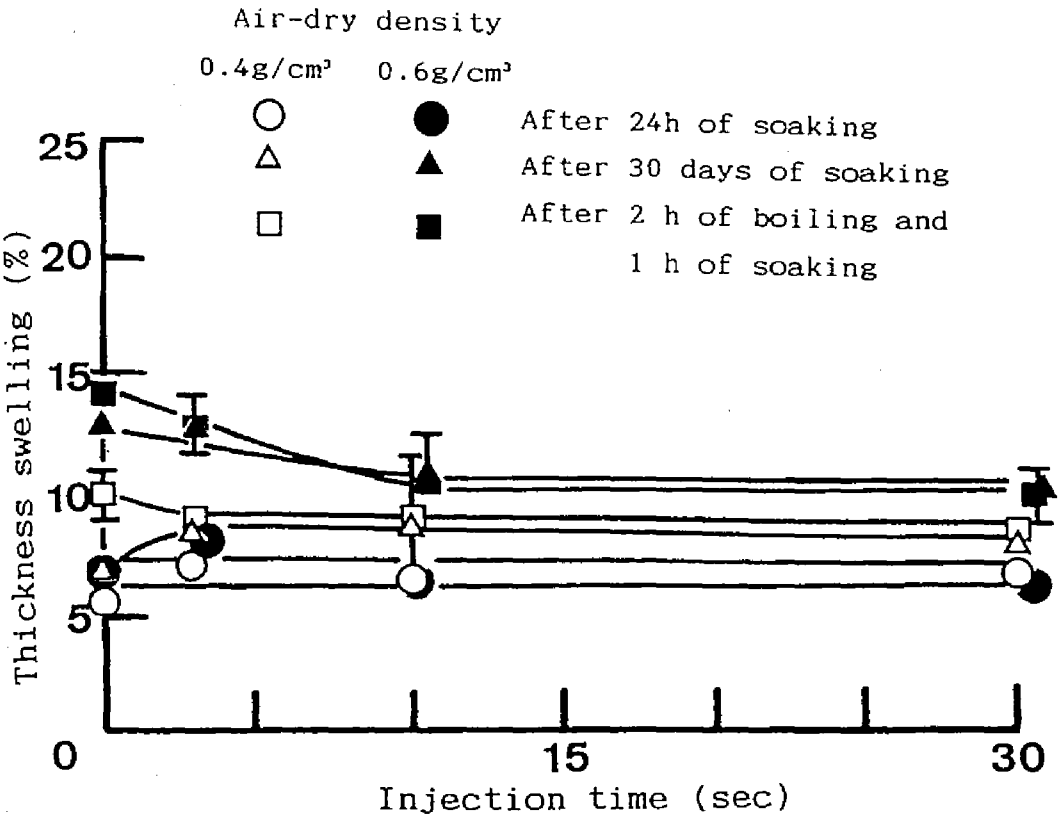

Fig.4.4 Relationships between steam-injection time and thickness swelling.

with 2-hour boiling or in 30-day water immersion.

Effect of steam-injection timing

The effect of steam-injection timing on MOE and MOR under wet and dry conditions is shown in Fig. 4.5. The effect of steam-injection timing on bending properties was not significant for board density of 0.4 g/cm³ but was significant for board density of 0.6 g/cm³. The MOE and the MOR values increased with delayed steam-injection timing. This corresponds with the tendency that delaying steam-injection timing forms surface layers with higher density.

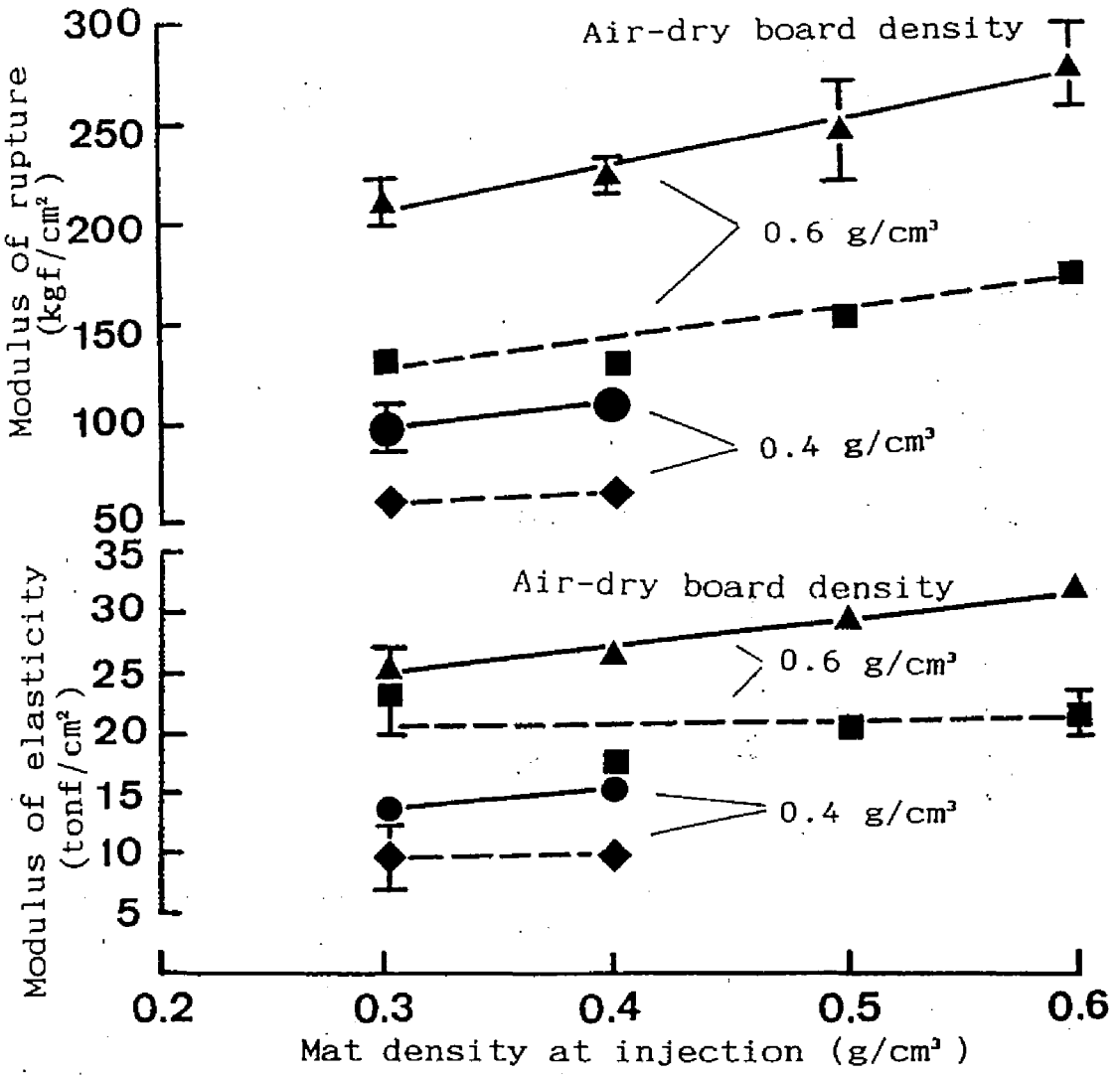

Fig.4.5 Relationships between mat density at steam-injection and modulus of elasticity and modulus of rupture in dry and wet condition.

Legend: ●, ▲ : in dry condition; ■, ◆ : in wet condition. The ranges of the mean value show 95% confidence intervals.

Figure 4.6 shows the relationship between steam-injection timing and IB. According to the above mentioned mechanisms of forming high density surface layer in conventional pressing, later steam-injection timing would form higher density surface layer and lower density core layer, which results in a certain decrease of IB. However, the effect of steam-injection timing on IB was not clear on boards with 0.6 g/cm³ density as shown in the Figure. This may be due to the negative effect of pre-cure of adhesive which occurred when steam was injected at lower mat density. Namely, earlier injection timing compensates for the effect of higher core density.

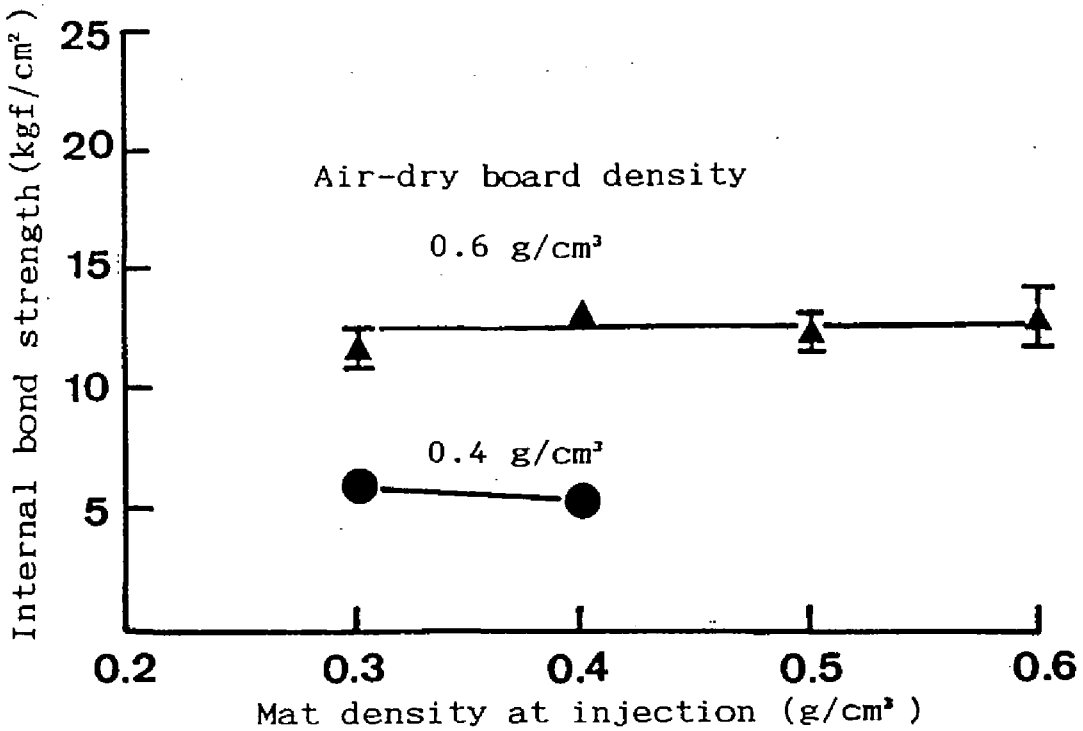

Fig.4.6 Relationships between mat density at steam-injection and internal bond strength.

The effect of steam-injection timing on TS is shown in Figure 4.7. Later steam-injection timing gave lower TS values

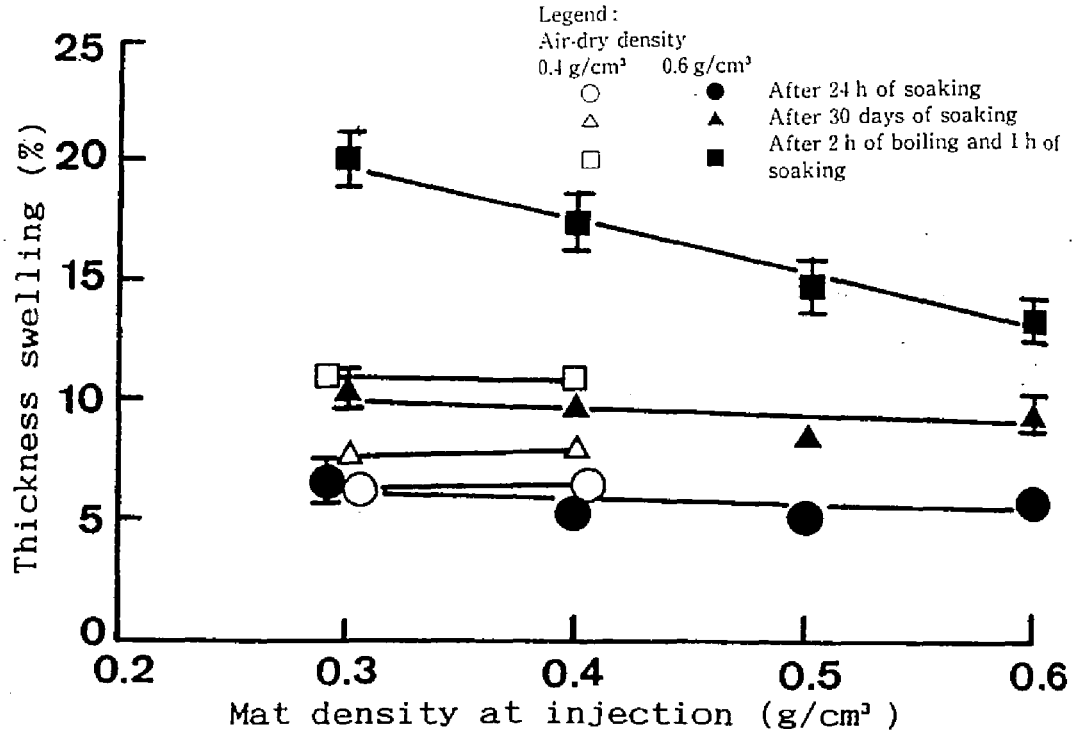

Fig.4.7 Relationships between mat density at steam-injection and thickness swelling.

Note: Legend is the same as in Fig.4

for board density of 0.6 g/cm³. From these experimental results, steam should injected when bulk density of mats increased up to a certain level where the particles had enough contact each other. In production of high density boards, greater compaction of particle mat is needed. Therefore, higher pressure and longer time are necessary to compress the mat to the target density. However, the press-time is shortened and less energy is required if steam is injected with an early timing. The economical choice of the injection timing results the injection at early stage in the press cycle. Considered the balance of these conflicts, the injection timing is better adjusted when the bulk density of mats reaches at least the compaction ratio of 1.0-1.3.

4.2 Effect of particle geometry on board properties[88)]

4.2.1 Experimental

Prepared materials and the methods of manufacturing the boards are the same as those of the experiment on the air permeability of boards in Chapter 3 [88)]. Each of seven types of Japanese red pine particles with different dimensions, which are shown in Table 4.1, strictly controlled for length (l), width (w), and thickness (t), was prepared in producing particleboards with a density range of 0.3–0.6 g/cm^3 using an isocyanate compound adhesive under different pressing conditions.

Table 4.1.

a. Prepared particles.

Particle No.	l (mm)	w (mm)	t (mm)	Particle No.	l (mm)	w (mm)	t (mm)
1	10	2	0.3	5	20	10	0.3
2	20	2	0.3	6	20	2	0.6
3	50	2	0.3	7	20	2	0.9
4	80	2	0.3				

b.Measurement of particle size.

l (mm) Target	l (mm) Measured	S.D.	C.V.	w (mm) Target	w (mm) Measured	S.D.	C.V. (%)	t (mm) Target	t (mm) Measured	S.D.	C.V. (%)
10	10.02	0.04	0.00	2	2.04	0.05	0.02	0.3	0.303	0.03	0.10
20	20.01	0.02	0.00	10	9.99	0.10	0.01	0.6	0.602	0.02	0.04
50	49.99	0.06	0.00					0.9	0.906	0.04	0.04
80	79.92	0.27	0.00								

Legend: l, w, and t : Particle length, width, and thickness, respectively.
S.D. and C.V.: Standard deviation and coefficient of varience, respectively.
Note: The number of particles measured in each configuration = 50–100 particles.

Two experimental boards with a size of 10 mm x 340 mm x 340 mm were conditioned for two weeks at 20 °C and 65 % RH (relative humidity), followed by cutting test specimens for each level of

particle geometry and pressing conditions. The mechanical and the physical properties of the boards were tested in accordance with Japanese Industrial Standard (JIS) A 5908. These were the modulus of elasticity (MOE), modulus of rupture (MOR), internal bond strength (IB), and thickness swelling (TS) after a 24 hr water soak at 25 °C. Statistical analyses of the data were made to determine the effects of the various factors on the board properties.

4.2.2 Results and discussion

Features of the voids among the particles from side views of the manufactured boards were as follows: as the particles became longer, more contact between them was observed, and the thicker the particles, the greater were the voids for both 2 mm and 10 mm wide particles. The sizes and distributions of the voids depended very much on the board densities. However, the injection timing and the initial steam pressure had little influences on the sizes and distributions of the voids.

Fig. 4.8 shows the effects of l, w, and t on MOR, and Fig. 4.9 shows their effects on MOE. The 0.4 g/cm^3 air-dry density boards surpassed the Type 200 of JIS in MOR in the case of 50 mm long, 2 mm wide, and 0.3 mm thick particles. The bending properties tended to increase with increases of l and with decreases of t (the latter at the length of 20 mm) when the other two dimensions were constant. This corresponded to the results for conventional boards. However, t had little influence on the bending properties at the length of 80 mm, and the bending properties had wide confidence intervals. This may have been due to the inhomogeniety of the steam diffusion in the mat. More steam diffuses between the sides of particles than between upper and lower particle surfaces when the particles are

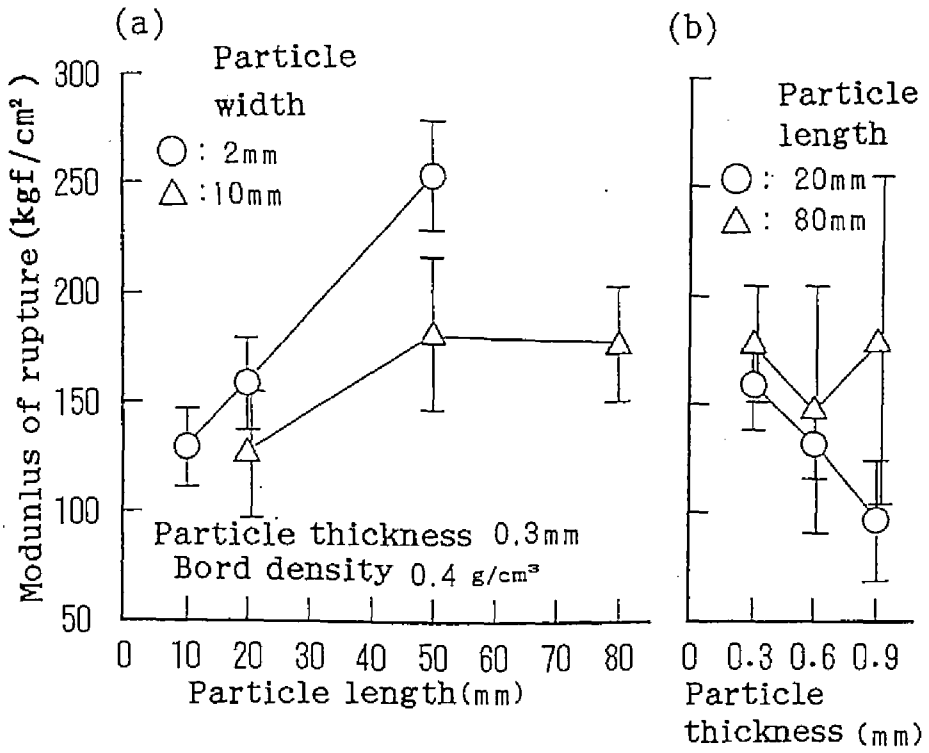

Fig.4.8 Effect of particle configuration on the modulus of rapture.
Note: The ranges of the mean value show 95 % confidence intervals.

longer. Little difference in MOE compared to MOR, was shown at the same particle width resulting from less sensitivity in MOE for board structures.

Fig. 4.10 shows the effect of the particle geometry on the IB. Although the target board density is as small as 0.4 g/cm³, greater IB value of about 6 kgf/cm² is obtained at 2 mm particle width, while it is lower value of about 1 kgf/cm² at 10 mm width. This may attribute to the lesser air permeability in the case of greater w. In general, the greater the thickness, the greater is the pressure applied on upper and lower particle surfaces. IB increased remarkably with increases of t in the

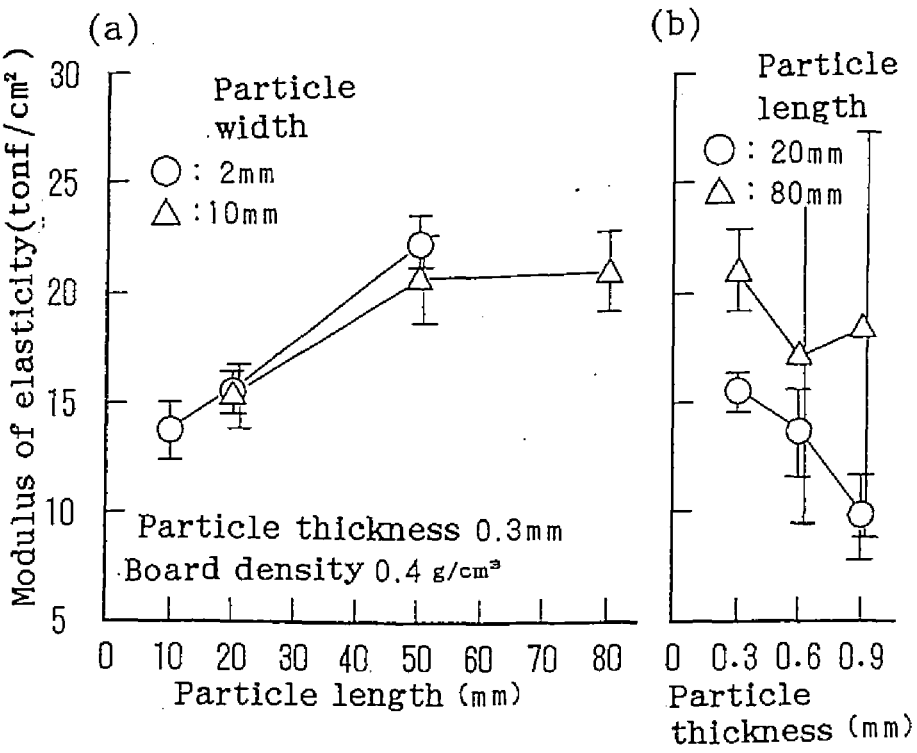

Fig.4.9 Effect of particle configuration on the modulus of elasticity.
Note: The ranges of the mean value show 95 % confidence intervals.

case of 80 mm long and 10 mm wide particles. This corresponded to the results of previous studies[88]. With increases of t, larger voids could be seen in the cross-sections, and the air permeabilities showed their maximums at 0.9 mm particle thicknesses. However, IB decreased at 0.9 mm thicknesses in the case of 20 mm long and 2 mm wide particles. These decreases may have been due to the greater ratio of steam flowing between particle sides instead of moving between the upper and lower particle surfaces.

Fig.4.11 shows the effect of the particle geometry on TS. TS increases with an increase of l. Although TS has the same tendency in the case of 10 mm long particles as that of previous

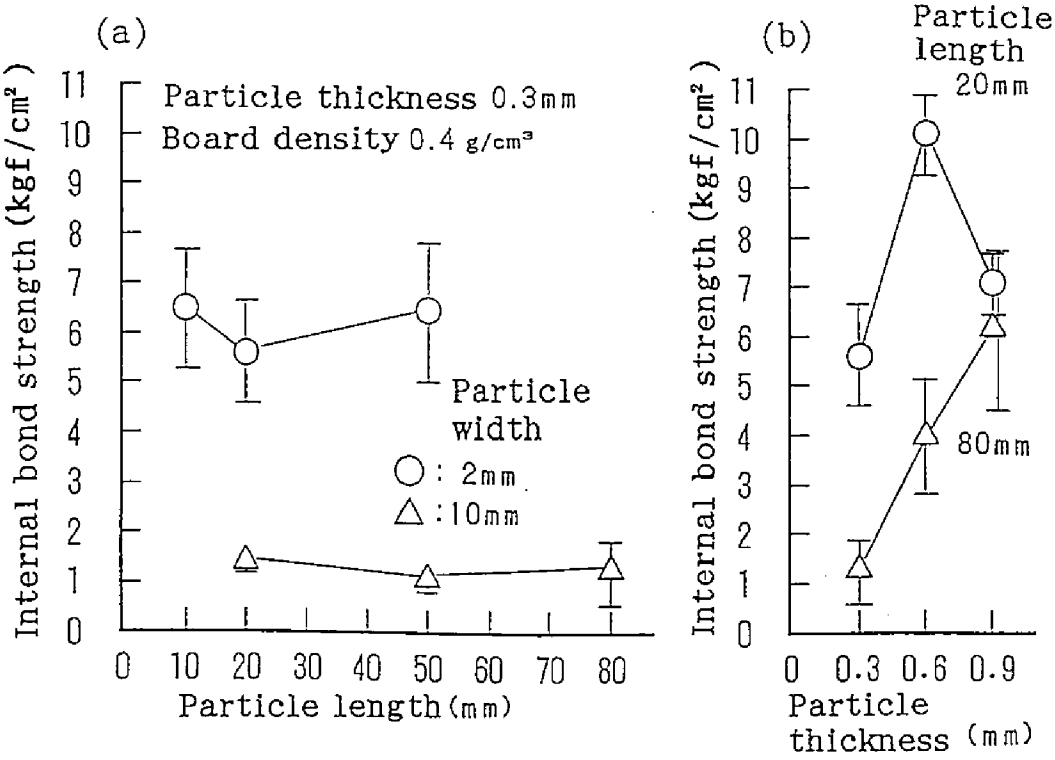

Fig.4.10 Effect of particle configuration on the internal bond strength.
Note: The ranges of the mean value show 95 % confidence intervals.

studies, it is almost independent of l in the case of 2 mm particle width. This may have been due to the inhomogeniety of the steam diffusion as mentioned before.

TS increased with an increase of t in the case of the 20 mm length and 2 mm width particles, whereas the TS decreased at the thickness of 0.6 mm, and little difference was observed between the TS at 0.3 mm and that of a 0.9 mm particle thickness. This may have been due to the lesser bonding strength at the 0.3 mm particle thickness resulting from the lesser air permeability in the mat.

Fig. 4.12 shows the effects of the mat densities at steam-injection on MOR and MOE. The larger MOR value of 350 kgf/cm²

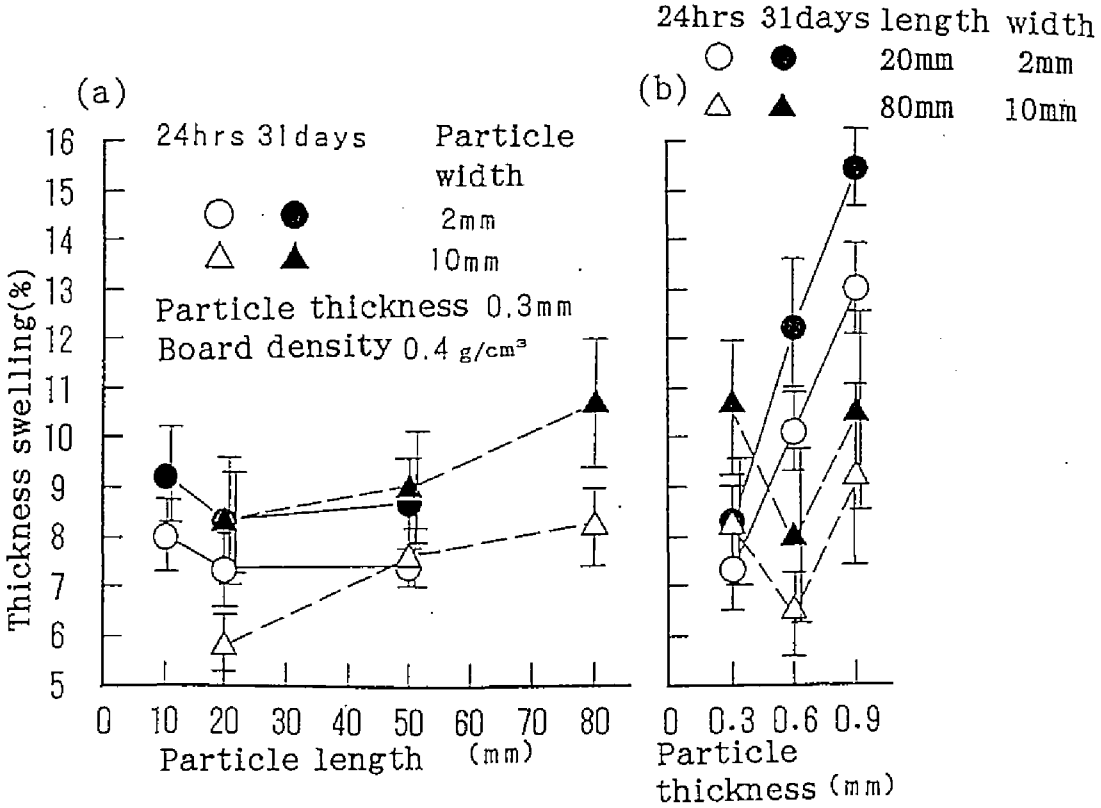

Fig.4.11 Effect of particle configuration on the thickness swelling.
Note: The ranges of the mean value show 95 % confidence intervals.

was obtained for 0.6 g/cm³ density board. MOE and MOR were a little less at the mat density of 0.4 g/cm³ at injection in the case of 0.4 g/cm³ density board, whereas those of 0.6 g/cm³ density boards seemed to be independent of injection timings.

Fig. 4.13 shows the effects of the mat densities at steam-injection on IBs and on TSs. IB was independent of the mat density at injection, whereas it was less at the mat density at injection for 0.6 g/cm³ density board. This result can be predicted from the results of the temperature behavior in the mat. When steam is injected at a greater mat density, the temperature increases more slowly because of less air permeabil-

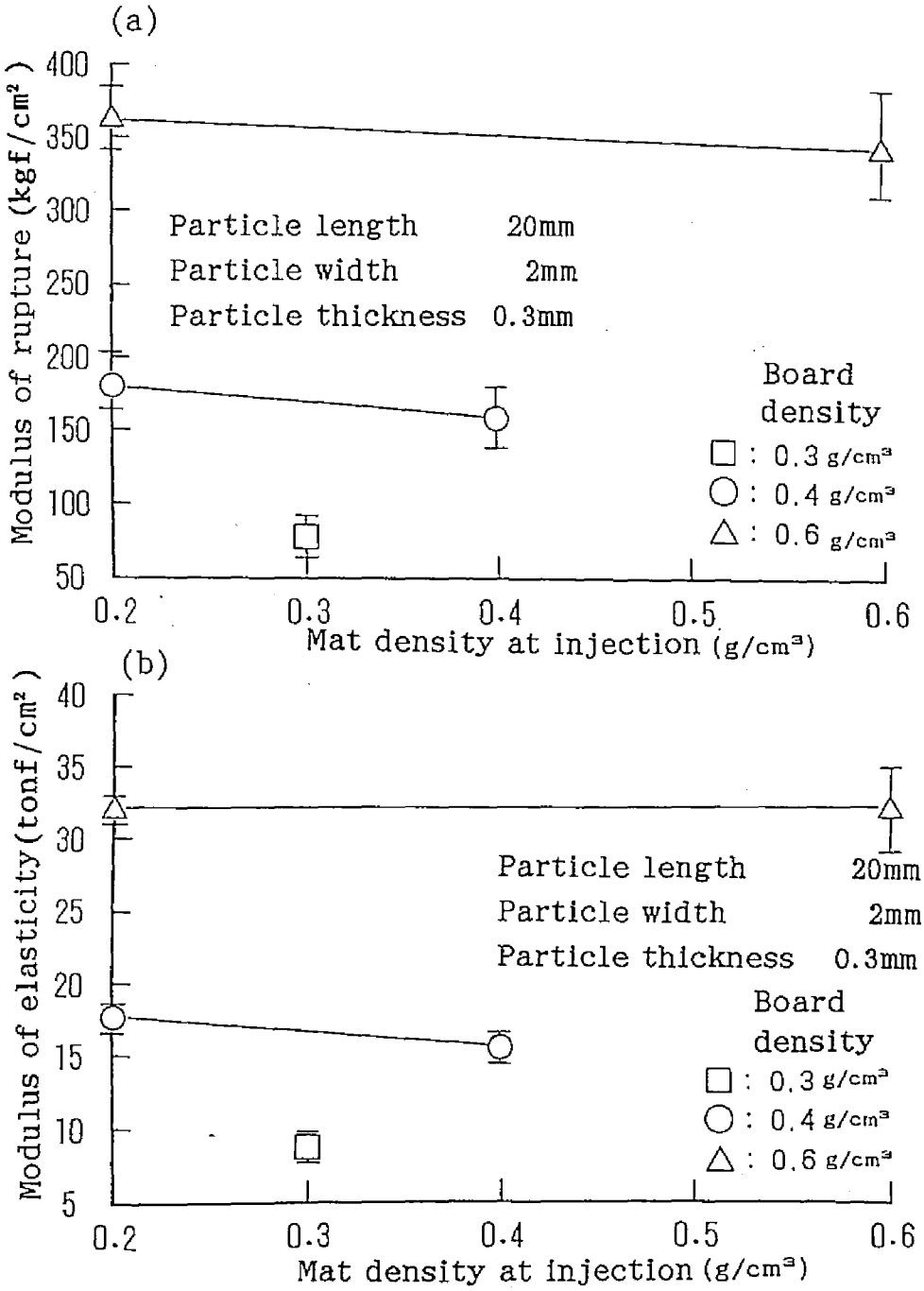

Fig.4.12 Effect of mat density at injection on MOR and MOE.

Note: The ranges of the mean value show 95 % confidence intervals.

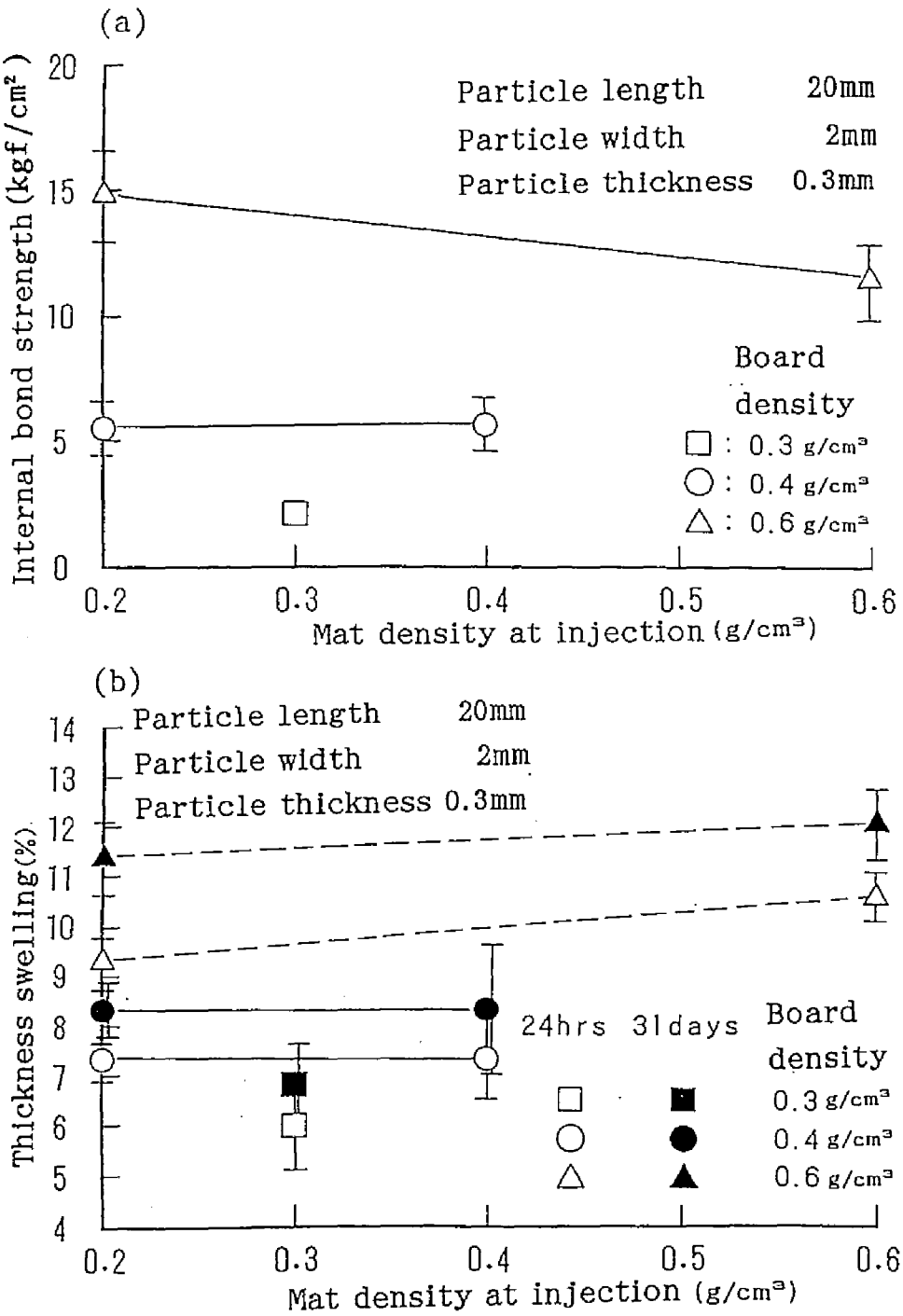

Fig.4.13 Effect of mat density at injection on the internal bond strength and on the thickness swelling.

Note: The ranges of the mean value show 95 % confidence intervals.

ity in the case of the 0.6 g/cm³ density board. On the other hand, little difference in temperature behavior was observed for 0.4 g/cm³ density board, because the air permeability of the mat was large enough for the steam to diffuse in the mat at the smaller density of 0.4 g/cm³.

The same tendencies were observed in the results of TS. The TS of 0.6 g/cm³ density board after a 24-hr water immersion was greater at the mat density at injection of 0.6 g/cm³ because of lesser bonding strength between particles resulting from the smaller air permeability of the mat.

The effects of the initial steam pressure on board properties also were investigated. However, little differences were observed with an initial steam pressure range of 2 to 6 kgf/cm².

4.3 Shortening press cycle with steam-injection pressing[74]

4.3.1 Experimental

Raw material used was Seraya (Shorea Spp.) with an air-dry density of 0.4 g/cm³. Chips of the materials prepared by a drum chipper were converted into flake-type particles with a knife-ring flaker (Pallmann PZ-8). The average dimensions of particles were 5.7 mm in length and 0.38 mm in thickness. Particles were conditioned to 11 % moisture content. The adhesive resin used was an isocyanate compound (IC) resin, UL-4800, formulated by Gun-ei Kagaku Kogyo Co. Ltd. The resin content level was ten percent of resin solid based on oven-dry weight of particles. In order to obtain a suitable vicosity of the adhesive for spraying, acetone was added to the IC resin at 20 percent based on weight of the resin solids. The resin was sprayed on the particle in a drum-type rotary blender by means of an airless

gun. Hand-formed particle mats were pressed to a board thickness of 20 mm.

In the case of steam-injection pressing, steam was injected for 3 seconds at mat bulk desnsity of 0.4 g/cm^3 for both the target board densities of 0.4 and 0.6 g/cm^3. The target steam pressure was 6 kgf/cm^2 (about 160 °C) with an effective steam pressure of 4 kgf/cm^2 (140°C). The temperature of the hot-platens was set at 160 °C with a press pressure of 5 to 10 kgf/cm^2. Total press-time were 30, 45, 60, and 120 seconds for a board density of 0.4 g/cm^3, and 30, 60, 90, and 120 seconds for a board density of 0.6 g/cm^3. The total press-time was measured from pressure build-up. In the case of conventional pressing, temperature of platens was set at 160 °C. The first stage pressure was set at 15 to 20 kgf/cm^2 for 30 seconds, and the second stage pressure was set at 5 to 10 kgf/cm^2 for 2.5, 3.5, and 4.5 minutes which correspond to the total press-time 3, 4 and 5 minutes. One board of 500 x 400 x 20 (thickness) mm was prepared for each condition mentioned above and for each target density of 0.4 and 0.6 g/cm^3.

Specimens cut from the above were tested after conditioning for 2 weeks at 20 °C and 65 % relative humidity (RH). Modulus of elasticity (MOE) and modulus of rupture (MOR) in both air-dry and wet conditions, internal bond strength (IB), screw withdrawal resistance (SW) and thickness swelling (TS) were measured according to Japanese Industrial Standard (JIS) A 5908.

4.3.2 Results and discussion

The effects of press time on MOE and MOR under dry and wet conditions are shown in Fig. 4.14 and 4.15. The steam-injection pressed boards showed no decrease in MOE and MOR properties both in air-dry and wet conditions for densities level of 0.4 and 0.6

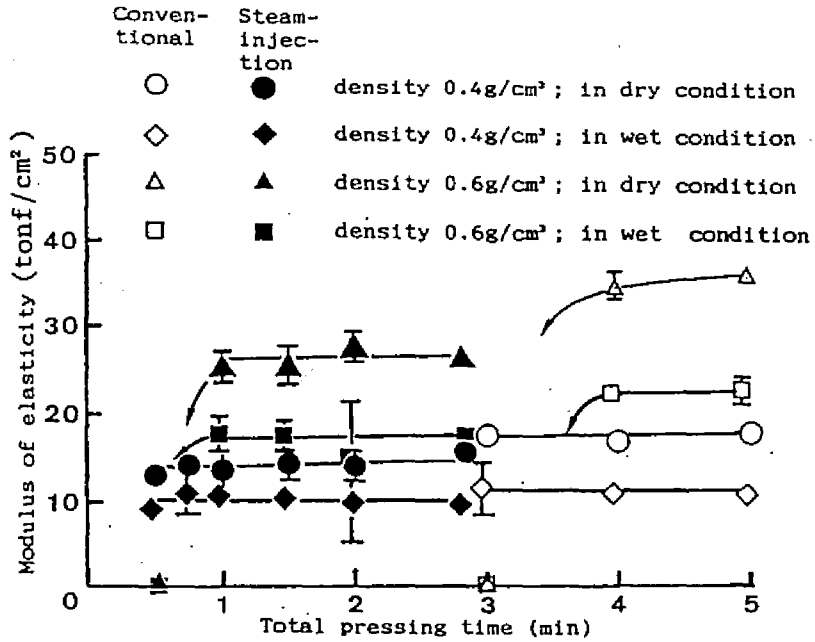

Fig.4.14 Relationships between total pressing time and modulus of elasticity in dry and wet condition.

Note: The ranges of the mean values show 95% confidence intervals.

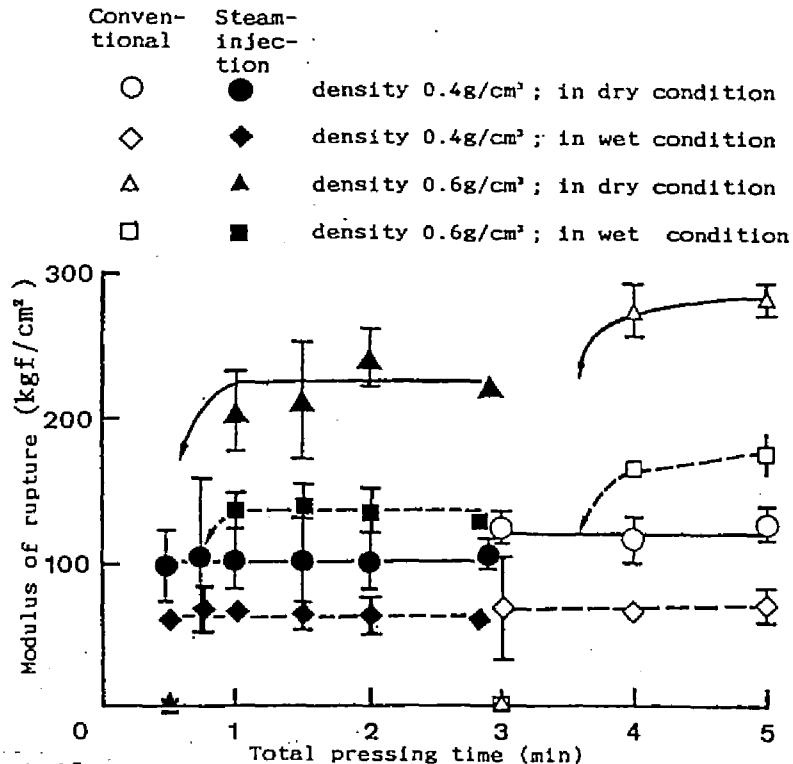

Fig.4.15 Relationships between total pressing time and modulus of rupture in dry and wet condition.

Note: The ranges of the mean values show 95% confidence intervals.

g/cm³, with reduction of total press time including 3 sec steam-injection down to 30 sec and 1 minute, respectively. On the other hand, for the conventional pressing, the press-time can be shortened to 3 and 4 minutes for board densities of 0.4 and 0.6 g/cm³, respectively. Delamination of board was observed for board density of 0.6 g/cm³ when press-time were 30 sec and 3 minutes for board produced by steam-injection and conventional pressing, respectively. The difference in the minimum press-time with different board densities may be attributed to the difference in internal stress, diffusion resistance during steam-injection and a rising rate of temperature in the core of mats. The values of MOE and MOR were similar to each other for the boards with a density of 0.4 g/cm³ produced with both pressing systems. However, higher values of MOE and MOR were obtained in conventional pressing than in steam-injection pressing in the case of 0.6 g/cm³ density board. This may be due to differences on density distribution across board thickness as described in the Section 2.3.

The relationship between press-time and IB is shown in Fig. 4.16. For board density of 0.4 g/cm³, though the IB value did not decrease when press-time was shortened to 45 sec, it began to decrease at a press-time of 30 sec. In the case of 0.6g/cm³ board density, the margin of press-time was about 60 sec. On the other hand, for both boards with densities of 0.4 and 0.6 g/cm³ produced by conventional pressing, this corresponded with the temperature behavior in the core of particle mat. The IB expresses the bonding strength of the weakest bonded layers. In other words, it is a direct measure of curing grade of adhesive in the middle layer when reducing press-time. This experimental result suggested that required press-time using steam-injection pressing was 45 and 60 sec for board densities of 0.4 and 0.6

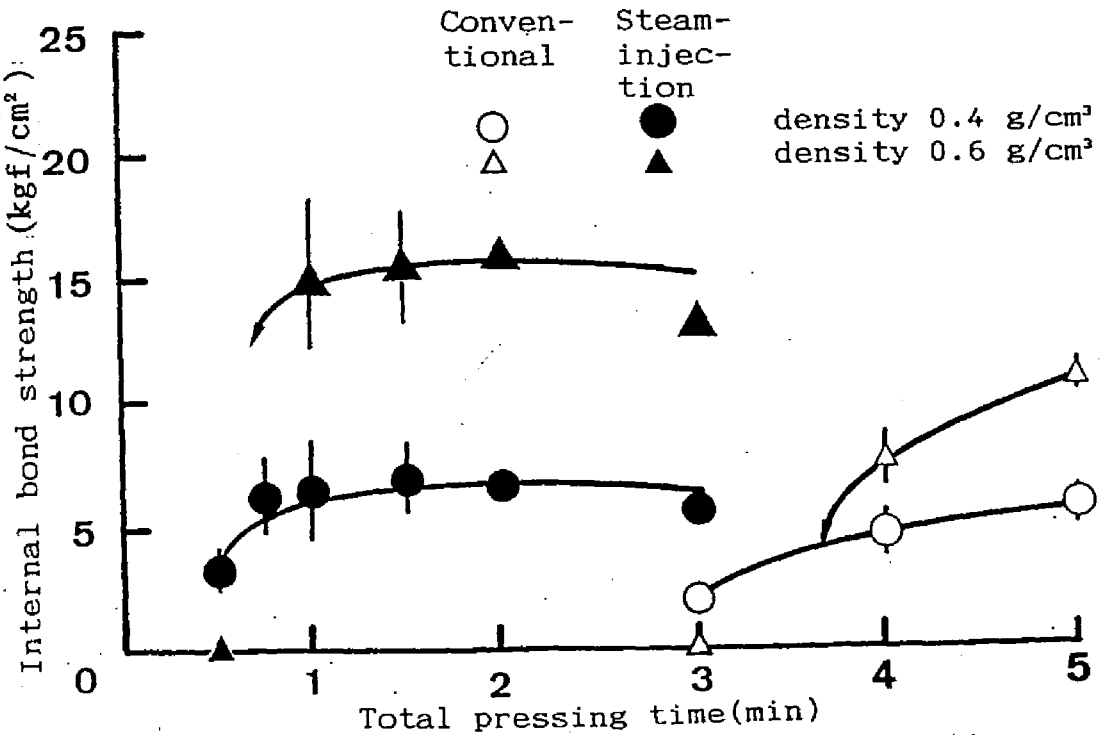

Fig.4.16 Relationships between total pressing time and internal bond strength.
Note: The ranges of the mean values show 95% confidence intervals.

g/cm³, respectively. This corresponds to only 1/5 to 1/6 of the press-time necessary for the conventional pressing. The results of this experiment agree well with the results obtained in the foregoing chapter concerning curing condition of particleboard adhesive using isocyanate resin[37].

The relationships between SW, TS properties and press time are shown in Figures 4.17 and 4.18, respectively. The results were similar with those obtained in IB test mentioned above.

4.4 Summary

First, the effect of steam-injection time and timing on the physical properties of particleboard was examined to get the optimum conditions for steam-injection pressing. Owing to the the difference of the density distribution through the board

thickness, the flexure properties of the greater density boards made with steam-injection pressing had values a little smaller than those made with conventional hot-platen pressing and their dimensional stability under wet conditions also tended to increase. The board properties were almost independent of the steam-injection time. The bending properties tended to increase with the delay of the initiation of the steam injection in most dense particleboards. This means that sufficient contact between particles before steam injection was best. In spite of the above results, initiation of the steam injection at the compaction ratio of 1.0 to 1.3 would be rational for shortening the total press time because a longer pressing time and a greater pressure were needed to compress the mats to a target density in the production of boards of greater densities.

Secondly, each of seven types of Japanese red pine particles with different dimensions, strictly controlled for length, width, and thickness, was prepared in order to produce particle boards with a density range of 0.3-0.6 g/cm^3 under different pressing conditions. Mechanical and physical properties of these boards were determined and the effect of particle geometry and pressing conditions were discussed. It revealed that particle geometry influenced the way how steam diffuses into the mat. Based on the experiments conducted, it can be surmised that both steam diffusion and particle geometry have correlation on the properties of the final products.

Finally, the minimum and necessary press-time of steam-injection pressed, particleboards with a thickness of 20 mm using an adhesive and the effect of total press-time on the particleboard properties were investigated. Steam-injection pressing made it possible to produce particleboards in only 1/5 - 1/6 of the press time of conventional hot-platen pressing.

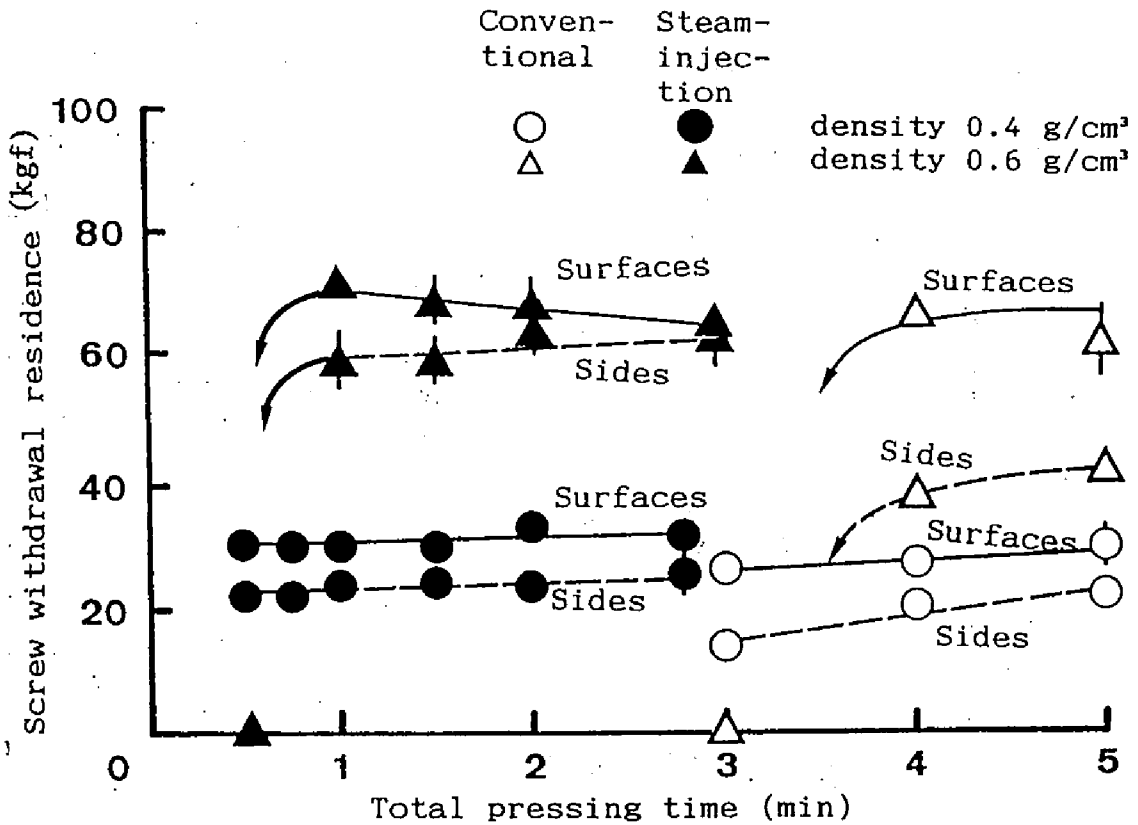

Fig.4.17 Relationships between total pressing time and screw withdrawal residence.
Note: The ranges of the mean values show 95% confidence intervals.

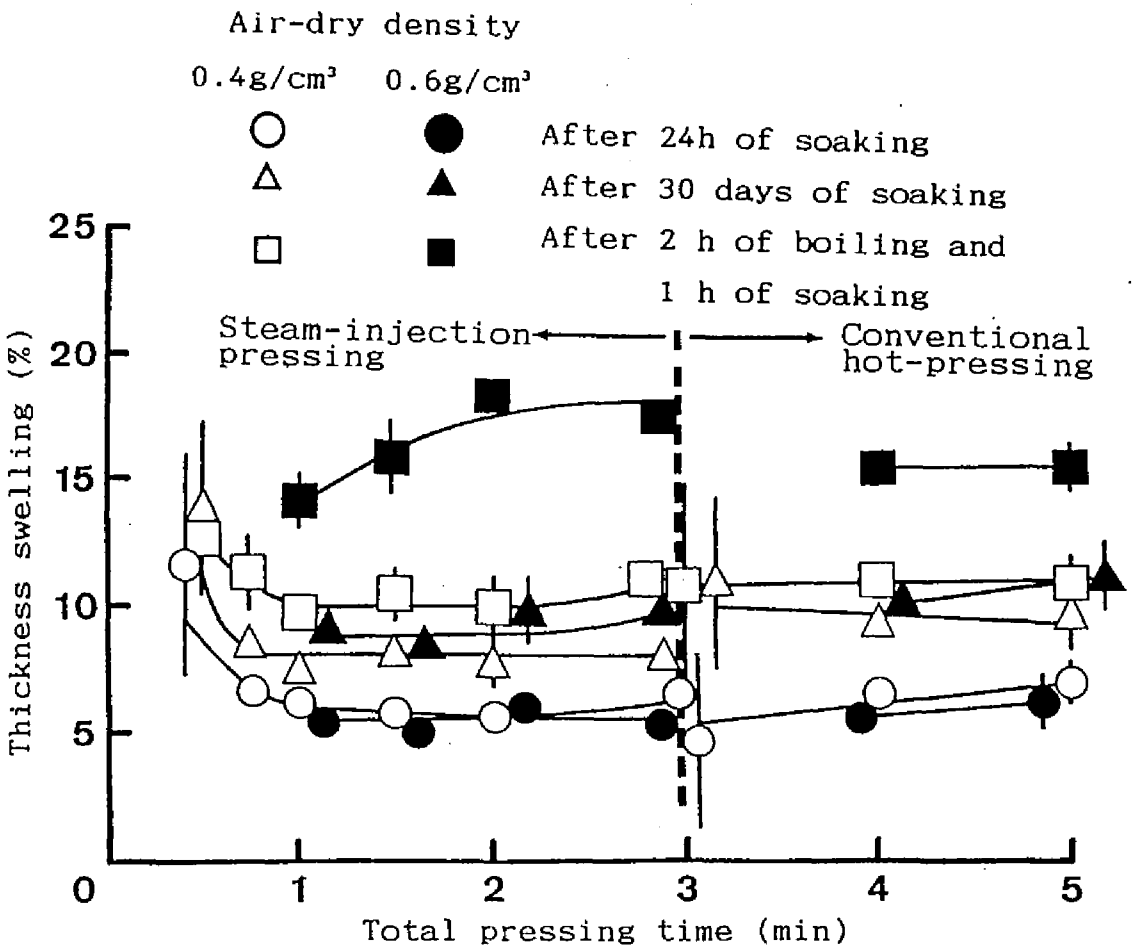

Fig.4.18 Relationships between total pressing time and thickness swelling.

Note:The ranges of the mean values show 95 % confidence intervals.

CONCLUSION

This thesis is written in four chapters with the aim of establishing the basic theories of the steam-injection pressing which is the most effective technology to improve the productivity of the wood-composite-products, while the effective utilization of low-quality wood resources is kept in mind.

It was surveyed in Chapter 1 that the steam-injection pressing made it possible to improve the productivity of wood composite boards as a substitute for wood and to positively make use of them in the situation where wood resources are reducing and that this process would become the breakthrough in wood industry which has been in a bad way.

First, the temperature behavior of the particle mat during hotpressing and steam-injection pressing was analyzed under various conditions in Chapter 2. With an increase of moisture content, the time necessary for the middle layer to reach 100 ℃ tended to shorten, whereas the time to maintain a constant temperature (about 100 °C) was prolonged in the case of hotpressing. The temperature in the middle layer of a mat with a higher moisture content in the face layers increased more than that of a mat with a uniform distribution of moisture content. In the case of steam-injection pressing, the temperature in the middle layer of the mats immediately increased to a specific degree decided by injection pressure and the characteristics of mats at the moment of steam-injection, and maintained a constant level during steam-injection. After stopping steam-injection, the temperature decreased a little, and then started to rise again. The rates of temperature increase in the middle layers of mats were independent of thickness, moisture content and density in the range of the experimental conditions.

Secondly, the temperature distribution in particle mats during steam-injection pressing was numerically analyzed with the finite element method under various conditions in this Chapter. Calculated results agreed comparatively well with the observed results, which proved that the analytical theory was useful to predict the temperature behavior of particle mats during hotpressing and steam-injection pressing. In steam-injection pressing, with increases of mat thickness, the injection time necessary for raising core temperature up to 100 ℃ gradually increased. For example, it will take about 8 seconds for the core temperature of a 1000-cm-thick-mat, to reach 100 °C.

The temperature behavior in the mat and the air permeability of the boards were investigated in Chapter 3, using each of seven types of particles with different dimensions, strictly controlled for length, width, and thickness. The variables influencing the temperature behavior in the mat by steam-injection press was directly related to the air permeabilities of mats. The air permeabilities of the boards in the horizontal direction to the heat platen was always higher than in the vertical direction. A functional equation with a higher coefficient of determination that explains the air permeabilities was obtained by a multiple regression analysis. It was inferred that the steam diffusion in the mat result from the repetition of the steam moving among particles in two dimensions.

First, the effects of injection time and injection timing of high-pressure steam from hot platens on the physical properties of particleboards using an isocyanate-compound adhesives were investigated and the optimum conditions for steam-injection pressing was determined in Chapter 4. Owing to

the difference of the density distribution through the board thickness the flexure properties of the greater density boards made with steam-injection pressing had values a little smaller than those made with conventional hot-platen pressing and their dimensional stability under wet conditions also tended to increase. The board properties were almost independent of the steam-injection time. The bending properties tended to increase with the delay of the initiation of the steam injection in most dense particleboards. This means that sufficient contact between particles before steam injection was best. In spite of the above results, initiation of the steam injection at the compaction ratio of 1.0 to 1.3 would be rational for shortening the total press time because a longer pressing time and a greater pressure were needed to compress the mats to a target density in the production of boards of greater densities.

Secondly, this chapter showed the experiment where each of seven types of Japanese red pine particles with different dimensions, strictly controlled for length, width, and thickness, was prepared in order to produce particleboards under different pressing conditions, mechanical and physical properties of these boards were determined, and the effect of particle geometry and pressing conditions were discussed. It revealed that particle geometry influenced the way how steam diffuses into the mat. Based on the experiments conducted, it can be surmised that both steam diffusion and particle geometry have correlation on the properties of the final products.

Thirdly, the effects of pressing time on the physical properties were investigated in this chapter to find the minimum press time required to produce particleboards using an isocyanate-compound adhesive with the steam-injection pressing. Steam-injection pressing made it possible to produce

particleboards in only 1/5 - 1/6 of the press time of conventional hot-platen pressing.

As mentioned above, it shows in the first part of this study that the steam-injection pressing fulfilled the requirements for lower density or thicker boards. The temperature behavior of particle mats during pressing was then investigated from the experiments and the computer simulation. It was made clear that this technology made it possible to produce boards with excellent properties and will improve productivity. The results of the experiment on the effects of particle geometry on air permeabilities will offer useful information in the development of a full scale continuous steam-injection press as well as the potential of the applied process of the steam-injection pressing in the production of wood composite products.

It follows from what has been said that this study would give us a deeper significance because the purpose of this research is the effective utilization of lower quality wood and the effective production of value-added functional materials with saved energy in order to face the inadequate supply of wood and its subsequent adverse effect on wood quality.

In relation to this study, many interesting subjects are still left and these are as follows: The development of new and thick wood composite products; The development of a full scale continuous steam-injection press; A study on the improvement of the dimensional stability and endurance of the products; and a study of the board production with applied technology of the steam-injection pressing; and so on. I would like to evolve the study and further aim at developing new materials.

ACKNOWLEDGEMENT

I would like to express gratitude for the privilege of being able to study under Professor Dr. Hikaru Sasaki, Wood Research Institute, Kyoto University, and for his invaluable supervision. I would also like to thank Professor Dr. Takeshi Sadoh, Faculty of Agriculture, Kyoto University, and to Professor Dr. Misato Norimoto, Wood Research Institute, Kyoto University, as co-supervisor.

Special thanks are due to Associate Professor Dr. Shuichi Kawai, Wood Research Institute, Kyoto University, for reading the manuscript and making a number of helpful suggestions. I would also like to thank Professor Dr. Shigehisa Ishihara, Associate Professor Dr. Yuji Imamura and Instructor Mr. Shinjiro Takino of the above Institute for their constant support and instructions. My further thanks are extended to Dr. Toru Ebihara, Forestry and Forest Products Research Institute, Ministry of Agriculture, Forestry and Fishries, for his help and suggestions on some parts of this research.

I would also like to acknowledge the invaluable support of Mr. Hisayoshi Suda, Sumitomo Ringyo Co. Ltd., Mr. Divino. E. Teixeria, Laboratorio De Productos Florestais, Bambanmg Subiyanto, Research and development Center for Applied Physics. Mr. Nakano Masashi, Iwate Prefectural Forestry and Forest Products Research Center, Mr. Yoki Suzuki, Forestry and Forest Products Research Institute, and Mrs. Hiromi Hata. Thanks must also be extended to members in the Research Section of Composite Wood and in the Forestry and Forest Products Research Institute for their help and encouragement; in particular to Dr. Orlando R. Pulido and Mr. Dweight A. Eusebio for his critical reading this manuscript.

REFERENCES

1) Kawai,S.; Hata,T., *Wood Industry* , 42 (12), 562-565(1987).

2) Geimer, R. L., Proc. Wash. State Univ. Int. Symp. Part. 16: 115-134 (1982).

3) Nakaji,M.; Kawai,S.; Morita,S., *Wood preservation*, 26, 53-59(1985).

4) Greten, B., *Holz als Roh- und Werkstoff*, 44, 371-378 (1986).

5) Soinè, H., *Holz als Roh- und Werkstoff* , 42, 63-66 (1984).

6) Soinè, H., *Holz als Roh- und Werkstoff* , 42, 93-98 (1984).

7) Soinè, H., *Holz als Roh- und Werkstoff* , 44, 371-378 (1986).

8) Williams,W., *Wood Based Panels North America* , 2, 25-27, (1989).

9) Deppe,H.J. & Ernst,K., *Holz als Roh- und Werkstoff*, 29 (2) 45-50 (1971).

10) Roffael, E.; Rauch, W., *Holz als Roh-und-Werkstoff*, 31 (10), 402-405 (1973).

11) Johns, W. E.; Malony, T. M.; Huffaker, E. M.; Saunders, J. B; Lentz, M. T., Proceeding of the fifteenth washington state universty international symposium on particleboard, Pullman, Washington, 31 (3), 213-239 (1981).

12) Kawai, S.; Sasaki, H.; Nakaji, M., *Wood Research* , 72 27-36(1986).

13) Kawai,S.; Sasaki, H., *Mokuzai Gakkaishi* , 32 (5) 324-330 (1986).

14) Yoshida, Y. et. al., *Mokuzai Gakkaishi* , 32 (12), 965-971 (1986).

15) Deppe, H- J. & Ernst, K.,*Holz als Roh-und-Werkstoff* , 23 (11) 441-445 (1965).
16) Tanishita,I., Heat Conduction Technology, Houkabou (1986).
17) Fahrni, F., *Holz als Roh- und Werktoff*, 14 (1),8-10 (1956).
18) Klauditz, W., Springer Verlag, Berlin (1966).
19) Kollmann, F., *Holz als Roh- und Werkstoff*, 15 (1), 35-44 (1959).
20) Klauditz, W., German Patent 1056358 (1959).
21) Corbin, R. L.; Hall, J. A. (Weyerhaeuser Co.), U. S. Patent 3280237 (1966).
22) Stegmann, G.; May, H. A., *Holz Zentralblatt* , 94 (23), 361-363 (1968).
23) Voelscow, P.; Shafer, K. (G. Siempelkamp and Co.), German Patent, 2,058,820 (1972).
24) Shen, K. C., U. S. Patent, 3,891,738 (1975).
25) Alenius, N. R., German Patent, 2,312,159 (1973).
26) Okhotskii, Y. V.; Pischikov, V. V.; Vuedensky, E. M. 1974 French Patent 2,206,701; Jun 7.
27) Thoman, B., & Pearson, R. G., *Forest. Prod. J.* 26 (11), 46-50 (1976).
28) Nyberg, D. W., Canadian Patent 1,075,140, April 8, 1980.
29) Nishikawa, S. et al., *Rinsanshi Geppou*, 12 (1981).
30) Nisikawa, S. et. al., *Rinsanshi Geppou*, 9 (1983).
31) Geimer, R. L., U. S. Patent 4,393,019. July 12. (1983).
32) Geimer,R. L., USDA Forest Serv. Res. Pep. 456, 1-16 (1985).
33) Taylor,M.N.; Reid,T.H., US Patent 4,517,147. May 14 (1985)
34) Geimer, R. L., & Price, E. W., Proceedings of the 20th international particleboard/composite materials symposium, 367-384 (1986).
35) Hsu, W. E. US Patent 4,850,849, July 25, 1989

36) Hsu, W. E. Spring Meeting, Eastern Canadian Section, For. Prod. Res. Soc. (1990).
37) Bambang Subiyanto; Kawai, S.; Sasaki, H.; Kahar, N.; Shigehira, H., *Mokuzai Gakkaishi*, 34 (4), 333-336 (1988).
38) Sasaki, H.; Kawai, S.; Bambang Subiyanto; Hata, T. *Mokuzai Kogyo Gijutsu Tanshin* 6 (1), 1-14 (1988).
39) Bambang Subiyanto; Kawai, S.; Tanahashi, M.; Sasaki, H., *Mokuzai Gakkaishi*, 35 (5), 419-423 (1989).
40) Bambang Subiyanto; Kawai,S.; Sasaki,H., *Mokuzai Gakkaishi*, 35 (5), 424-430 (1989).
41) Sasaki, H., Report of the Grants-in-Aid for Scientific Research (No.62860020) from the Ministry of Education, Sience and Culture of Japan, March (1989).
42) Bambang Subiyanto, Docter thesis of agriculture (1991).
43) Sasaki, H., Report of the Grants-in-Aid for Scientific Research (No.01860023) from the Ministry of Education, Sience and Culture of Japan, March (1990).
44) Tomimura, Y. et al., *Mokuzai Gakkaishi*,32 (1), 67-69 (1986).
45) Hata, T; Ebihara, T., Pacific Rim Bio-Based Composites Symposium, Rotorua New Zealand, November, 64-72 (1992).
46) Pamphlet of Sunds Defiberator, Sunds Defiberator & Falco Cement Flakeboard Technology (1990).
47) Anonym, Wood based panels intn'l, 2, Feb. (1987).
48) Iwashita, M., *Mokuzai Kogyo*, 42, 12 (1987).
49) Anonym, Wood based panels intn'l, 3, Feb. (1986).
50) Walter, K., Wood based panels intn'l, 36-38, Nov. (1988).
51) Walter, K., *Holz als Roh- und Werkstoff*, 47, 117-120 (1989).
52) Williams, W.,Wood Based Panels Intn'l, 34-35, April (1990).

53) Walter,K., F.R.I.(New Zealand) Bulletin No.177, 64-72 (1992).
54) Tansey,P., Wood Based Panels intn'l, 38-39, April (1992).
55) Sasaki, H., et al., *Mokuzai Kogyo*, 45 (9) (1988).
56) Bambang Subiyanto; Takino, S.; Kawai, S.; Sasaki, H., *Mokuzai Gakkaishi*, 37 (1) 24-30 (1991).
57) Hata, T.; Bambang Subiyanto; Kawai, S.; H. Sasaki, Abst. 39th Annu. Meet. Jpn. Wood Res. Soc., Okinawa, p.183, (1989).
58) Futo, L. P., *Holz als Roh-und-Werkstoff*, 28 (11) (1970).
59) Maku, T., *Mokuzai Kenkyu*, 3, 1-36 (1949).
60) Maku, T.; Matsuura, N., *Mokuzai Kenkyu*, 3, 37-53, (1949).
61) Hata, T.; Bambang Subiyanto; Kawai, S.; Sasaki, H., *Wood Sci. Technol* 23, 361-369, 12 (1989).
62) Maku,T.; Hamada, R.; Sasaki, H., *Wood Research*, 21, 47-50 (1959).
63) Maku, T.; Hamada, R.; Sasaki, H., *Mokuzai Kenkyu*, 21 (11), 34-46 (1958).
64) Shen, K. C., Forest Prod. J., 23 (3), 21-29 (1973).
65) Hata,T.; Kawai,S.; Sasaki,H., *Wood Sci. and Technol* 24, 65-78 (1990).
66) Yagawa, G.; Miyazaki, N., Analysis of Thermal Stress, Creep and Thermal Conduction by Finite Element Method, Science Co. (1985).
67) Canbell G. S., Soil Physics with Basic-Transport Models for soil-systems, ELSEVIER SCIENCE PUBLISHING COMPANY INC.40(1985).
68) HATA,T. et al., *Mokuzai Gakkaishi*,39 (2) 161-168 (1993).
69) HATA,T. et al. *Mokuzai Gakkaishi*,39 (2) 169-173 (1993).
70) Ogura, T., Bulletin of Forestry and Forest Products Research Institute 51, 61-75 (1951).

71) Suzuki, Y.; Haishi, T.; Saito, H., Abst. 39th Annu. Meet. Jpn. Wood Res. Soc., Okinawa, p.16, (1989).
72) Okuno, T.; Kume, H.; Saito, H., "Multivariate Analysis", Nikkagiren, 141 (1989).
73) Hata,T.; Bambang Subiyanto; Sasaki,H., *Mokuzai Gakkaishi*, 35 (12), 1080-1086 (1989).
74) Hata, T.; Kawai, S.; Sasaki, H., *Mokuzai Gakkaishi*, 35 (12), 1087-1091 (1989).